

jan 1958

CIRCULAR POLARIZATION
OF GAMMA RAYS EMITTED
FROM ORIENTED NUCLEI

W. J. HUISKAMP

Universiteit Leiden



1 481 265 0

CIRCULAR POLARIZATION OF GAMMA RAYS EMITTED FROM ORIENTED NUCLEI.

PROFESSOR DR. C. J. GOETHE

De heer CLAY en HARRISON hebben gevonden dat de cirkelpolarisatie van gammastraling van de beide kanten van een kristal van eenzelfde soort is, hoewel de kristalassen van de twee kanten in tegenovergestelde richtingen liggen.

PROEFSCHRIFT

TER VERKRIJGING VAN DE GRAAD VAN DOCTOR IN DE
WIS- EN NATUURKUNDE AAN DE RIJKSUNIVERSITEIT TE LEIDEN
OP GEZAG VAN DE RECTOR MAGNIFICUS DR. S. E. DE JONGH,
HOGLERAAR IN DE FACULTEIT DER GENEESKUNDE,
PUBLIEK TE VERDEDIGEN OP WOENSDAG 22 JANUARI 1958 TE 14 UUR

DOOR

WILLEMINUS JAN HUISKAMP

GEBOREN TE WINTERSWIJK IN 1925



1958

DRUKKERIJ 'DA COSTA' - UTRECHT

ORIENTED POLARIZATION OF GAMMA
RAYS EMITTED FROM ORIENTED NUCLEI

PROMOTOR: PROF. DR. C. J. GORTER

PROEFSCHRIFT

VOOR
DE ACADEMIE VAN WETENSCHAPPEN
VAN NEDERLANDSE INDIA
IN VERBAND MET
DE UNIVERSITEIT VAN
NEDERLANDSE INDIA
TE SOERABAYA

WETENSCHAPPELIJK INSTITUTE
TE SOERABAYA



WETENSCHAPPELIJK INSTITUTE
TE SOERABAYA

STELLINGEN

I

De door CLAY en HEREFORD gemeten korrelatie tussen de cirkulaire polarisatie's van de beide fotonen, welke ontstaan bij twee-kwantumannihilatie van positonen in rust, verschilt in teken van de theoretisch voorspelde korrelatie.

F. P. CLAY en F. L. HEREFORD, *Phys. Rev.* **85** (1952) 675.

II

Het zou aanbeveling verdienen om de metingen van de gemiddelde levensduur van positonen in vloeibaar helium uit te breiden tot temperaturen beneden het lambda-punt en aan te vullen met metingen van de richtingskorrelatie der annihilatiekwanta.

D. A. L. PAUL en R. L. GRAHAM, *Phys. Rev.* **106** (1957) 16.

J. WACKERLE en R. STUMP, *Phys. Rev.* **106** (1957) 18.

III

Gebruik makend van bestaande technische hulpmiddelen, moet het mogelijk geacht worden om protonen en mesonen van hoge energie met behoorlijke opbrengst te laten verstrooien door gerichte cobalt-kernen.

IV

De bepaling van het magnetisch dipoolmoment van een aangeslagen toestand van een kern uit metingen van de gamma-gamma-richtingskorrelatie, kan bijzondere moeilijkheden opleveren indien deze kern behoort tot een paramagnetisch ion. In zo'n geval kan het van belang zijn om de ionen te polariseren, bijvoorbeeld in een sterk magneetveld en bij temperaturen van vloeibaar helium.

V

Bij het bestuderen van zwakke resonantiesignalen van kernspins (met inbegrip van kern-quadruupoolmomenten) of electronspins, waarbij het uitwendig magneetveld of de frekwentie worden gemoduleerd, verdient het aanbeveling om slechts de tweede harmonische komponent van het signaal te versterken met een fasegevoelige versterker.

VI

Bij de direkte polarisatie van atoomkernen in een sterk uitwendig magneetveld (ook „brute force” methode genoemd) is de temperatuur van het kernspinsysteem veelal onvoldoende bekend. In een dergelijke situatie kan men door middel van demagnetisatie temperaturen van ongeveer 10^{-5} °K bereiken.

Uit metingen van de kernmagnetische susceptibiliteit bij deze temperatuur zou men kunnen afleiden, welke temperatuur vóór de demagnetisatie heeft bestaan.

STILLINGEN

ARTIKEL 1. VAN DE VERBODEN

De heer GAY en HENRIOD kunnen voortaan niet de rechten van de heer GAY en HENRIOD in de zaak van de heer GAY en HENRIOD tegenover de heer GAY en HENRIOD uitoefenen.

DE HEER GAY en HENRIOD, advocaat te Brussel.

II

Het eenzijdig verzoek van de heer GAY en HENRIOD tot de rechterlijke bevoegdheid van de heer GAY en HENRIOD is niet gegrond op de wet van 15 april 1894, art. 10, § 1, en art. 10, § 2, van de wet van 15 april 1894.

DE HEER GAY en HENRIOD, advocaat te Brussel.

DE HEER GAY en HENRIOD, advocaat te Brussel.

III

De heer GAY en HENRIOD kunnen voortaan niet de rechten van de heer GAY en HENRIOD in de zaak van de heer GAY en HENRIOD tegenover de heer GAY en HENRIOD uitoefenen.

IV

De heer GAY en HENRIOD kunnen voortaan niet de rechten van de heer GAY en HENRIOD in de zaak van de heer GAY en HENRIOD tegenover de heer GAY en HENRIOD uitoefenen.

V

De heer GAY en HENRIOD kunnen voortaan niet de rechten van de heer GAY en HENRIOD in de zaak van de heer GAY en HENRIOD tegenover de heer GAY en HENRIOD uitoefenen.

VI

De heer GAY en HENRIOD kunnen voortaan niet de rechten van de heer GAY en HENRIOD in de zaak van de heer GAY en HENRIOD tegenover de heer GAY en HENRIOD uitoefenen.

De heer GAY en HENRIOD kunnen voortaan niet de rechten van de heer GAY en HENRIOD in de zaak van de heer GAY en HENRIOD tegenover de heer GAY en HENRIOD uitoefenen.

VII

Het zou aanbeveling verdienen om bij de metingen van de richtingskorrelatie tussen β -deeltjes en cirkulair gepolariseerde fotonen, een controleproef uit te voeren, waarbij het verstrooiende, gemagnetiseerde ijzer is vervangen door messing.

H. SCHOPPER, *Phil. Mag.* 2 (1957) 710.

A. LUNDBY, A. P. PATRO en J. P. STROOT, *Nuovo Cimento* 6 (1957) 745.

VIII

Bij het onderzoek van MALAKER naar de soortelijke warmte van cobalt-ammonium-Tuttonzout bij zeer lage temperaturen, is gebruik gemaakt van een elektromagnetisch wisselveld met een frekwentie van 35 Hz. MALAKER'S argumenten voor de keuze van deze frekwentie zijn aan bedenkingen onderhevig.

S. F. MALAKER, *Phys. Rev.* 84 (1951) 133.

IX

Bij de bestudering van de fotoelektrische verschijnselen in éénkristallen van cadmium-sulfide, opgewekt door beschieting met α -deeltjes, is het van belang niet alleen te letten op de pulsgrootte, maar ook op de gelijkstroom. De invloed van infrarood licht op deze gelijkstroom verdient in het bijzonder de aandacht.

P. J. v. HEERDEN, 106 (1957) 468.

X

In de door BEUN aangegeven entropieberekeningen betreffende chroom-aluinen bij de temperatuur van ongeveer 1° K en in verschillende magneetvelden, is onvoldoende rekening gehouden met de splitsing van de grondtoestand van het chromion onder invloed van elektrische kristalvelden.

J. A. BEUN, *Akademisch proefschrift*, Leiden, 1957.

XI

Het valt ernstig te betwijfelen of het door REICHSTEIN uit de bijnier geïsoleerde desoxycorticosteron in het menselijk lichaam (op natuurlijke wijze) wordt gevormd.

REICHSTEIN en v. EUW, *Helv. Chim. Acta* 21 (1938) 1197.

XII

Tegen de onderstelling van RÜMKE, dat de zogenaamde „exploratieve aandrift” slechts een ondergeschikte rol zou spelen bij het ondernemen van buitenlandse reizen, zijn ernstige bedenkingen aan te voeren.

H. C. RÜMKE, *Ned. Tijdschrift voor Geneeskunde* 101 (1957) 1525.

XIII

Gezien de noodzakelijk geachte uitbreiding van het hoger onderwijs in ons land, is het gewenst om een nieuwe universiteit te stichten buiten de randstad-Holland, bijvoorbeeld in het Oosten des lands.

De auteur is lid van de wetenschappelijke staf van de "Stichting voor Fundamenteel Onderzoek der Materie" (F.O.M.), die finantieel wordt gesteund door de „Nederlandse Organisatie voor Zuiver Wetenschappelijk Onderzoek" (Z. W. O.). Het onderzoek betreffende gerichte radioactieve atoomkernen werd verricht in samenwerking met de F.O.M.-werkgroep voor kernphysica, Rijksuniversiteit Groningen, onder leiding van
Prof. Dr. H. Brinkman.

Teneinde te voldoen aan het verzoek van de Faculteit der Wis- en Natuurkunde volgt hier een overzicht van mijn academische studie.

De basis voor deze studie was de opleiding aan de R.H.B.S. te Winterswijk, in het bijzonder de wiskundelessen van de heer T. Hoogeveen. Na het eindexamen B in 1941 te hebben afgelegd, bezocht ik gedurende 1½ jaar de Rijksuniversiteit te Utrecht teneinde chemie te studeren. In de daarop volgende onderduikperiode besteedde ik veel tijd aan wiskunde. Bij de hervatting van de universitaire studie in 1945 koos ik natuurkunde als hoofdvak en in juli 1947 legde ik het candidaatsexamen D af. Vanaf maart 1948 tot september 1950 vervulde ik de dienstplicht bij het wapen der Veldartillerie; de tweede helft van de diensttijd werd op Oost-Java doorgebracht.

Vervolgens experimenteerde ik in het Natuurkundig Laboratorium te Utrecht achtereenvolgens onder leiding van Dr. L. N. M. Duysens in de afdeling biofysika en van A. J. L. van Egmond in de afdeling elektronika. Daarna werkte ik aan een onderzoek van de fotoelektrische eigenschappen van CdS-kristallen. Voor het doctoraal examen, hoofdvak natuurkunde, afgelegd te Utrecht in 1954, volgde ik de colleges van o.a. Prof. Dr. P. M. Endt, Prof. Dr. S. R. de Groot, Prof. Dr. H. Freudenthal, Prof. Dr. J. M. Bijvoet en Prof. Dr. B. R. A. Nijboer.

In juli 1954 trad ik in dienst van de F.O.M. bij de werkgroep voor experimenten met gerichte atoomkernen, Kamerlingh Onnes Laboratorium, Leiden. Het werk, waarop deze dissertatie is gebaseerd, werd verricht onder de leiding van mijn promotor, Prof. Dr. C. J. Gorter en van Dr. M. J. Steenland.

Van groot belang voor het tot stand komen van dit proefschrift waren de theoretische bijdragen van Dr. H. A. Tolhoek, o.a. de suggesties voor de meting der circulaire polarisatie van gammastraling. De metingen, beschreven in hoofdstuk IV, werden uitgevoerd onder leiding van en in samenwerking met Prof. Dr. J. C. Wheatley, Universiteit van Illinois. Voorts zij vermeld de medewerking van Dr. A. N. Diddens, A. R. Miedema en Dr. J. C. Severiens. Voor het welslagen van voornoemde experimenten waren de medewerking en raadgevingen van de heren J. van Weesel, A. R. B. Gerritse en E. S. Prins onontbeerlijk.

In 1956 werkte ik mee aan metingen van lineaire polarisatie van gammastraling en in 1957 aan experimenten betreffende het niet-behoud van pariteit bij het beta-verval.

... ..

... ..

... ..

... ..

... ..

... ..

CHAPTER I.

INTRODUCTION AND SUMMARY.

§ 1. Methods for nuclear orientation.

Nuclear orientation means that different directions in space are not equally probable for the ensemble of nuclei under consideration and hence is meaningless for nuclei with zero spin, which many stable nuclei have. Ordering the nuclear spin system implies (under the condition of equilibrium) a decrease of entropy of the system, which in turn is connected with a decrease of temperature, hence nuclear orientation is generally carried out at low temperatures.

A simplified discussion of three methods for nuclear orientation will be given here, which are schematically indicated in fig. 1. For this discussion it will be assumed that the magnetic moment μ of the nucleus is positive, which means that \mathbf{I} , the nuclear spin, is parallel to μ .

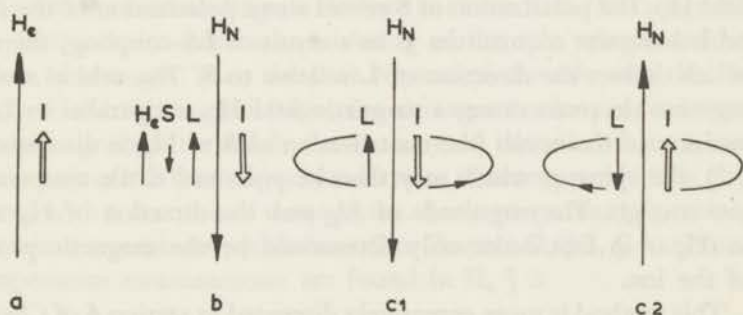


Fig. 1. a) Nuclear polarization in an external magnetic field H_e .
 b) Magnetic hyperfine structure polarization.
 c) Magnetic hyperfine structure alignment.

a) External field polarization (Gor 34, Kur 35).

An external magnetic field H_e is applied for polarization of μ (and \mathbf{I}). A considerable polarization will occur only if the interaction energy between μ and H is not small compared with the energy kT of thermal motions. Since $\mu \approx 10^{-23}$ ergs/Gauss and $k \approx 10^{-16}$ ergs/degree, values of $H/T \approx 10^7$ are required. Although magnetic fields of 10^4 Oe and temperatures of a few times 10^{-3} °K can be realized, combination of both large magnetic fields and very low temperatures is experimentally very difficult and has been achieved in only a few cases. In prin-

principle the method is applicable to all nuclei having non-zero μ .

- b) Magnetic hyperfine structure polarization (Gor 48 a, b, Ros 48). Atomic electrons may cause magnetic fields of the order of 10^5 — 10^6 Oe at the position of the nucleus, which occurs for many atoms with non-zero angular momentum. The interaction of these fields with μ gives rise to hyperfine structures in optical spectra. At the temperatures required (10^{-2} °K) free atoms very rarely occur, but paramagnetic ions may be used instead, because they also have non-zero angular momentum from unpaired electrons which interact with μ , as is evidenced from hyperfine structures in paramagnetic resonance spectra (Ble 53).

The orbital motion of unpaired electrons of paramagnetic ions in a solid is often modified to a considerable degree by the influence of crystalline electric fields, particularly for the iron group elements. Consequently, as will be discussed in Chapter II, § 2, the spin angular momentum \mathbf{S} will be mainly responsible for the magnetic moment \mathbf{M}_{ion} of the ion in a crystal. Since \mathbf{M}_{ion} is of the order 10^3 as large as μ , it is relatively easy to polarize \mathbf{M}_{ion} , hence \mathbf{S} , in a small external magnetic field \mathbf{H}_e . The polarization of \mathbf{S} causes also a polarization of the residual orbital angular momentum \mathbf{L} as a result of \mathbf{LS} -coupling, the sign of which defines the direction of \mathbf{L} relative to \mathbf{S} . The orbital motion of negative electrons causes a magnetic field \mathbf{H}_N antiparallel to \mathbf{L} at the position of the nuclei (the contribution of \mathbf{S} to \mathbf{H}_N is discussed in II, § 2), the spins of which may then be polarized if the temperature is low enough. The magnitude of H_N and the direction of \mathbf{H}_N relative to \mathbf{H}_e is in first order only determined by the magnetic properties of the ion.

This method is more extensively discussed in section 4 of Chapter II.

- c) Magnetic hyperfine structure alignment (Ble 51b). Crystalline electric fields often cause a strong anisotropy of the orbital motion of the unpaired electrons of a paramagnetic ion. For instance, this orbital motion may occur preferably in a plane perpendicular to one of the crystal axes. This preference can, even at room temperatures, be so pronounced that the orbital angular momentum \mathbf{L} is practically tied to that crystal axis. Since the interaction between the crystalline electric field and the circulating electrons will be independent of the sense of circulation, situation c1 and c2 of fig. 1 have equal energies and are therefore equally probable. It is seen that, if the temperature is decreased, the nuclear moments and spins will line up in the direction of \mathbf{L} , hence of the crystal axis, one half of the nuclear

spins being in opposite direction to the rest of the spins. This is called nuclear alignment, which is discussed in Chapter II, particularly in II.5.

It should be mentioned that the use of single crystals of paramagnetic salts is essential.

Ferromagnetic or antiferromagnetic substances might also be useful. For instance it has been shown that nuclear alignment can be achieved at low temperatures in a single crystal of Co-metal (Kur 55). However the preferred direction for L is in such cases not merely determined by the crystalline electric field since exchange forces play an important role.

§ 2. Low temperature technique.

Temperatures down to about 1° K can be obtained by the use of liquid helium under a reduced vapour pressure. For nuclear orientation appreciably lower temperatures are required and can be obtained by the technique of adiabatic demagnetization of paramagnetic salts (Kle 55, 56, Amb 55a). This process is carried out in two stages. In the first stage a large magnetic field is isothermally applied to the salt and the heat of magnetization is carried off to the surroundings, a He-bath at about 1° K. The magnetization of the electron spins implies an ordering of the spin system and hence a reduction of entropy. Then the heat contact of the salt with the He-bath is removed and the second stage, the demagnetization, is, consequently, an adiabatic process in which the entropy of the salt remains constant. The net result of the two stages is a decrease of entropy, which is generally connected with a decrease of temperature. Some properties of paramagnetic salts at low temperatures are discussed in Chapter II, § 3, § 4 and methods for temperature measurements are found in II, § 3.

§ 3. Anisotropy of radiations from oriented radioactive nuclei.

Nuclear orientation becomes particularly interesting if the oriented nuclei are radioactive. As the experimental procedure requires half lives of at least a few days, our discussion will be confined to nuclei decaying by α and β -emission. Since β -decay of unstable nuclei is often followed by gamma decay of the daughter nucleus, also gamma radiations from oriented nuclei may be studied.

All these radiations carry integral units (\hbar) of angular momentum, which may be connected with a change of spin I_i of the initial nucleus to the spin I_f of the final nucleus by integral units of \hbar . We will consider the simple case that unit angular momentum is carried off by α -particle, β -particle plus neutrino and photon respectively and that $I_i = 1$, $I_f = 0$.

This is pictured in fig. 2, where also Z , the nuclear charge, is indicated.

A system characterized by a wave function ψ having non-zero angular momentum, cannot be spherically symmetric in all respects. If the radiation, with wave function ψ , has non-zero orbital angular momentum \mathbf{L} (with respect to the nucleus as a center), then the probability density $\psi^*\psi$ will not be spherically symmetric about the nucleus. On a macroscopic scale, for a system

of polarized nuclei, the intensity \mathcal{W} of the radiation will generally show a (non-spherical) directional distribution, the orientation of the distribution in space being determined by the direction of \mathbf{L} , hence of \mathbf{I}_i .

Non-zero spin angular momentum of the radiation is connected with polarization, which will not be spherically symmetric either.

Anisotropy of the intensity of α -, β - and γ -radiation from oriented nuclei has been observed experimentally and the angular distributions are schematically shown in fig. 3.

There are, however, important differences among the three cases. α -particles have zero spin and the angular momentum of the particle is equal to \mathbf{L} , which defines the directional distribution \mathcal{W} , which, for the case of fig. 2, is proportional to $1 - \cos^2\theta$, θ being the angle between \mathbf{W} and \mathbf{I}_i (Bru 57).

It will be discussed in Chapter III, section 4, that spin 1 must be attributed to photons but that the intensity distribution of gamma radiation is nevertheless only determined by its total angular momentum. For the case of fig. 2 with $I_i = 1$ and $I_f = 0$ the radiation has necessarily an angular momentum of one unit \hbar and is then called dipole radiation, the angular

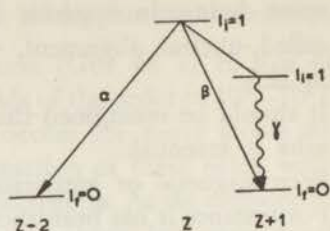


Fig. 2. α -, β^- and γ -decay drawn in one (fictitious) decay scheme. For all three radiations the initial state has spin $I_i = 1$ and the final state has spin $I_f = 0$.

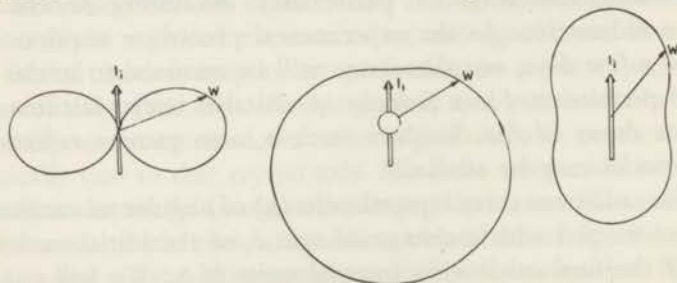


Fig. 3. Anisotropy of the intensity distribution \mathcal{W} for (from left to right) α -, β^- and γ -decay from $I_i = 1$ to $I_f = 0$.

distribution of which could also be obtained from 2 mutually perpendicular, oscillating, classical dipoles in a plane perpendicular to the nuclear spin \mathbf{I}_i . The directional distribution W is proportional to $W \propto 1 + \cos^2\vartheta$, where ϑ is the angle between \mathbf{W} and \mathbf{I}_i , and is pictured in fig. 3.

As will be seen from fig. 3 the directional distributions for both α - and γ -decay are symmetric with respect to reversal of the nuclear spin direction and consequently the distributions for polarized and aligned nuclear spins will be equal. This symmetry can be understood from the invariance under space reflection of the interactions which lead to α - and γ -decay, namely the combination of "strong" interactions between the nucleons and the Coulomb interaction for α -decay and the electromagnetic interaction for γ -decay. In a transition between initial and final nuclear states with a definite parity the emitted radiation must also be in a state of definite parity if the interaction is invariant under space reflection. Hence, for instance, for the wave function of an emitted α -particle either $\psi(\mathbf{r}) = \psi(-\mathbf{r})$ or $\psi(\mathbf{r}) = -\psi(-\mathbf{r})$ where \mathbf{r} is the radius vector to the nucleus. In either case however, $\psi^*(\mathbf{r})\psi(\mathbf{r}) = \psi^*(-\mathbf{r})\psi(-\mathbf{r})$, making $W(\mathbf{r}) = W(-\mathbf{r})$.

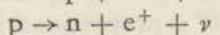
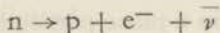
β -decay is more complicated since two particles with spin $\frac{1}{2}$ are emitted, namely an electron^{*}(e) and a neutrino (ν) or their anti-particles. For the simplest case of allowed β -decay both e and ν are emitted in states with total angular momentum $j = \frac{1}{2}$. Our discussion will be confined to the example of fig. 2, where $I_i - I_f = 1$, making $\mathbf{j}(e)$ and $\mathbf{j}(\nu)$ parallel to \mathbf{I}_i .

Until recently it was always assumed that parity is conserved in all processes with elementary particles, or alternatively, that the interactions between these particles are invariant under space reflection. In this case the state of the emitted electron + neutrino must have a definite parity and one can then show that for polarized nuclei an isotropic intensity distribution would be obtained.

YANG and LEE (Lee 56), however, conjectured in 1956 on the basis of certain facts on K-mesons that parity might not be conserved in the so called "weak interactions" to which β -decay belongs. If β -interaction is not invariant under space reflection, the β -particles will be emitted in a superposition of two $j = \frac{1}{2}$ states of opposite parity, which produces an asymmetric directional distribution of β -particles from polarized nuclei, as will be discussed hereafter. (Fel 57).

In case of parity non-conservation the general proposal for the β -interaction made by YANG and LEE contains, as a special case, a formalism with less arbitrary parameters: the two-component neutrino theory (Lee 57 b, Lan 57, Sal 57, Tou 57) with the aid of which a number of phenomena are more easily visualized. This theory is further simplified if conservation

of leptons is assumed, in which case the fundamental processes of β -emission are:



and where the neutrino ν and antineutrino $\bar{\nu}$ may be assumed to have their spin respectively parallel and antiparallel to their momentum. For the case of fig. 2 it is then seen that the antineutrino is emitted preferably with spin parallel to \mathbf{I}_i , hence with momentum antiparallel to \mathbf{I}_i .

Now, assuming the β -interaction to be a tensor interaction, the $(e, \bar{\nu})$ angular correlation law for this interaction says, that the momenta of e^- and $\bar{\nu}$ are preferably parallel. Consequently the electron is then emitted preferably antiparallel to \mathbf{I}_i as was recently observed (Wu 57).

The same reasoning leads to β^+ -emission with a preference in the direction of \mathbf{I}_i (again in case $I_f = I_i - 1$) as the spin-momentum relation for the emitted ν is opposite to that for $\bar{\nu}$, while the (e, ν) angular correlation law is the same for e^+ and e^- . This was also shown experimentally (Amb 57, Pos 57 a, b). The intensity distribution W for β^- -emission is proportional to $(1 - a \cos \vartheta)$ where ϑ is the angle between \mathbf{W} and \mathbf{I}_i and a is approximately v/c , v being the velocity of the electron.

It is discussed in Chapter III, § 1, 3, how the anisotropy of the intensity of gamma radiations depends on temperature according to theory. One of the parameters involved is the magnitude of the nuclear magnetic moment μ and from the experimentally observed magnitude of the anisotropy as a function of temperature one can in principle deduce the value of μ . In § 4 of Chapter V it is found that the most probable value of μ for ^{52}Mn is 2.8 n.m. From the discussion in that section it will become clear that a high accuracy for μ could not be obtained, which is due to insufficient knowledge about the magnitude of H_N .

§ 4. Polarization of radiations from oriented nuclei.

For the particular case of β^- -decay considered in the preceding section it will be clear that for electrons, emitted in directions parallel and perpendicular to the nuclear spin, the electron spin will be respectively parallel and perpendicular to the direction of propagation, which is called longitudinal and transverse polarization respectively (Tol 56). In order to observe longitudinal polarization of electrons, it is not necessary to use polarized nuclei, since also for randomly oriented nuclear spins longitudinal polarization of the emitted β -particles can be observed (Waa 57, Fra 57). This is connected with the fact that, for instance in the case of fig. 2, the spin of the electron is preferably parallel to \mathbf{I} , whereas the direction of emission is preferably antiparallel to \mathbf{I} , which gives a correlation between spin and direction of

propagation of the electron. Transverse polarization of the electrons will only occur, however, for polarized nuclear spins.

The situation for photon polarization is somewhat different. Photons emitted in directions parallel and antiparallel to the nuclear spin will have their spins pointing respectively in and opposite to the direction of propagation. In the former case we will, according to the optical convention, speak of left circularly polarized (l.c.p.) radiation and in the latter case of right circularly polarized (r.c.p.) radiation. Conversely, if the sense of polarization can be determined, the direction of the nuclear spin will be known.

In Chapter III, § 6, some aspects of such a method will be discussed. It will be seen there that circular polarization can be detected by means of Compton scattering at magnetized iron, in which the electron spins are (partially) polarized. The intensity of the scattered radiation depends strongly on the relative directions of the electron spin and photon spin. If the direction of the electron spin is reversed, one obtains the direction of the photon spin, hence of the nuclear spin, from the change of the scattered intensity. Since the direction of the nuclear spin \mathbf{I} relative to the polarizing magnetic field \mathbf{H}_e is determined by the sign of the magnetic moment μ , such experiments can establish the sign of μ for radioactive nuclei. In Chapters IV and V experiments are described from which it could be concluded that the signs of the nuclear magnetic moments of ^{60}Co and ^{52}Mn are positive.

An experimental determination of the relative directions of \mathbf{I} and \mathbf{H}_e is also of interest for experiments on the asymmetry of β -emission from polarized nuclei. Conversely, if all data concerning β -decay are known, the sign of μ may be determined from the observed asymmetry.

In contrast to the case for electrons, the photon spin can be only parallel or antiparallel to the direction of propagation. Nevertheless, photons emitted in directions perpendicular to the nuclear spin are polarized, namely linearly polarized. The state of linear polarization is related to the parity of the emitted radiation, which is even or odd for $\mathbf{H}(\mathbf{r}) = \mathbf{H}(-\mathbf{r})$ and $\mathbf{H}(\mathbf{r}) = -\mathbf{H}(-\mathbf{r})$ respectively, where \mathbf{H} is the magnetic vector, which is perpendicular to the electric vector and to the direction of propagation for r much larger than the nuclear radius. In fig. 2 where $I_i = 1$, $I_f = 0$, the photons which are emitted in directions perpendicular to the nuclear spin \mathbf{I}_i will be polarized with the electric vector in the direction of I_i for even parity and perpendicular to \mathbf{I}_i for odd parity of the radiation. Since parity is conserved for electromagnetic interactions, the difference in parity between the initial and final state of the nucleus can be determined from the direction of polarization. In chapter V it is discussed that the radiations of ^{52}Mn possess even parities.

CHAPTER II

ORIENTATION OF NUCLEAR SPINS.

§ 1. General remarks.

Various methods for nuclear orientation have been proposed and a review may be found in (Ste 57). Nearly all these methods are based upon the electromagnetic interaction of the nucleus with its environment. However, "strong" interactions and in principle even "weak" interactions can also be used for obtaining nuclear polarization. Polarized radioactive nuclei can be obtained, for instance, by absorption of polarized thermal neutrons by randomly oriented nuclei (Tru 56). Similarly, a small number of almost completely polarized, radioactive nuclei might be obtained by absorption of a beam of neutrinos or polarized electrons (i.e. inverse β -decay) by randomly oriented stable nuclei, thereby making use of parity non-conservation in weak interactions.

The electromagnetic interaction consists, for all practical purposes, of two terms: 1) the interaction between the nuclear magnetic moment and a magnetic field. If such a field is due to atomic electrons, this will hereafter be called the magnetic h.f.s. interaction, 2) the interaction of the nuclear electric quadrupole moment with inhomogeneous electric fields, which can be caused, for instance, by neighbouring ions in crystals.

The orientation methods may be divided into static and dynamic methods. In the static methods the temperature is lowered in order to cause considerable differences in (Boltzmann-) population between the various levels, belonging to different values of I_z , the z-component of the nuclear spin. In the dynamic methods, such differences are induced by transitions between the various levels, for instance by means of magnetic resonance (Jef 57). We will not go into further details, since they can be found elsewhere (Ste 57), but it may be mentioned that for a number of dynamic methods it has become customary to speak of nuclear polarization in case the differences between the populations of the various levels are considerably enhanced, for instance if $\langle I_z \rangle / I$ has been multiplied by a factor of 100 from its room temperature value (of the order 10^{-5}) by means of electronic paramagnetic resonance (Car 56). This has important consequences if one wants to apply nuclear resonance, but for a practical nuclear physical experiment one requires values of $\langle I_z \rangle / I$ of about 0.1 or larger. In order to achieve this by dynamic methods, so far available,

one has to start with temperatures in the liquid helium range. JEFFRIES *et al.* (Abr 57) and PIPKIN *et al.* (Pip 57) have, by using paramagnetic resonance, successfully achieved nuclear polarization which could be observed by measurements of an anisotropy of the gamma ray intensity.

We will discuss two static methods in more detail, namely the methods of magnetic h.f.s. polarization (§ 4) and of magnetic h.f.s. alignment (§ 5).

§ 2. Crystal fields and hyperfine structures.

2.A. Introduction.

The coupling between a nuclear magnetic moment and its surrounding electrons give rise, as is well known, to hyperfine structures in optical and paramagnetic resonance spectra. The h.f.s. interaction in free atoms or ions, first suggested by PAULI (Pau 24), is mainly due to unpaired s-electrons and consequently, is a coupling between electron spin and nuclear spin. Even when in the ground state no unpaired s-electrons are present, in many cases the observed h.f.s. splitting of this state has to be ascribed to configurational mixing with a higher state, possessing an unpaired s-electron. As has been shown by ABRAGAM *et al.* (Abr 55), the degree of configurational mixing required is about ten times larger than what one expects on basis of a calculation from first principles.

Paramagnetic ions in crystals have no unpaired s-electrons, but will have unpaired 3d and 4f electrons for the iron group and rare earth elements respectively. As will be seen below, ABRAGAM and PRYCE assumed that configurational mixing of states with unpaired s-electrons also occurs in paramagnetic ions to roughly the same degree as in free atoms and they were able to explain the magnitude of h.f.s. splittings for a number of ions rather well (Abr 51a).

A modification of the h.f.s. coupling is due to the fact that especially the 3d-electrons of ions from the iron group elements, when incorporated in a crystal, will feel a strong inhomogeneous electric field from neighbouring ions and this will result in "quenching" the orbital motion (see section 2.B.). Since the h.f.s. splitting for most of the 3d ions must be attributed mainly to the orbital motion of the 3d electrons, as will be shown for one particular example in § 2.B., quenching of the orbital motion will generally lead to a reduction of the h.f.s. splitting.

The quenching of orbital angular momentum and the absence of unpaired s-electrons in paramagnetic ions will make the h.f.s. splittings of these ions smaller than those of, for instance, alkali atoms or singly ionized atoms of the 3d iron group elements. For Cu in the state $3d^94s^2$ the total

h.f.s. splitting $\approx 0.5 \text{ cm}^{-1}$, in the state $3d^{10}4s$ even $\approx 0.8 \text{ cm}^{-1}$, whereas the overall h.f.s. splittings in Cu-salts do not exceed 0.2 cm^{-1} .

More quantitatively, the h.f.s. interaction energy E is deduced from FERMI's formula (Fer 30):

$$E = 2\beta\mu \sum_{\mathbf{k}} \left[\left\{ \frac{\mathbf{l}_{\mathbf{k}} \cdot \mathbf{I}}{r_{\mathbf{k}}^3} \right\} - \left\{ \frac{\mathbf{s}_{\mathbf{k}} \cdot \mathbf{I}}{r_{\mathbf{k}}^3} - \frac{(\mathbf{r}_{\mathbf{k}} \cdot \mathbf{s}_{\mathbf{k}})(\mathbf{r}_{\mathbf{k}} \cdot \mathbf{I})}{r_{\mathbf{k}}^5} \right\} \right] \quad (1)$$

in which β and μ are the Bohr magneton and nuclear magnetic moment respectively; $\mathbf{l}_{\mathbf{k}}$ and $\mathbf{s}_{\mathbf{k}}$ are the orbital and spin angular momentum of the electron \mathbf{k} ; $\mathbf{r}_{\mathbf{k}}$ is the radius vector from the nucleus to the electron \mathbf{k} ; and \mathbf{I} is the nuclear spin. The first term represents the interaction between μ and a magnetic field due to orbital motion of the electron, the second term is the classical expression for two interacting magnetic dipoles: the intrinsic magnetic moment of the electron and the nuclear magnetic moment. For free ions with unpaired d or f electrons, the second term is considerably smaller than the first term. It was shown (Abr 51a) how the $\mathbf{r}_{\mathbf{k}}$ can be expressed in \mathbf{L} , the total orbital angular momentum of the electrons and how this can be worked out for paramagnetic ions in crystalline electric fields of various symmetries.

2.B. Discussion of the Cu^{++} ion.

The modification of the electronic wave functions of a paramagnetic ion under the influence of a crystalline inhomogeneous electric field, has been discussed by many authors. (Vle 32, Ble 53, Bow 55). For instance BETHE (Bet 29) has shown, by means of group theoretical methods, how the orbital and spin degeneracy of the ground state of free ions will be partly or completely removed by fields of various symmetries.

We will consider a particular example, which is a somewhat simplified discussion of the consequences of the crystal field interacting with the Cu^{++} -ion (Pol 42). This ion has a ground state ${}^2D_{5/2}$, which means $L = 2$, $S = 1/2$ and a negative spin-orbit coupling constant λ , so that $\lambda \mathbf{L} \cdot \mathbf{S}$ has the lowest energy for $J = L + S = 5/2$.

For ions in the iron group and for a large number of salts, the crystal field has predominantly cubic symmetry. This is due in many cases to an octahedron of water molecules, surrounding the magnetic ion. For iron group ions, the magnitude of the crystalline electric potential V is much larger than the spin-orbit coupling energy; consequently one has to begin the perturbation calculation from the state 2D with V as the main perturbing potential and $\lambda \mathbf{L} \cdot \mathbf{S}$ as a secondary interaction. For the orbitally 5-fold degenerate ground state, one might take as wave functions the eigenfunctions of the (L, L_z) operators i.e. $Y_{LM} f'(\mathbf{r})$ where

$f'(r)$ is the radial dependent part of the wave functions. It is, however, more convenient to take the following linear combinations of $Y_{LM}f'(r)$:

$$\begin{aligned}
 \psi_{-2} &= \sqrt{15} xy f(r) \\
 \psi_1 &= \sqrt{15} xz f(r) \\
 \psi_{-1} &= \sqrt{15} yz f(r) \\
 \psi_2 &= \frac{1}{2} \sqrt{15} (x^2 - y^2) f(r) \\
 \psi_0 &= \frac{1}{2} \sqrt{5} (3z^2/r^2 - 1) f'(r) = \frac{1}{2} \sqrt{5} (2z^2 - x^2 - y^2) f(r) \\
 f(r) &= f'(r)/r^2.
 \end{aligned}
 \tag{2}$$

These wave functions are linearly independent and normalized; they are plotted in fig. 4. One easily verifies that $\psi_2 \pm i\psi_{-2}$, $\psi_1 \pm i\psi_{-1}$ and ψ_0 are eigenfunctions of L_z with eigenvalues ± 2 , $\pm 1, 0$ respectively. In order to account for the twofold degeneracy due to the electron spin $S = 1/2$, the ψ 's should be multiplied by the eigenfunctions of S^2 , S_z , called $|\xi\rangle$ and $|\eta\rangle$ ($S_z|\xi\rangle = \frac{1}{2}|\xi\rangle$ and $S_z|\eta\rangle = -\frac{1}{2}|\eta\rangle$).

Then we have a complete set of eigenfunctions for the 10-fold degenerate ground state 2D . Because the electrostatic field interacts only with the orbits and not with the spins of the electrons, we will omit ξ and η in the first part of the discussion.

It may be assumed that the cubic crystalline field is caused by the negative charges of the H_2O -dipoles surrounding the positive Cu ion. If the body diagonals of the octahedron of water molecules are chosen as coordinate

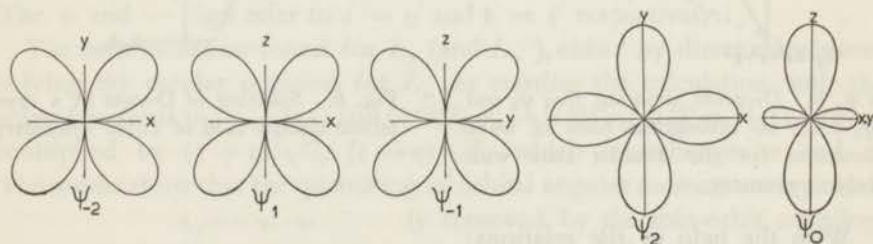


Fig. 4. Angular dependence of d-orbital wave functions ψ which are eigenfunctions of a crystalline electric field potential with cubic symmetry. The angular dependent part of ψ_M is a linear combination of spherical harmonics $Y_{L=2}^M$ and $Y_{L=2}^{-M}$. x , y and z are the axis of the cubic field, the z -axis being also the axis of quantization.

system, the negative charges are located on the x , y and z axes. The wave functions ψ refer to a hole in the 3d shell of the Cu ion ($3d^9$) and consequently $\psi^*\psi$ represents a positive charge cloud. It will be seen from fig. 4 that the electrostatic energy of the states ψ_0 and ψ_2 is lower than the energy of the states ψ_{-2} , ψ_1 and ψ_{-1} , which for reasons of symmetry, have equal

energies. Also the states ψ_0 and ψ_2 have equal energies, as can be explained with the help of fig. 5. ψ_0 and ψ_2 are apparently linear, mutually orthogonal combinations of the functions $x^2 - y^2$, $z^2 - x^2$ and $y^2 - z^2$, which are symmetric with respect to the x , y , z axes. Alternatively one might have chosen another linear combination of ψ_0 and ψ_2 as a basis of orthogonal wave functions, for instance

$$\frac{\sqrt{3}}{2} \psi_2 - \frac{1}{2} \psi_0 = \frac{\sqrt{5}}{2} (2x^2 - y^2 - z^2) \quad \frac{1}{2} \psi_2 + \frac{\sqrt{3}}{2} \psi_0 = \frac{\sqrt{15}}{2} (z^2 - y^2)$$

and these can also be obtained from ψ_0 and ψ_2 by exchange of z and x . Therefore ψ_2 and ψ_0 form an arbitrary basis of wave functions for a state, which has essentially cubic symmetry; this will be used later in the discussion.

The splitting of the 2D state by the cubic field has been indicated in fig. 6.

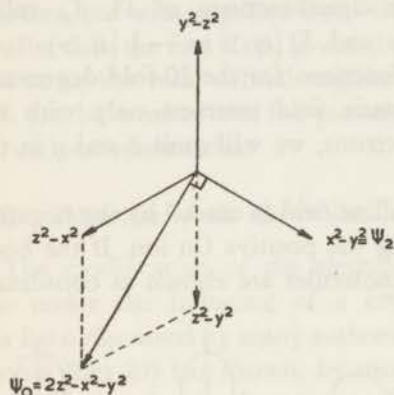


Fig. 5. Diagram showing that ψ_0 and ψ_2 form an orthogonal basis of wave functions for the doublet state with cubic symmetry.

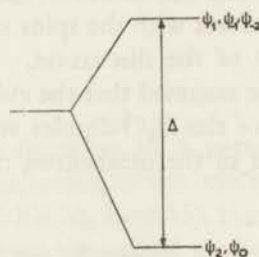


Fig. 6. Splitting of D-state in a crystalline electric field of cubic symmetry.

With the help of the relations:

$$L_z \psi_0 = 0; \quad L_z \psi_{\pm 1} = \mp \frac{\hbar}{i} \psi_{\mp 1}; \quad L_z \psi_{\pm 2} = \mp \frac{2\hbar}{i} \psi_{\mp 2} \quad (3)$$

one easily checks, that $\langle \psi_i^* | L_z | \psi_i \rangle = 0$ for all i . And because of cubic symmetry, also one finds: $\langle \psi_i | L_x | \psi_i \rangle = \langle \psi_i | L_y | \psi_i \rangle = 0$. This is called quenching of the orbital angular momentum by the (cubic) crystalline electric field: the expectation values of L_x , L_y , L_z are zero for all states. If there were no electronic spin, the upper triplet state and the lower doublet would be non-magnetic, because the Zeeman-energy splitting in a magnetic field is determined by:

$$(e\hbar/2mc) H \langle \psi_i | L_z + 2S_z | \psi_i \rangle = \beta H \langle \psi_i | L_z | \psi_i \rangle = 0.$$

For $S = 1/2$ both triplet and doublet would split in two Zeeman levels: the magnetism is caused by the electron spin only.

Now we have, however, not yet taken into account the spin-orbit coupling: $\lambda \mathbf{L} \cdot \mathbf{S} = \lambda(L_x S_x + L_y S_y + L_z S_z)$.

The diagonal elements of $\lambda \mathbf{L} \cdot \mathbf{S}$ in the ψ -representation are zero: there is no first order energy shift in the doublet and triplet due to $\mathbf{L} \cdot \mathbf{S}$ -coupling. There is, however, in first order, a mixing of the wave functions ψ , given by the non-diagonal matrix elements, according to

$$|\psi'_i \epsilon'_i\rangle = |\psi_i \epsilon_i\rangle + \sum_k \frac{\langle \psi_k \epsilon_k | \lambda \mathbf{L} \cdot \mathbf{S} | \psi_i \epsilon_i \rangle}{E_i - E_k} |\psi_k \epsilon_k\rangle \quad (4)$$

$$|\psi'_0 \xi'\rangle = |\psi_0 \xi\rangle - \frac{\lambda \sqrt{3}}{2i\Delta} |\psi_{-1} - i\psi_1, \eta\rangle$$

$$|\psi'_0 \eta'\rangle = |\psi_0 \eta\rangle - \frac{\lambda \sqrt{3}}{2i\Delta} |\psi_{-1} + i\psi_1, \xi\rangle \quad (5)$$

$$|\psi'_2 \xi'\rangle = |\psi_2 \xi\rangle + \frac{\lambda}{i\Delta} |\psi_{-2} \xi\rangle - \frac{\lambda}{2i\Delta} |\psi_{-1} + i\psi_1, \eta\rangle$$

$$|\psi'_2 \eta'\rangle = |\psi_2 \eta\rangle - \frac{\lambda}{i\Delta} |\psi_{-2} \eta\rangle - \frac{\lambda}{2i\Delta} |\psi_{-1} - i\psi_1, \xi\rangle$$

where Δ is the energy difference between the doublet and the triplet. As a result of this first order perturbation, the expectation values of L_x , L_y and L_z are no longer zero:

$$\langle \psi'_2 \epsilon' | L_z | \psi'_2 \epsilon' \rangle \approx \pm 4\lambda \hbar / \Delta \quad \langle \psi'_0 \epsilon' | L_z | \psi'_0 \epsilon' \rangle \approx 0.$$

The + and - sign refer to $\epsilon' = \eta'$ and $\epsilon' = \xi'$ respectively.

The same values are found for L_x (and L_y), either by direct calculation, solving the secular equation for L_x , or starting the calculation with the wave functions $\psi_1, \psi_{-1}, \psi_{-2}$ and $(\sqrt{3}/2)\psi_2 - (1/2)\psi_0, (1/2)\psi_2 + (\sqrt{3}/2)\psi_0$ multiplied by $(\xi + \eta)/\sqrt{2}, (\xi - \eta)/\sqrt{2}$, which interchanges z and x . The results show that the quenching of orbital angular momentum is partially removed by the spin-orbit coupling.

In general crystals will not have perfect cubic symmetry, but, according to JAHN and TELLER (Jah 37), tend to distort in such a way as to remove the degeneracy in the energy levels. Let us assume, for instance, that the deviation from cubic symmetry can be considered as a tetragonal distortion round the z -axis, caused by a compression of the octahedron in the z -direction which brings the negative charges on the z -axis closer to the

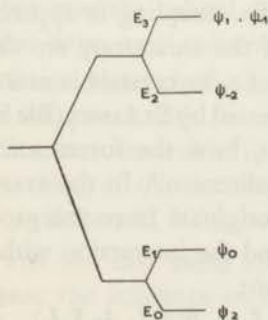


Fig. 7. Splitting of D-state in a cubic crystal field with tetragonal distortion.

paramagnetic ion. The energies of the states $\psi_2 (\propto x^2 - y^2)$ and $\psi_{-2} (\propto xy)$ are lowered with respect to the states $\psi_0 (\propto 2z^2 - x^2 - y^2)$ and ψ_1, ψ_{-1} respectively. In fig. 7 the effect of the tetragonal field is indicated. The states ψ_1 and ψ_{-1} have still equal energies and a crystalline field distortion of lower than tetragonal symmetry may remove also this degeneracy, leaving only the twofold spin degeneracy. According to a theorem of Kramers this spin degeneracy cannot be removed by crystalline electric fields. We will not discuss further these questions, but we will only consider the ground state ψ_2 which has a twofold spin degeneracy. After introduction of the $\lambda \mathbf{L} \cdot \mathbf{S}$ coupling, we find again the formula (5) for the perturbed wave functions of the ground state ψ_2 , except for different E 's (E_1 is defined in fig. 7). The expectation values for L_z are:

$$\begin{aligned} \langle \psi'_2 \xi' | L_z | \psi'_2 \xi' \rangle &= -\langle \psi'_2 \eta' | L_z | \psi'_2 \eta' \rangle = -4\lambda\hbar/(E_2 - E_0) \\ \langle \psi'_2 \varepsilon' | L_x | \psi'_2 \varepsilon' \rangle &= \langle \psi'_2 \varepsilon' | L_y | \psi'_2 \varepsilon' \rangle = \mp \lambda\hbar/(E_3 - E_0). \end{aligned} \quad (6)$$

where $\varepsilon' = (\xi' \pm \eta')/\sqrt{2}$ or $\varepsilon' = (\xi' \pm i\eta')/\sqrt{2}$, which gives a representation in which L_x, S_x (and respectively L_y, S_y) are diagonal. Clearly the expectation value for L_z is different from that of L_x and L_y . This has two important consequences:

1) If a magnetic field \mathbf{H} is applied, the Zeeman splitting which is given by

$$\beta \mathbf{H} \langle \psi'_2 \xi' | \mathbf{L} + 2\mathbf{S} | \psi'_2 \xi' \rangle - \beta \mathbf{H} \langle \psi'_2 \eta' | \mathbf{L} + 2\mathbf{S} | \psi'_2 \eta' \rangle$$

(where \mathbf{L} and \mathbf{S} are in the direction of \mathbf{H}) will be different, if \mathbf{H} is in the z -direction compared with \mathbf{H} in the x or y directions. This is expressed by the anisotropic g -factor:

$$g_z = 2 [1 - 4\lambda/(E_2 - E_0)], \quad g_x = g_y = 2 [1 - \lambda(E_3 - E_0)].$$

For Cu, with $\lambda = -850 \text{ cm}^{-1}$, $E_3 - E_0 \approx E_2 - E_0 \approx 17000 \text{ cm}^{-1}$, $g_z \approx 2.4$, $g_x \approx g_y \approx 2.1$.

2) The magnetic fields at the position of the nucleus, no longer have cubic symmetry, but will be stronger in the direction of the tetragonal crystal axis than in any other direction: the h.f.s. coupling is apparently anisotropic and the direction and magnitude of the anisotropy are determined by the crystal field. The anisotropy of h.f.s. in crystals is essential for the h.f.s. alignment of nuclear spins, first suggested by BLEANEY (Ble 51b).

ABRAGAM and PRYCE (Abr 51a) have shown, how the forementioned state of affairs can be expressed by a "spin-Hamiltonian". In the example given above, the energies of the levels which originate from the ground state under the influence of the magnetic field and the interaction with the nucleus, may be calculated from the Hamiltonian:

$$H = g_{\perp} \beta (H_x S_x + H_y S_y) + g_{\parallel} \beta H_z S_z + A S_z I_z + B (S_x I_x + S_y I_y) \quad (7)$$

S is called the "fictitious" spin and has the properties of a spin operator. The anisotropy of g and the h.f.s. coupling constant is expressed by

$g_{\perp} \neq g_{\parallel}$ ($g_x = g_y = g_{\perp}$, $g_z = g_{\parallel}$) and $A \neq B$.

For our case $S = 1/2$; this implies that the ground state ψ_2 which has twofold spin-degeneracy, is split by a magnetic field H into two Zeeman-levels, separated by the energy difference $g_{\parallel}\beta H$ (for $H = H_z$).

2.C. Other ions.

2.C. I. For other paramagnetic ions the calculations are similar and lead to spin-Hamiltonians, which contain the expression (7) though some additional terms may be required in more complicated examples. Some of the complications encountered are:

1) The ground state of the ion in a cubic field with a trigonal or tetragonal distortion may have higher than twofold degeneracy. Higher order perturbations or crystal fields having lower symmetry (rhombic for instance) will lift the degeneracy and result in comparatively small splittings of the energy levels. This can be described by introduction of terms like $D S_z^2$, as for instance in the case of Mn^{++} (with $S = 5/2$) where D is of the order $D = 0.01 \text{ cm}^{-1}$, or for Ni^{++} (with $S = 1$) and D ranging from 0.1 cm^{-1} to a few cm^{-1} in various salts.

In case of rhombic symmetry an additional term $E(S_x^2 - S_y^2)$ may be required. Moreover then the g -values and the h.f.s. splittings are also no longer equal in x and y directions, although the differences between g_x and g_y and also between A_x and A_y (in $A_x I_x S_x + A_y I_y S_y + A_z I_z S_z$) are generally small.

2) The crystal field splitting may be smaller than in the case of Cu (see also § 4). In Co^{++} the energy splitting of the tetragonal or trigonal field, superposed on the cubic field splitting, is of roughly the same magnitude as the L - S -coupling energy. The L - S -coupling can then no longer be considered as a small perturbation and calculations are more complicated. In that case the orbital angular momentum may not be nearly quenched so that large, very anisotropic g -values and h.f.s. splittings can occur.

3) Excited states in the free ion may have energies not far from the ground state compared with the magnitude of the cubic field potential. In Co^{++} for instance the cubic field apparently mixes the ground state 4F with about 25% of the next higher state 4P and this has a profound effect on the g -values and h.f.s. constants.

4) For the rare earth ions a somewhat different treatment is required, because the influence of the crystal field on the $4f$ -electrons is screened off by the $5s$ and $5p$ electrons and the effective field potential is smaller than the L - S -coupling energy. This has two important consequences:

a) The orbital angular momentum is quenched to only a small degree.

As a result the g -values may be appreciably different from the "spin-only" value $g = 2$; the h.f.s. splittings are often larger than for the iron-group ions. b) $J(\mathbf{J} = \mathbf{L} + \mathbf{S})$ remains a "good" quantum number and the influence of the crystal field can be calculated using a (J, J_z) representation for the wave functions.

The crystal field for the trivalent ions of the rare earth group may not have predominantly cubic symmetry, for instance, in the ethylsulfates the rare earth ion is surrounded by triangles of water molecules, giving trigonal symmetry to the crystalline field, which may then be considered, in a first approximation, to have axial symmetry. A crystal field potential V with axial symmetry is invariant for rotations about the z -axis and consequently, commutes with L_z . Because V is a scalar potential, it also commutes with S_z and therefore with $J_z = L_z + S_z$, so that V is diagonal in the (J, J_z) -representation. Because V has also reflection symmetry with respect to the xy -plane, the ground state is split into a number of doublets with $J_z = \pm J, J_z = \pm(J - 1)$ etc. A real crystal field cannot have axial symmetry and trigonal or tetragonal components of V will admix wave functions of different L_z and consequently of J_z . Because then the lowest doublet cannot be rigorously characterized by one pair $\pm J_z$, the spin-Hamiltonian is again written with the aid of the fictitious spin $S = 1/2$, but very anisotropic g -values.

5) The interaction of the electronic orbital motion with a nuclear electric quadrupole moment may give rise to appreciable h.f.s. splittings. These interactions are ignored in the following because they are small for the iron group and rare earth group ions compared with the magnetic h.f.s. interaction.

6) The direct interaction of the nuclear magnetic moment with an external magnetic field is neglected, because the magnitude of the interaction is small compared to the h.f.s. interaction.

2.C. II. Mn^{++} . Configuration $3d^5, {}^6S$.

The five $3d$ electrons fill one half of the $3d$ shell and according to HUNDS rule, give an S state for the free ion. Because there is no total orbital angular momentum, in first order approximation no effects of the crystalline field on the magnetic properties of the free ion are to be expected.

The ground state has $S = 5/2$ and has six fold spin-degeneracy, which will be removed by a magnetic field and since only the spins contribute to the magnetic moment of the ion, the g -value should be 2 and isotropic. These predictions are verified by susceptibility measurements.

It has been shown (Vle 34, Coe 49, Ble 51c) that a small fine structure splitting of the electronic levels exists. Pryce (Pry 50) has suggested that in second order approximation the influence of a tetragonal or trigonal crystal field on the strong spin-spin interaction gives rise to such a splitting. In simple terms, this can be understood from an elongation (or contraction) of the spherical electron density in the direction of the tetragonal axis, because then the interaction energy between the magnetic moments of the 3d electrons depends on the direction of the spins relative to the crystal axis and for $S_z = 5/2$ may be different from the case $S_z = 1/2$. Phenomenologically, results can be described by adding to the spin-Hamiltonian a term DS_z^2 , where D is of the order of 10^{-2} cm^{-1} in most salts.

A high order effect of the cubic field has to be included in the Hamiltonian by means of the additional term:

$$a(S_\xi^4 + S_\eta^4 + S_\zeta^4) \quad (8)$$

ξ , η and ζ are the cubic axes. In case of a cubic field distortion having trigonal symmetry, as is the case for Ce-Mg-nitrate, the z-axis is the (1.1.1) direction with respect to the (ξ , η , ζ) coordinate system. For Mn^{++} in Bi-Mg-nitrate $a \approx 10^{-3} \text{ cm}^{-1}$ and gives a small correction to the DS_z^2 term. The g -values and h.f.s. splittings are not affected by the a -term to any appreciable extent.

The h.f.s. splitting is according to (Abr 51a), exclusively due to configurational coupling of the ground state with higher states with unpaired s-electrons and is therefore practically unconnected with orbital electronic motion. The h.f.s. splitting is expected to be isotropic and independent of the particular crystalline surrounding. This indeed is experimentally found: in all ionic salts $A = B \approx 0.009 \text{ cm}^{-1}$ (for ^{55}Mn with $I = 5/2$).

2.C. III. Co^{++} -ion. Configuration $3d^7$, 4F .

The ground state of the free ion is, according to Hund's rule, $^4F_{9/2}$. The cubic crystal field splits the 4F state in 2 triplet states and 1 singlet, the lowest state being an (orbital) triplet. About 25% of the 4P state of the free ion is admixed to this lower triplet by the cubic field. Taking the spin angular momentum $S = 3/2$ into account, the lowest level has a twelvefold degeneracy. The L-S coupling combined with the influence of a tetragonal or trigonal field causes a splitting of the level into 6 Kramers doublets, of which we will further consider only the lowest one. This doublet may be characterized by a fictitious spin $S' = 1/2$ and is split in a magnetic field in two states $S'_z = 1/2$ and $S'_z = -1/2$. $S'_z = 1/2$ is a mixture of states with $S_z = 3/2$, $S_z = 1/2$ and $S_z = -1/2$, whereas $S'_z = -1/2$ is a mixture of $S_z = -3/2$, $S_z = -1/2$, $S_z = 1/2$. This shows

that the overall Zeemansplitting has to be smaller than could be expected for a free spin $S = 3/2$ (in case of no $L \cdot S$ -coupling and completely quenched orbital angular momentum). Since, however, g -values even larger than 6 occur, it will be seen, that the orbital angular momentum contributes appreciably to the g -value. In the ammonium Tutton salt $g_{||} = 6.45$ and $g_{\perp} = 3.06$. Semi-empirically it has been found, that the approximate contribution from the orbital angular momentum is $g_{||}^L = 1.8$ and $g_{\perp}^L = 0.55$, whereas the contribution from the electron spins is roughly $g_{||}^S = 4.7$ and $g_{\perp}^S = 2.5$ (Abr. 51b).

In Mg-Bi-nitrate there are two crystallographically different positions for the divalent Co^{++} -ion, one has $g_{||} = 7.29$, $g_{\perp} = 2.34$, the other $g_{||} = 4.11$ and $g_{\perp} = 4.39$.

These facts have to be taken into account in the discussion of the h.f.s. of the Co-ion. Using the nomenclature of ABRAGAM and PRYCE the h.f.s. coupling constant A in $A I_z S_z + B(I_x S_x + I_y S_y)$ may be separated as follows:

$A = A_L + A_{Sd} + A_{Ss}$ and analogous for B ;

A_L is the h.f.s. interaction due to orbital electron moments;

A_{Sd} is the h.f.s. interaction due to the electron spins of the 3d-electrons and A_{Ss} is a term, which accounts for the effect of unpaired 4s-electrons on the nucleus.

Writing for $(2\beta\mu/I)\overline{(1/r^3)} \equiv P$, it is found that in order to get agreement with experimentally observed h.f.s. splittings in ^{59}Co , $P = 0.0225 \pm 0.005$ cm^{-1} .

For the Tutton salts the calculated values are

$A_L = P g_{||}^L = 1.78 P$ $A_{Sd} = 0.08 P$ $A_{Ss} = (\kappa/2) P g_{||}^S = -0.76 P$
 $B_L = P g_{\perp}^L = 0.56 P$ $B_{Sd} = -0.06 P$ $B_{Ss} = (\kappa/2) P g_{\perp}^S = -0.41 P$
 (κ is related to the expectation value of spin angular momentum of unpaired s-electrons at the position of the nucleus).

If these values are added, one finds:

$A = 0.0248 \text{ cm}^{-1}$ } which may be compared with { $A = 0.0245 \text{ cm}^{-1}$
 $B = 0.0021 \text{ cm}^{-1}$ } the experimental values: { $B = 0.0020 \text{ cm}^{-1}$

It should be mentioned that the A_{Sd} and B_{Sd} terms are small compared with A_L and B_L ; A_{Sd} and B_{Sd} are relatively still smaller for the Co^{++} -ion in a cubic field with some trigonal instead of a tetragonal distortion, like it is encountered in the fluosilicate and Ce-Mg-nitrate.

It may be noted that A_{Sd} and B_{Sd} are not equal to $P g_{||}^S$ and $P g_{\perp}^S$ respectively; this is one reason why, unlike the h.f.s. splittings for many rare earth ions, A/B is not equal to $g_{||}/g_{\perp}$ (Ell 53a). The main reason for the inequality $A/B \neq g_{||}/g_{\perp}$ is the contribution of the unpaired s-electrons.

The h.f.s. splittings of Co^{++} in Ce-Mg-nitrate are, of course different for the two lattice positions. The ion with $g_{\parallel} = 7.29$, $g_{\perp} = 2.34$ has, for ^{59}Co , $A = 0.0283 \text{ cm}^{-1}$ and B is practically zero.

For the other lattice position:

$$g_{\parallel} = 4.11 \quad A = 0.0085 \text{ cm}^{-1}$$

$$g_{\perp} = 4.38 \quad B = 0.0103 \text{ cm}^{-1}$$

It should be mentioned that, whereas experimentally the B -values in a number of cases are very small (B in the potassium Tutton salt is 0.007 cm^{-1}), theoretically a small B value has to be explained by cancelling of the h.f.s. due to orbital angular momentum by the unpaired 4s-electron effect. This may cast some doubt on the validity of the explanation (see also Hei 57). However, the s-electron effect seems to be the only plausible explanation for the magnitude of the h.f.s. splitting in Mn and is also in agreement with the fact that the h.f.s. splittings in the Co-salts, can be explained with the use of only two parameters (κ and P).

2.C. IV. Ce^{+++} -ion. Configuration $4f^1$, 2F .

The state 2F is split by spin-orbit coupling in $J = 7/2$ and $J = 5/2$, $J = 7/2$ lying about 2250 cm^{-1} above $J = 5/2$. An axially symmetric crystal field would split the 6-fold degenerate state $J = 5/2$ into three Kramers doublets $J_z = \pm 1/2$, $J_z = \pm 3/2$ and $J_z = \pm 5/2$.

$J_z = \pm 3/2$ would give $g_{\perp} = 0$, which is in complete disagreement with experiment. From the experimental g -values it is probable that $J_z = \pm 1/2$ is lowest, giving g -values: $g_{\perp} = 18/7$ and $g_{\parallel} = 6/7$. Crystal fields of trigonal symmetry will mix the states $J_z = \pm 1/2$ with $J_z = \pm 5/2$. Approximate agreement with experiment (table 1) can be obtained for a $|J_z = 1/2 \rangle - b |J_z = -5/2 \rangle$ with $a = 0.91$, $b = 0.4$ and a $|J_z = -1/2 \rangle - b |J_z = 5/2 \rangle$ as the two states of the doublet.

This gives g -values: $g_{\parallel} = (6/7)(a^2 - 5b^2) \approx 0$ and $g_{\perp} = 18a^2/7 \approx 2.1$. If admixtures of the level $J = 7/2$ are taken into account, better agreement with experiment is obtained. (Jud 55, Ell 53b).

From the formula for g_{\perp} it will be seen, that a small change in the ratio a/b has a profound effect on the g_{\parallel} -value, but is relatively unimportant for g_{\perp} . It may be suggested, that small variations in the crystal structure in various crystals may result in appreciable differences in g_{\perp} . This might explain the discrepancy between paramagnetic resonance experiments (Coo 53) and the adiabatic demagnetization experiments of WHEATLEY and ESTLE (Whe 56), who find g_{\perp} practically zero: $g_{\parallel} < 0.03$. An error in the paramagnetic resonance experiments is also a possibility since a crystal must be carefully aligned with respect to the magnetic field.

Since the stable Ce nucleus has $I = \mu = 0$, no h.f.s. has been measured.

Apart from a relatively unimportant admixture of the $J = 7/2$ level, one would expect $A/B = g_{||}/g_{\perp}$ and consequently $A = 0$. Nuclear spins would, at low temperatures, therefore preferably be oriented perpendicular to the trigonal crystalline axis (c- or z-axis) and this has been confirmed experimentally by gamma ray anisotropy measurements of ^{141}Ce in Ce-Mg-nitrate (Amb 55b).

2.C. V. Table of g-values and h.f.s. splitting constants.

Table 1. Hyperfine structure splitting constants for a nuclear gyromagnetic ratio $\mu/I = 1$, expressed in degrees Kelvin. Also the g-values are given.

| Ion | Salt | A/k | B/k | $g_{ }$ | g_{\perp} |
|-----------------------------------|------------------------------|---------|----------------------------------|----------|------------------------------|
| V ⁺⁺ | NH ₄ -Tutton salt | 0.0086 | — | 1.95 | — |
| Mn ⁺⁺ | Bi-Mg-nitrate | -0.0094 | -0.0094 | 2.00 | 2.00 |
| Co ⁺⁺ | K-Tutton salt | 0.0310 | 0.0071 | 6.56 | 2.50 |
| | NH ₄ -Tutton salt | 0.0265 | 0.0022 | 6.45 | 3.06 |
| | Rb-Tutton salt | 0.0318 | 0.0053 | 6.6 | 2.7 |
| | Bi-Mg-nitrate $\frac{1}{3}$ | 0.0307 | — | 7.29 | 2.338 |
| | $\frac{2}{3}$ | 0.0092 | 0.0112 | 4.108 | 4.385 |
| | Fluosilicate | 0.0199 | 0.0051 | 5.82 | 3.44 |
| Cu ⁺⁺ | NH ₄ -Tutton salt | 0.0124 | $A_x = 0.0024$ $A_y = 0.0033$ | 2.46 | $g_x = 2.12$ $g_y = 2.05$ |
| | Bi-Mg-nitrate | 0.0105 | 0.0016 | 2.454 | 2.096 |
| | Fluosilicate | 0.0105 | <0.0029 | 2.46 | 2.10 |
| Ce ⁺⁺⁺ | Bi-Mg-nitrate | 0.0044 | 0.072 | ≈ 0 | 1.84 |
| Pr ⁺⁺⁺ | La-Mg-nitrate | 0.073 | — | 1.55 | — |
| | Ethylsulfate | 0.078 | — | 1.69 | 0.3 |
| Nd ⁺⁺⁺ | La-Mg-nitrate | 0.025 | 0.155 | 0.45 | 2.72 |
| | Ethyl sulfate | 0.189 | 0.099 | 3.535 | 2.072 |
| Sm ⁺⁺⁺ | Sm-Mg-nitrate | 0.222 | <0.07 | 0.76 | 0.40 |
| | Ethylsulfate | 0.0386 | 0.161 | 0.596 | 0.604 |
| Tb ⁺⁺⁺ | Ethylsulfate | 0.292 | — | 17.72 | <0.3 |
| Dy ⁺⁺⁺ | Acetate | 0.025 | — | 13.60 | — |
| Ho ⁺⁺⁺ | Ethylsulfate | 0.511 | 0.03 | 15.36 | — |
| Er ⁺⁺⁺ | Ethylsulfate | 0.0051 | 0.0310 | 1.47 | 8.8 |
| Yb ⁺⁺⁺ | Ethylsulfate | 0.151 | — | 3.4 | 0 |
| (NpO ₂) ⁺⁺ | Uranyl-Rb-nitrate | +0.0987 | +0.0106 | 3.40 | 0.20 |
| (PuO ₂) ⁺⁺ | Uranyl-Rb-nitrate | 0.148 | — | 5.32 | <0.4 |

Remarks:

- 1) In strong magnetic fields the splitting Δ between two successive nuclear magnetic sublevels is given by $\Delta = A/2$ if $S = 1/2$; for all ions $S = 1/2$, except Mn⁺⁺ ($\Delta = 5A/2$) and V⁺⁺ ($\Delta = 3A/2$). Irrespective of the value of I , A is also the overall h.f.s. splitting per nuclear

magneton in strong magnetic fields if $S = 1/2$; for Mn and V the overall splitting is $5A$ and $3A$ respectively.

- 2) For the Co-Tutton salts B and g_{\perp} are the minimum values measured in the plane of the tetragonal axes of the two magnetic ions, which are in different lattice positions.
- 3) Only one Mn-salt occurs in the table since the splittings in other salts have, within experimental accuracy, the same magnitude.
- 4) For Cu only one Tutton salt is given, as the splittings in other Tutton salts are not very different.
- 5) No experimental errors are indicated but they amount to a few units in the last decimal. For the rare earth elements the error may be a few percent, due to inaccurate knowledge of the nuclear magnetic moment.
- 6) The signs of A and B are unknown from experiment, unless explicitly indicated.
- 7) The constants A and B for Ce are theoretical estimates. The measured value for ^{141}Ce is $B = 0.0126$ ($I = 7/2$, μ unknown).
- 8) H.f.s. constants, ranging from 0.001 to 0.01 cm^{-1} have also been measured for Eu in SrS and for Mo, Ru and Ir compounds; they are omitted from the table since it has not been shown, that cooling of these compounds to temperatures below 0.01°K is experimentally feasible.
- 9) The value of A for Yb is actually measured in Yb-acetate, but it is a reasonable assumption that A/g_{\parallel} is practically constant in various Yb-salts.
- 10) Most of the data are calculated from the values given in (Bow 55). For references the reader is referred to that paper.

§ 3. Low temperature aspects of nuclear orientation.

3. A. *Adiabatic demagnetization.*

Nearly all methods for nuclear orientation require temperatures below 1°K . At present nearly (Men 55) the only available technique for reaching temperatures below that of the liquid helium range ($0.9\text{--}4^{\circ}\text{K}$ under practical experimental conditions) is the adiabatic demagnetization of paramagnetic salts, first suggested by GIAUQUE and DEBYE (Gia 27, Deb 26). This subject has been treated in a number of review articles (Kle 55, 56, Amb 55a, Han 56) and will not be discussed here in any more detail than is required for an understanding of the experiments of chapter IV and V.

The experimental arrangement, used for our experiments, is described in (Kle 48, 56, Ste 52a, Beu 57) and may be seen particularly from fig. 4 of

(Kle 56), fig. 3.1 in (Beu 57). A favourable aspect of the arrangement is the powerful (80 kW) electromagnet, which easily gives a field of 23000 Oe in a pole gap of 7 cm and which is homogeneous to within 1% over a region with a diameter of 5 cm. This homogeneity enables one to demagnetize large samples (more than 10 cc) of paramagnetic salts, which stay cold for a long time because the heat leak is practically independent of the sample size.

Many salts may be chosen for reaching low temperatures: roughly 25 salts have been studied in some detail with respect to their properties below 1°K. (Coo 55a)

If the oriented nuclei are contained in the cooling salt itself, this will be called "internal cooling", as opposed to the case of "external cooling", where a paramagnetic salt is used to cool another substance in which one wants to orient nuclei. External cooling has been applied only in a small number of nuclear orientation experiments, because this method requires heat transfer from the cooled substance to the cooling salt. This heat transfer problem has only been reasonably solved for $T > 0.05^\circ\text{K}$; if the temperature is further decreased heat conductivity decreases rapidly and the heat transfer through the surfaces of connected substances in particular becomes very poor. Nevertheless, for the so called external field polarization, or brute force method, of nuclear orientation, external cooling is essential.

It may be useful to discuss a few of the most important thermodynamic aspects of adiabatic demagnetization.

a) Suppose the demagnetization is carried out from an initial field H_i of the order 10^4 Oe and from an initial temperature T_i of about 1°K, to a final field H_f corresponding to a temperature T_f . If both H_i and H_f are large enough so as to induce equidistant Zeeman splittings of the paramagnetic ion, then in both cases the Boltzmann distribution is completely determined by the factor $g\beta H/kT$. The entropy remains constant during an adiabatic demagnetization, therefore the distribution of ions among the various energy states also remains constant, which implies that H/T is constant during the whole process. In many salts H/T is roughly constant for values of H_f greater than 1000 Oe. If H_i is further reduced, the proportionality between the Zeeman splittings and H may be appreciably disturbed by the "natural" field splittings in the crystal, which may be caused, for instance, by crystalline electric fields or magnetic dipole-dipole interaction between neighbouring ions. These natural splittings determine the value of T which is obtained when H is reduced to zero.

b). The entropy S in zero external magnetic field as a function of temperature can generally be represented by a curve like that in fig. 8, where the entropy of Ce-Mg-nitrate has been plotted. Mathematically $S(T)$ can

be reasonably well described, particularly for not too low temperatures, by

$$S = R \ln(2J + 1) - b/2T^2 \quad (9)$$

where R is the gasconstant and J is the electronic angular momentum (in most cases equivalent to the fictitious spin in the spin-Hamiltonian for the ion and salt under consideration). b is a constant, which is related to the specific heat c_0 according to:

$$c_0 = dQ/dT = T dS/dT = b/T^2. \quad (10)$$

For a constant heat input per unit time dQ/dt , as is experimentally encountered in case of radioactive heating of the sample, we have:

$$\begin{aligned} dQ/dt &= (dQ/dT)(dT/dt) = \\ &= -T^2(dQ/dT)d(1/T)/dt = \\ &= -b d(1/T)/dt \end{aligned}$$

hence a constant value of $d(1/T)/dt$. In a nuclear orientation experiment the magnetic susceptibility χ , roughly $1/T$, is directly measured as a function of time. $1/T$ versus t curves

were for instance obtained in the experiments of Chapter V, and an example is given in fig. 9. It can be seen that $d(1/T)/dt$ was approximately constant for Ce-Mg-nitrate in magnetic fields of a few hundred oersteds. The influence of magnetic fields on the specific heat will be discussed hereafter.

c) If a small magnetic field H is isothermally applied to the sample, the entropy S_H is related to the entropy in zero field, S_0 , according to:

$$S_H = S_0 - CH^2/2T^2 \quad (11)$$

where C is the Curie constant, C/R being given by $J(J+1)g^2\beta^2/3k^2$. Comparing S_0 , S_H and S_1 , as defined in fig. 10, one easily derives with the aid of (9, 11):

$$T_0/T_1 = \sqrt{1 + CH^2/b}. \quad (12)$$

For H small compared with $\sqrt{b/C}$, (12) gives $\Delta T = T_0 - T_1 \approx H^2$. It should be noted that (11) has been derived with the aid of Curies law $M = CH/T$; consequently (12) may not be valid for large H or at the

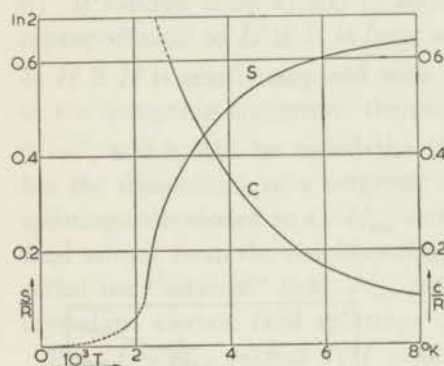


Fig. 8. Entropy S and specific heat c per half-mole of $Ce_2Mg_3(NO_3)_{12} \cdot 24 H_2O$ as a function of temperature T , according to (Dan 53, Kle 56). S and c are expressed in units $R = 8.317$ Joule/degree and T is given in millidegrees Kelvin.

lowest temperatures, where large deviations of Curie's law may occur. However, the validity of $\Delta T \propto H^2$ requires only that M can be written as $M = H\chi(T)$; for a number of salts it was found that indeed ΔT is approximately proportional to H^2 . In the experiments described in Chapter V it was found that in Ce-Mg-nitrate the relation (12) is approximately fulfilled for $H < 1000$ Oe, if H was applied in the $g_{||}$ direction.

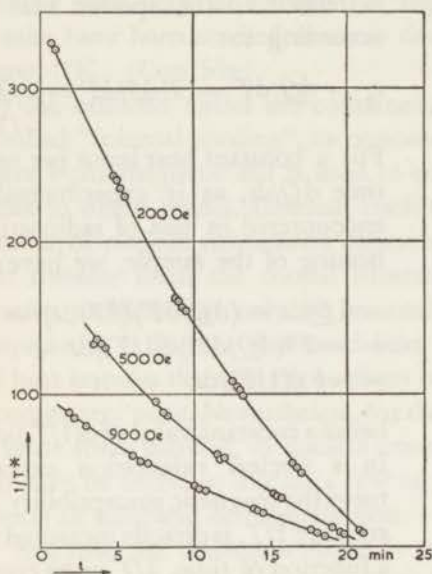


fig. 9

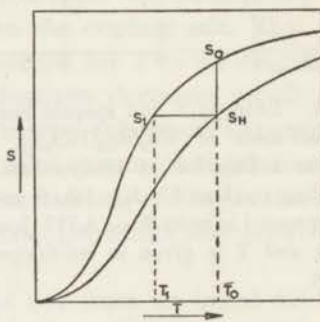


fig. 10

Fig. 9. Magnetic susceptibility ($\propto 1/T^*$) of Ce-Mg-nitrate crystals in various magnetic fields, applied in the $g_{||}$ -direction; t is the time after adiabatic demagnetization. The circles represent χ -measurements in one typical run of the experiments described in V, § 4. It may be seen that $d(1/T)/dt$ is approximately constant.

Fig. 10. Entropy S versus temperature T in the absence of a magnetic field (upper curve) and in a field H (lower curve). The diagram shows the temperature increase if H is adiabatically applied at the temperature T_1 , T_0 being determined by $S_0 - S_1 = S_0 - S$.

If (12) is valid, then the curve S_H can be obtained from the curve S_1S_0 by a change in scale factor of T . Hence $c = dQ/dT = T(dS/dT)$ is not changed by introducing a magnetic field adiabatically.

One finds $c_H = (b + CH^2)/T^2$ for the specific heat in a magnetic field. This makes $dQ/dt = -(b + CH^2) d(1/T)/dt$, which shows that $d(1/T)/dt$ is decreased by the magnetic field.

In fig. 9 the $(d/T)/dt$ curves for different values of the magnetic field may be compared; the expression for dQ/dt shows that for a constant heat input also $d(1/T)/dt$ should be constant (if (9) and (11) are valid), as was actually found for Ce-Mg-nitrate (fig. 9). From the slopes of the $1/T$ vs t curves, heat input, dQ/dt , can be calculated if b and C are known.

d) It follows from a) and c) and particularly from formula (12) that T is proportional to H if H is large and that T is in first order independent of H if H is small compared with $\sqrt{b|C}$. The words "small" and "large" in the foregoing statements therefore refer to the comparison of H with $\sqrt{b|C}$, which will be called the "natural" field H_{nat} . This natural field has the dimensions of a magnetic field and is related to the natural field splittings mentioned in a). H_{nat} should not be confused with the magnetic field arising from the neighbouring magnetic dipoles, which is sometimes called the "internal" field. H_{nat} may also be due to exchange interaction, crystalline electric field splittings or h.f.s. interactions.

For $H \approx H_{\text{nat}}$ neither $H/T = \text{constant}$ or $\Delta T \propto H^2$ are good approximations.

Since g and hence the Curie constant C are not scalar quantities but tensors, one must be careful in applying these concepts to ions with very anisotropic g -values.

§ 3. B. *Temperature measurements.*

The temperature of a paramagnetic salt was determined by measuring its magnetic susceptibility χ by means of two mutual inductance coils around the sample. The primary coil is wound around the He-dewar and gives a magnetic field of roughly 25 Oe/Amp. This field was homogeneous to within 0.3% over the sample volume and showed two equal (within 10^{-3}) maxima at a distance of 2 cm apart. The secondary coil was 2 cm long and wound around the glass vessel which contained the sample in such a way that the specimen was located approximately at the center of the coil. The upper and lower edge of the secondary coil were then adjusted so that they were located at the two forementioned maxima. The purpose of this procedure is to reduce the effect of any movement of the secondary coil with respect to the primary, which can arise from differences in thermal expansions and contractions of He-dewar and sample vessel if the cryostat is cooled from 4 to 1°K. In this temperature range one wants a very constant mutual induction of the coils themselves, the measured change in induction is then entirely due to the change in the susceptibility of the salt. The change in susceptibility as a function of the

temperature T between 4 and 1°K serves as a calibration of the susceptibility thermometer. In fact, since Curies law $\chi = C^*/T$ is obeyed to a very good approximation for the usual salts in the He-temperature range, the calibration determines the constant C^* , (for one gram ion C^* is equal to the Curie constant C).

After demagnetization a measurement of χ yields the temperature providing Curies law remains valid. This, however, is the ideal case and in practice one has to know the relation between $\chi \equiv C/T^*$ and T , which has been determined for many salts.

The measurement of the mutual inductance is made by means of a Hartshorn bridge; for the calibration the high accuracy required is obtained by using a.c. current and a vibration galvanometer as a zero reading instrument. For the susceptibility measurements after adiabatic demagnetization, mostly ballistic methods are used (Kle 55, 56) in order to avoid a.c. losses either in the sample at low temperatures or in the surroundings, for instance an iron core magnet.

It must be mentioned, that whereas the axis of the external magnetic field is horizontal, the susceptibility measurements are made in the vertical direction since the coils are wound around the cryostat, with a vertical axis. For both the adiabatic demagnetization and the susceptibility measurements one prefers large g -values ($\chi \propto g^2$). If one uses monocrystals of a salt which possesses a small g -value in two directions, for instance $g_{\perp} \approx 0$, this would present an experimental problem. One could wind the coils skewly around the cryostat and sample vessel, such that the mutual inductance of the coil will also be influenced by horizontal components of the magnetization of the sample. Alternatively, one could arrange the coils outside the cryostat, which has, apart from a number of disadvantages, the advantages: 1) the relative position of the two coils can be rigidly fixed, 2) one set of coils can be used for many experiments.

For a salt with a small g -value along only one crystal axis ($g_{\parallel} \approx 0$), the mounting of the crystal is determined by the two foregoing requirements of vertical susceptibility measurements and horizontal magnetic field direction. (see also fig. 13).

A small magnetic field for nuclear h.f.s. polarization has, from an experimental point of view, preferably to be placed with its axis horizontal. Otherwise one measures the susceptibility in a direction, along which H is far from zero. Small variations of the field cause serious perturbations in the ballistic readings. Moreover one measures the susceptibility in a field, χ_H , and the reduction of χ_H to χ_0 , the susceptibility in zero field, requires additional knowledge about the magnetic properties of the salt. The reduction of χ_H to χ_0 is calculated in general as follows. Suppose

the spin-Hamiltonian, neglecting h.f.s. interactions, is: $H = g_{\parallel}\beta H_z S_z + g_{\perp}\beta(H_x S_x + H_y S_y)$ with $S = 1/2$. The energy levels in a magnetic field are calculated from this Hamiltonian, if written in the form

$$H = g_{\parallel}\beta H_z S_z + \frac{1}{2}g_{\perp}\beta(H_+ S_- + H_- S_+)$$

$$\text{where } \begin{aligned} H_+ &= H_x + iH_y & S_+ &= S_x + iS_y \\ H_- &= H_x - iH_y & S_- &= S_x - iS_y \end{aligned}$$

$$\text{Since } \begin{aligned} \langle \pm 1/2 | S_z | \pm 1/2 \rangle &= \pm 1/2 \\ \langle -1/2 | S_- | +1/2 \rangle &= \langle +1/2 | S_+ | -1/2 \rangle = 1 \end{aligned}$$

the secular equation is:

$$\begin{vmatrix} \frac{1}{2}g_{\parallel}\beta H_z - E & \frac{1}{2}g_{\perp}\beta H_- \\ \frac{1}{2}g_{\perp}\beta H_+ & -\frac{1}{2}g_{\parallel}\beta H_z - E \end{vmatrix} = 0$$

$$E_{\pm} = \pm \frac{1}{2} \sqrt{g_{\parallel}^2 \beta^2 H_z^2 + g_{\perp}^2 \beta^2 (H_x^2 + H_y^2)}$$

From the partition function $Z = \sum_i \exp(-E_i/kT)$ the susceptibility is calculated by means of the formulae

$$F = -kT \ln Z, \quad M = -(\delta F / \delta H)_T \quad \text{and} \quad M = \chi H.$$

If the susceptibility is measured along the x, y or z-axis the result is:

$$\left(\frac{\chi_H}{\chi_0} \right) = \frac{Tha}{a} \left\{ \frac{Tha - a/Ch^2a}{a^2} \right\} \left[\frac{g_k^2 H_k^2}{g_{\parallel}^2 H_z^2 + g_{\perp}^2 (H_x^2 + H_y^2)} \right] \quad (13)$$

where $k = x, y$ or z and $a = (\beta/2kT) \sqrt{g_{\parallel}^2 H_z^2 + g_{\perp}^2 (H_x^2 + H_y^2)}$

The validity of (13) is based upon the assumption that $E_+ - E_-$ is large compared with the other interactions of the paramagnetic ion, or that $H > H_{nat}$.

The accuracy of the temperature determination is limited by the following factors:

1) Sensivity of the measurements.

Because the susceptibility is inversely proportional to the temperature, the measurements at high temperatures are relatively not very accurate. During the calibration from 4 to 1°K, the entire change in mutual inductance of the coils is of the order of one per thousand (for 10 grams of crystals) and the figure, which determines the calibration constant C^* , usually cannot be determined with an accuracy that is better than a few percent. The relative accuracy of all T^* -measurements is limited to that of the constant C^* .

2) Demagnetizing effects.

In the foregoing discussion (particularly in the second paragraph of § 3 B) it has been tacitly assumed, that if Curie's law is valid, the measured

temperature T^* is equal to the thermodynamic temperature T . This, however, is a simplification. In the mutual inductance measurements one measures essentially the induction and therefore the magnetization M of the sample in the field H_{ext} of the primary coil. The relation between M and T is expressed by Curie's law $M = CH_{\text{ext}}/T$ only in the case that the field acting on the paramagnetic dipoles, called H_{loc} is equal to H_{ext} (i.e. in the case of free ions). In a crystal, however, H_{loc} may be quite different from H_{ext} due to a) the demagnetizing effects from the magnetization on the crystal surfaces, b) the field of the neighbouring ions, which may be very complicated. Adopting the Lorentz approximation for the field of the neighbouring ions, then for a spherical sample the effects of a) and b) cancel and $H_{\text{loc}} = H_{\text{ext}}$. The measured T for a spherical sample, called T^\otimes should then be equal to T , and if so, it is said that Curie's law holds. In the literature on low temperature physics, the distinction between T^* and T^\otimes is usually neglected, particularly if spherical samples are used and no confusion can arise. However, the samples used in nuclear orientation experiments usually consist of one or more single crystals and the sample form will then be very much different from a sphere. We will therefore mostly be concerned with T^* . If the form of such a sample can be approximated by an ellipsoid, it is possible to account for the demagnetizing effects, because one can calculate (Kle 56) that

$$H_{\text{loc}} = H_{\text{ext}} + (4\pi/3 - N)M \quad (14)$$

Here N is called the demagnetizing factor, which is related to the excentricity of the ellipsoid; $N = 4\pi/3$ for a sphere. M is the magnetization per unit volume and therefore, at high temperatures (for instance in the calibration) where M is small, the demagnetizing effects can be neglected. From (14) one easily derives

$$T^\otimes = T^* + \Delta \text{ with } \Delta = (4\pi/3 - N)C' \quad (15)$$

where C' is the Curie-constant per unit volume. In a non-ellipsoidal sample H_{loc} is no longer constant over the sample volume and therefore the demagnetizing factor becomes, strictly speaking, meaningless. Nevertheless, it is assumed here that, because the susceptibility measurement is an average over the sample volume, it is possible to account for the demagnetizing effects in an approximate fashion by means of (14, 15). A method for measuring N will be discussed in Chapter V, § 4 B. It is shown there, that Δ/T^* can amount to 50%. Because of the approximations involved, the deduced T^\otimes values may be in error by as much as 5%.

3) $T^\otimes - T$ relation.

It turns out, that the Lorentz model for the field of the surrounding ions

is in many cases only a rough approximation. At low temperatures, this is shown by large deviations of T^\otimes from T , or alternatively, deviations from Curie's law. These deviations have been measured for many salts and the ratio T^\otimes/T has been given for a wide range of temperatures with an accuracy of a few percent. The real T^\otimes/T values may, however, differ from the observed values by appreciably more than 5% at the lowest temperatures, in which we are particularly interested. This may be seen, for instance, from page 141 of (Kle 56). It should be mentioned, that a difference between T^\otimes and T is not necessarily a result of dipole-dipole or exchange interactions with neighbouring ions, but may also result from electric field splittings or h.f.s. interactions in the ion itself. In some cases this difference has, to a first order approximation, a constant value θ called the Curie-Weiss constant: $T^\otimes = T - \theta$ if $T \gg |\theta|$.

§ 4. Magnetic h.f.s. polarization.

4. A. Electronic polarization.

H.f.s. polarization of the nuclear spins requires first of all polarization of the ions, or more precisely, of the electronic angular momenta. Hence we will neglect h.f.s. splittings in the first part of the discussion, which consists of a rough calculation of the fields and temperatures required to polarize the magnetic ions.

For that purpose we will assume that the salt under consideration is in the form of a single crystal and contains only one sort of paramagnetic ion, the nuclei of which we want to polarize, and that the spin-Hamiltonian for these ions can be written as

$$H = g_{\parallel}\beta H_z S_z + g_{\perp}\beta(H_x S_x + H_y S_y) + AS_z I_z + B(S_x I_x + S_y I_y) \quad (16)$$
for $S = 1/2$. If a magnetic field H is applied in the z-direction, the doublet ($S_z = \pm 1/2$) is split and the energy difference between the two levels with $S_z = -1/2$ and $S_z = 1/2$ will be $g_{\parallel}\beta H_z$. In practice it is sufficient to reach an electronic polarization $f_e \equiv |\langle S_z \rangle / S|$ of 90%, and since

$$f_e = \text{Th } g_{\parallel}\beta H_z / 2kT, \text{ this requires } g_{\parallel}\beta H_z / kT > 3.0$$

or $H/T \geq \frac{4.5 \times 10^4}{g_{\parallel}} \text{ Oe/degree Kelvin} \quad (17)$

A field of 25000 Oe and a temperature of 1°K would be sufficient, unless $g_{\parallel} < 1.8$.

For nuclear polarization, however, lower temperatures are needed. These can be obtained by lowering the magnetic field adiabatically, since then H/T remains approximately constant. Taking the forementioned values $H_i = 25000$ Oe, $T_i = 1^\circ\text{K}$, we get for $H_f = 1000$ Oe: $T_f = 0.04^\circ\text{K}$, while f_e should remain constant. In the following discussion the viewpoint

is adopted, that h.f.s. polarization is achieved by adiabatic demagnetization, not to zero field, but to such a value H_f that f_e is practically unchanged from its initial value while T_f is low enough as to obtain nuclear polarization. Sometimes, however, we will consider h.f.s. polarization as a result of applying a small magnetic field ($\approx 10^2$ Oe) to the salt at low temperatures (10^{-2} °K); this means that the demagnetization was then already carried out to zero field. In any case, it is seen, that a large field is favourable for high f_e . This follows for instance from (12):

$$T_H/T_{H=0} = \sqrt{1 + CH^2/b} \text{ or } H/T_H = \frac{\sqrt{bH^2/(b + CH^2)}}{T_{H=0}}$$

so that the ratio H/T_H increases with increasing H .

The foregoing discussion shows that electronic polarization becomes difficult for small values of g : for $g_{\parallel} < 1$, $f_e < 0.7$, unless H/T -values larger than 25000 Oe/degree are experimentally feasible. Fortunately, practically all ions have a value of either g_{\parallel} or g_{\perp} which is greater than 1.

4. B. Nuclear polarization.

We will start the discussion from the simplifying assumptions $I = 1/2$, and $B = 0$ in equation (16). Then for $S_z = -1/2$ the nuclear magnetic

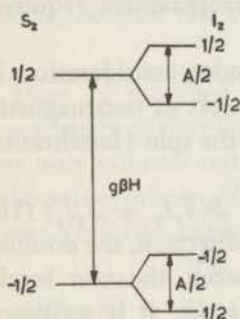


Fig. 11. H.f.s. energy levels in an external magnetic field H . S_z and I_z are the z -components of electronic and nuclear spin along the crystal symmetry axis (z -axis) which is also the axis of H ($H = H_z$). The fig. refers to the particular case that the spin-Hamiltonian can be written as $H = g_{\parallel} \beta H_z S_z + A S_z I_z$, where $S = I = \frac{1}{2}$, A positive.

sublevels $I_z = -1/2$ and $I_z = +1/2$ are separated by an energy difference $|A/2|$ as a result of the h.f.s. interaction (fig. 11). In order to make the nuclear polarization $f_N \equiv \langle |I_z| \rangle / |I|$ larger than 10%, the temperature should be low enough so as to satisfy $|A| / 2kT > 0.2$. Or alternatively, if we adopt a final temperature $T_f = 0.04$ °K, $|A|/k$ should be greater than 0.015 °K. For values of S or I larger than $1/2$, $|A|$ may be correspondingly smaller. However, small I is favourable, as follows from the approximate expression for f_N , valid for small values of f_N :

$$f_N \approx \frac{1}{3} \left(\frac{I+1}{I} \right) \frac{|AIS|}{kT} \quad (18)$$

so that for a fixed value of the nuclear magnetic moment and hence also of AIS , f_N decreases with increasing nuclear spin according to the factor $(I+1)/I$. Values of A of the mentioned magnitude can be found for a number of ions and salts, but values of f_N

larger than 0.1 are required if appreciable effects in nuclear physics are wanted, say $f_N \approx 0.5$. Moreover for many salts deviations from $H/T = \text{constant}$ occur for temperature above $T = 0.04$ °K, so that this temperature may then not be obtainable, even by complete demagnetization. In fact, only for a very restricted number of ions and salts does this h.f.s. polarization method yield values of $f_N \approx 0.5$.

4. C. *Other possibilities.*

If the salt, which contains the ions whose nuclear spins we wish to polarize, cannot be cooled sufficiently by demagnetization, then the cooling might be achieved by putting it in heat contact with another salt. Although this is experimentally not very simple because both heat contact and heat conduction are poor at low temperatures, such a procedure would increase considerably the possibilities for h.f.s. polarization. A serious drawback is, however, that the temperature in the cooled salt would not be homogeneous, thereby making quantitative interpretation of experimental results much more difficult. Only little could be gained by making a powdered mixture of the two salts because at these low temperatures heat contact would still be insufficient to equalize temperatures, unless a suitable binding agent could be found. A possible solution of the heat contact problem may be presented by the use of an alcoholic solution of the two sorts of paramagnetic ions. Preliminary experiments have shown, that with such a solution, which is suddenly frozen, temperatures below 0.01 °K can readily be obtained*. Little data are known about g -values and h.f.s. splittings for the ions in such an environment, but the medium in the neighbourhood of each ion is expected to vary considerably from place to place in the solidified "solution". Particularly since, if crystals of the paramagnetic salt are dissolved, the water of crystallization mixes with the alcohol, so that the ions may be surrounded by varying numbers of alcohol and water molecules, which have, however, not very different electric dipole moments. For ions with no orbital angular momentum in their ground state, like Mn^{++} , neither the g -value nor the h.f.s. splitting are very sensitive to the influence of the surrounding ions or molecules, so that such ions may be very suitable for the use in alcoholic solutions. This is also indicated by paramagnetic resonance experiments, carried out with Mn impurities in single crystals of NaCl and KCl. For ions like Co^{++} and also the rare-earth ions, one must expect the g -value and h.f.s. splittings to be very anisotropic; if the direction of large g -value and large A is randomly oriented for the various ions in the solution, as is to be expected, then quantitative experiments become very difficult. This objection is also valid for powdered mixtures.

* Communicated to the author by M. J. Steenland and A. R. Miedema

4. D. *Single crystals with two paramagnetic ions.*

It is sometimes possible to incorporate both the cooling paramagnetic ion and the ions, of which the nuclei are to be polarized, in one single crystal (Dan 51). This method is often used for alignment, by example: Mn and Co ions in Ni-fluosilicate, Nd-ions in Ce-Mg-nitrate and Ce-ethylsulfates. In these cases the bulk of the ions, Ni and Ce respectively, feel in the crystal a relatively small "natural" field $H_{\text{nat}} = \sqrt{b/C}$ (partly due to the absence of h.f.s. interaction in the Ce- and Ni-ions) and by demagnetization low temperatures can be obtained. The "foreign" ions in the lattice, Mn, Co, Nd, whose nuclei are to be polarized, should possess appreciable h.f.s. splittings. This method is also useful for h.f.s. polarization and becomes much more interesting if the two sorts of paramagnetic ions have very different g -values. Particularly Ce-Mg-nitrate in this respect is extremely suitable in combination with Co^{++} and Mn^{++} -ions, which can replace Mg^{++} -ions in the lattice. The advantages of Ce-Mg-nitrate are: 1) By adiabatic demagnetization temperatures as low as 0.003 °K can be reached. Because g_{\parallel} is very small the demagnetization must be carried out with the field in the direction of $g_{\perp} = 1.84$. 2) The polarizing magnetic field may be applied in the direction of g_{\parallel} instead of g_{\perp} because the g_{\parallel} -values of Co^{++} and Mn^{++} are large. Then the temperature rise, which is the consequence of the action of the field on the Ce-ions, can be kept very small, since $\Delta T \propto CH^2$ where C is proportional to g^2 . In fact, a polarizing field of 1000 Oe applied at $T = 0.003^{\circ}\text{K}$ in the g_{\parallel} -direction does not increase the temperature beyond 0.01 °K, if at least the thermodynamic properties of the crystal are merely determined by the Ce-ions and not also partly by the incorporated "foreign" ions.

4. E. *Properties of Ce-Mg-nitrate.*

$2 \text{Ce}(\text{NO}_3)_3, 3 \text{Mg}(\text{NO}_3)_2, 24 \text{H}_2\text{O}$ is one of the isomorphous series of double nitrates of the general formula $2 \text{M}^{+++}(\text{NO}_3)_3, 3 \text{M}^{++}(\text{NO}_3)_2, 24 \text{H}_2\text{O}$ in which M^{+++} is a paramagnetic ion of the 4f-group and M^{++} an ion of the 3d-group. The crystal structure is not fully known. Unpublished investigations of POWELL (Coo 53) showed, that the unit cell is rhombohedral and has the form of a cube pulled out along the trigonal axis. At the corner of the distorted cube there is one Ce-ion, whereas divalent ions Mg, Co, Mn etc. can be placed both at the face centres and at the body centres of the cube. The results of paramagnetic resonance measurements suggest that the divalent ion is surrounded by an octahedron of water molecules forming a nearly cubic arrangement with a small trigonal distortion. See also fig. 12. The principal axes of the g -tensors

for the three lattice positions coincide and the trigonal crystal axis can be considered as the z-direction or //direction for the spin-Hamiltonian of all ions. The x and y directions may be arbitrarily chosen perpendicular

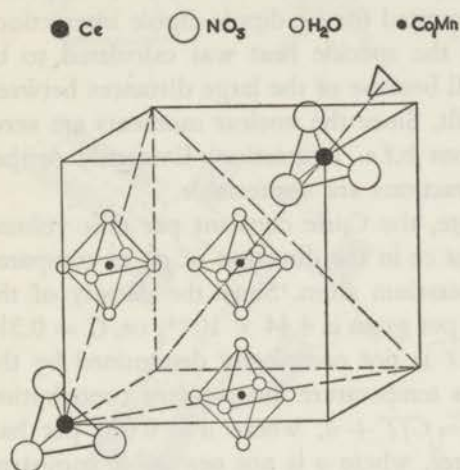


Fig. 12. Trigonal symmetry in the crystal structure of Ce-Mg-nitrate. This picture does not completely represent the unit cell of Ce-Mg-nitrate, many details being unknown. The diagram may show, however, that trigonal symmetry can arise for the trivalent Ce ions as well as for the divalent ions (Mg, Co, Mn) in both lattice positions (face centres and body centres). The data are given in Coo 53. According to these data the unit cell is rhombohedral as a result of an elongation of the cube along a body diagonal. This distortion may also affect the octahedrons of water molecules around the divalent ions; the crystalline field of these ions will then have predominantly cubic symmetry with a trigonal distortion around the trigonal crystal axis.

at low temperatures alignment of the electronic angular momentum occurs, which causes also alignment of the nuclear spins along the crystal c-axis (in spite of $A = B$).

Since $g = 2$, h.f.s. polarization with a field in the g_{\parallel} -direction is a favourable possibility also for Mn. From table 1 it follows, that the overall h.f.s. splittings for $\mu/I = 1$ are of the order of kT for $T = 0.1$ °K and hence appreciable nuclear polarization will occur.

to the z-direction. As the stable ¹⁴⁰Ce nuclei are even-even, there is no h.f.s. splitting.

For the Co⁺⁺-ion, the spin-Hamiltonian is

$$H = g_{\parallel}\beta H_z S_z + g_{\perp}\beta(H_x S_x + H_y S_y) + AI_z S_z + B(S_x I_x + S_y I_y). \quad (19)$$

The constants were given in table 1; we will recall only that $^{1/3}g_{\parallel} = 7.29$ and $^{2/3}g_{\parallel} = 4.108$, from which it is seen, with the aid of relation (17), that a large value of f_e can easily be obtained with a field of a few hundred Oersts and a temperature of 0.01 °K or lower.

For the Mn⁺⁺-ion, both the g -value and h.f.s. constants are practically isotropic. The spin-Hamiltonian is (neglecting 8).

$$H = g\beta\mathbf{H}\cdot\mathbf{S} + \mathcal{A}\mathbf{S}\cdot\mathbf{I} + D(S_z^2 - 35/12) \quad (20)$$

with $^{1/3}D/k = -0.0310$ °K and $^{2/3}D/k = -0.0115$ °K (Tre 53). In the absence of an external field H , the lowest levels are $S_z = \pm 5/2$, hence

The specific heat $c = b/T^2$ of Ce-Mg-nitrate is extremely small (Dan 53) $b/R = 7.5 \times 10^{-6}$ (0.87 ergs degree/gram) as compared to other salts: chromium potassium alum $b/R = 0.0165$, manganous ammonium sulfate $b/R = 0.034$ and cobalt ammonium sulfate $b/R = 0.0042$. The specific heat can be nearly completely accounted for by dipole-dipole interactions (Dan 53), whose contribution to the specific heat was calculated to be $b/R = 6.75 \times 10^{-6}$, which is small because of the large distances between the Ce-ions in this very diluted salt. Since the nuclear moments are zero, there is no contribution to b from h.f.s. interaction. Evidently neither exchange nor Stark splitting interactions are appreciable.

As the salt is magnetically dilute, the Curie constant per unit volume is also small: $C = 8.88 \times 10^{-4}$ per cc in the direction of g_{\perp} as compared to 67.0×10^{-4} for chromium potassium alum. Since the density of the crystals is 2.00, the Curie constant per gram is 4.44×10^{-4} ; or, $C = 0.318$ per half mole. The susceptibility χ is not completely determined by the Curie constant and T , since also a temperature independent contribution to χ was observed (Coo 53): $\chi = C/T + a$, where $a = 0.025$ per half mole. At liquid helium temperatures, where a is not negligible compared with C/T , the susceptibility is calibrated by the change of χ from 4 to 1° K and hence, only differences in χ are measured, making the term a irrelevant for our discussion.

For Ce-Mg-nitrate $b/C = 1970$ or $H_{\text{nat}} = \sqrt{b/C} = 44$ Oe, which is very low as contrasted to, for instance, Cr-K-alum, for which $b/C = 75 \times 10^4$ or $H_{\text{nat}} = 860$ Oe. It may be noted that a line width of about 40 Oe was also found in paramagnetic resonance experiments at liquid helium temperatures. The small value of b/C is in agreement with the fact that very low temperatures can actually be obtained by adiabatic demagnetization. For the $T-T^{\otimes}$ relation the reader is referred to (Dan 53, Kle 56). It was found that Ce-Mg-nitrate obeys Curie's law very well, the difference between T and T^{\otimes} being smaller than 10% for $T > 0.006^{\circ}\text{K}$, according to (Kle 56) even for $T > 0.004^{\circ}\text{K}$.

4. F. *Experimental procedure.*

Crystals of Ce-Mg-nitrate grow quickly in flat plates with trigonal symmetry, the trigonal c-axis being perpendicular to the plates. Since the magnetic properties show rotational symmetry around this axis, the z-axis or g_{\parallel} -direction, the choice of x and y-axis is arbitrary. In connection with the considerations of section 3. B., and Chapters IV and V, the mounting of the crystal relative to other parts of the apparatus is shown in fig. 13.

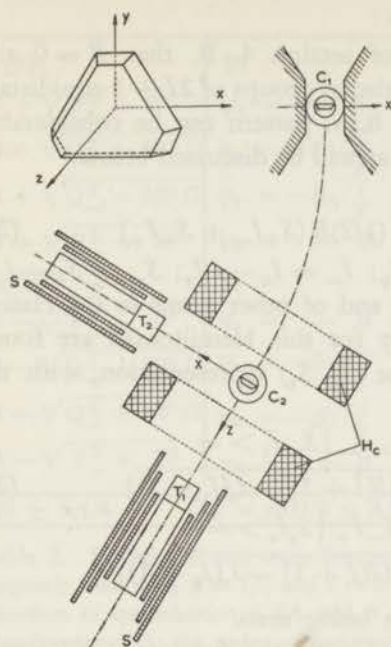


fig. 13

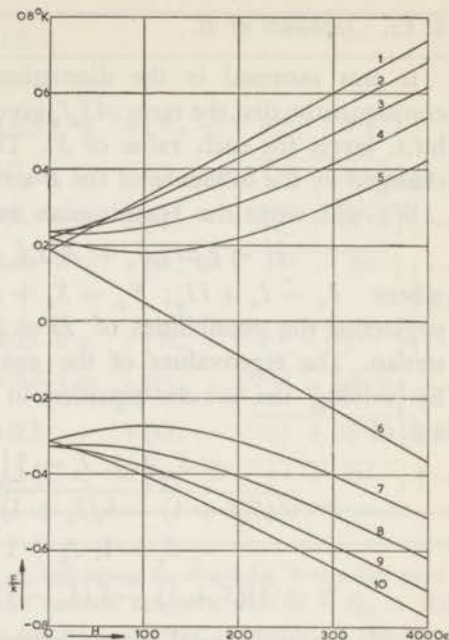


fig. 14

Fig. 13. Experimental arrangement for the h.f.s. polarization method (horizontal cross section). The cryostat C is first placed (position C1) between the poles of a large magnet, used for isothermal magnetization of Ce-Mg-nitrate in a direction of high g -value of the Ce-ions. After adiabatic demagnetization the cryostat is moved into position C₂. A magnetic field, produced by two Helmholtz coils H_c, is then applied in the direction of small g -value of the Ce-ions (c or z -axis); this field causes a polarization along the z -axis of spins of Co or Mn nuclei, which are incorporated in the crystal. The gamma ray intensities in the z -direction and perpendicular to it can be measured by the counters T₁ and T₂ which are magnetically shielded by concentric iron tubes S.

H_c and the counters are mounted on a table which can be raised and lowered by means of a hydraulic lift. The susceptibility measurements are carried out in the vertical direction (y -direction). The scale of the drawing may be inferred from the outside diameter of H_c, which is 36 cm.

Fig. 14. Calculated h.f.s. energy levels for $\frac{2}{3}$ of the Co-ions in Ce-Mg-nitrate, plotted as a function of the magnitude of the magnetic field H which is applied in the direction of small g -value (z -direction) of the Ce-ions. The level scheme refers to the case of ^{58}Co ($I = 2$ and $\mu = 4.05$ n.m.), assuming positive values for the h.f.s. parameters A and B , i.e. positive μ . The energies of the levels are calculated with the aid of table 2 and are expressed in degrees K. (The scale has been erroneously taken too large by a factor of 10: 0.8 should be read as 0.08 etc.). For $H = 0$ the energies are solely determined by the h.f.s. coupling, which is almost isotropic for $\frac{2}{3}$ of the Co-ions ($B \approx A$).

4. G. Influence of B .

It was assumed in the discussion of section 4. B. that $B = 0$ and consequently, that the term AS_zI_z gives rise to groups of $2I + 1$ equidistant h.f.s. levels for each value of S . The h.f.s. pattern can be considerably changed by the influence of the B -term as will be discussed below.

We will write the Hamiltonian as:

$$H = g_{\parallel}\beta H_z S_z + A S_z I_z + (1/2)B(S_+ I_- + S_- I_+) \quad (21)$$

where $I_+ = I_x + iI_y$; $S_+ = S_x + iS_y$; $I_- = I_x - iI_y$; $S_- = S_x - iS_y$ neglecting the possibilities of $H \neq H_z$ and of other terms in the Hamiltonian. The eigenvalues of the energy for this Hamiltonian are found by solving the secular equation in the (I_z, S_z) representation, with the aid of

$$\begin{aligned} & \langle S_z + 1, I_z - 1 | S_+ I_- | S_z, I_z \rangle = \\ & = \sqrt{\{S(S+1) - S_z(S_z+1)\} \{I(I+1) - I_z(I_z-1)\}} \quad (22) \\ & \langle S_z - 1, I_z + 1 | S_- I_+ | S_z, I_z \rangle = \\ & = \sqrt{\{S(S+1) - S_z(S_z-1)\} \{I(I+1) - I_z(I_z+1)\}} \end{aligned}$$

all other non-diagonal matrix elements being zero.

The energies of the levels, together with the (unnormalized) wave functions, found by diagonalizing the matrix, are listed in table 2 for the particular case of $S = 1/2$, $I = 2$, which refers to ^{58}Co .

The results are worked out numerically for the case of Co-ions in Ce-Mg-nitrate. For 1/3 of the ions, $B = 0$, but for the remaining 2/3 of the ions, B is somewhat larger than A and for these latter ions the energy levels have been plotted as a function of $H = H_z$ in fig. 14.

For $H = H_z = 300$ Oe the energies of the levels, taking the lowest level $E_{10} = 0$, and the normalized wave functions are shown in table 3. For later applications the expectation values of $\langle I_z \rangle$ and $\langle I_z^2 \rangle$ have also been indicated. The calculations have not been carried out to an accuracy higher than a few units in the last decimal for ψ and to one unit in $\langle I_z \rangle$ and $\langle I_z^2 \rangle$.

It is seen that a) the energy difference between the lowest levels is smaller than AS_z , which for this case would be $A/2$ b) even for $T = 0$, when only the lowest level would be populated, f_N is not equal to 1. Consequently, the B -term tends to decrease the nuclear polarization; this decrease is reduced by making H larger, but because then also the temperature is increased, the nuclear polarization will not necessarily be augmented.

A general quantitative discussion for the optimal value of H for obtaining maximum f_N cannot easily be given, but some remarks will be made for the case $S = 1/2$. We will first assume that $g\beta H > 2AI$ and

TABLE 2

| | | | |
|--------------------------------------|---------------|--|-----|
| $E_1 = A + g\beta H/2$ | $\psi_1 =$ | $ 1/2, 2 \rangle$ | $>$ |
| $E_2 = -A/4 + \sqrt{P_+^2 + B^2}$ | $\psi_2 =$ | $-B 1/2, 1 \rangle + \{P_+ - \sqrt{P_+^2 + B^2}\} -1/2, 2 \rangle$ | $>$ |
| $E_3 = -A/4 + \sqrt{Q_+^2 + 3B^2/2}$ | $\psi_3 =$ | $-B\sqrt{\frac{3}{2}} 1/2, 0 \rangle + \{Q_+ - \sqrt{Q_+^2 + 3B^2/2}\} -1/2, 1 \rangle$ | $>$ |
| $E_4 = -A/4 + \sqrt{Q_-^2 + 3B^2/2}$ | $\psi_4 =$ | $-B\sqrt{\frac{3}{2}} 1/2, -1 \rangle + \{Q_- - \sqrt{Q_-^2 + 3B^2/2}\} -1/2, 0 \rangle$ | $>$ |
| $E_5 = -A/4 + \sqrt{P_-^2 + B^2}$ | $\psi_5 =$ | $-B 1/2, -2 \rangle + \{P_- - \sqrt{P_-^2 + B^2}\} -1/2, -1 \rangle$ | $>$ |
| $E_6 = A - g\beta H/2$ | $\psi_6 =$ | $ -1/2, -2 \rangle$ | $>$ |
| $E_7 = -A/4 - \sqrt{P_-^2 + B^2}$ | $\psi_7 =$ | $-B 1/2, -2 \rangle + \{P_- + \sqrt{P_-^2 + B^2}\} -1/2, -1 \rangle$ | $>$ |
| $E_8 = -A/4 - \sqrt{Q_-^2 + 3B^2/2}$ | $\psi_8 =$ | $-B\sqrt{\frac{3}{2}} 1/2, -1 \rangle + \{Q_- + \sqrt{Q_-^2 + 3B^2/2}\} -1/2, 0 \rangle$ | $>$ |
| $E_9 = -A/4 - \sqrt{Q_+^2 + 3B^2/2}$ | $\psi_9 =$ | $-B\sqrt{\frac{3}{2}} 1/2, 0 \rangle + \{Q_+ + \sqrt{Q_+^2 + 3B^2/2}\} -1/2, 1 \rangle$ | $>$ |
| $E_{10} = -A/4 - \sqrt{P_+^2 + B^2}$ | $\psi_{10} =$ | $-B 1/2, 1 \rangle + \{P_+ + \sqrt{P_+^2 + B^2}\} -1/2, 2 \rangle$ | $>$ |
| $P_{\pm} = g\beta H/2 \pm 3A/4$ | | $Q_{\pm} = g\beta H/2 \pm A/4$ | |

Table 2. Energies E and wave functions ψ , belonging to the h.f.s. levels for paramagnetic ions with $S = 1/2$ and $I = 2$ in an external magnetic field $H = H_z$ in the direction of quantization z . (A and B are the h.f.s. splitting constants in the spin-Hamiltonian (21); the order of succession of the levels is such that $E_1 > E_2 > E_3$ etc. if $g\beta H \gg A > B > 0$ (fig. 14).

TABLE 3

| E/k in $10^{-3} \text{ }^\circ\text{K}$ | ψ | $\langle I_z \rangle$ | $\langle I_z^2 \rangle$ | | |
|--|---------------------|--|-------------------------|-------|------|
| $E_1 = 124.5$ | $\psi_1 =$ | $ 1/2, 2 \rangle$ | $>$ | 2.00 | 4.00 |
| $E_2 = 119.7$ | $\psi_2 = 0.980$ | $ 1/2, 1 \rangle + 0.198 -1/2, 2 \rangle$ | $>$ | 1.04 | 1.12 |
| $E_3 = 113.6$ | $\psi_3 = 0.965$ | $ 1/2, 0 \rangle + 0.263 -1/2, 1 \rangle$ | $>$ | 0.07 | 0.07 |
| $E_4 = 105.9$ | $\psi_4 = 0.948$ | $ 1/2, -1 \rangle + 0.318 -1/2, 0 \rangle$ | $>$ | -0.90 | 0.90 |
| $E_5 = 96.4$ | $\psi_5 = 0.943$ | $ 1/2, -2 \rangle + 0.330 -1/2, -1 \rangle$ | $>$ | -1.89 | 3.67 |
| $E_6 = 41.7$ | $\psi_6 =$ | $ -1/2, -2 \rangle$ | $>$ | -2.00 | 4.00 |
| $E_7 = 24.3$ | $\psi_7 = 0.943$ | $ -1/2, -1 \rangle - 0.330 1/2, -2 \rangle$ | $>$ | -1.11 | 1.33 |
| $E_8 = 13.9$ | $\psi_8 = 0.948$ | $ -1/2, 0 \rangle - 0.318 1/2, -1 \rangle$ | $>$ | -0.10 | 0.10 |
| $E_9 = 6.1$ | $\psi_9 = 0.965$ | $ -1/2, 1 \rangle - 0.263 1/2, 0 \rangle$ | $>$ | 0.93 | 0.93 |
| $E_{10} = 0$ | $\psi_{10} = 0.980$ | $ -1/2, 2 \rangle - 0.198 1/2, 1 \rangle$ | $>$ | 1.96 | 3.88 |

Table 3. Energies E and normalized wave functions ψ for the h.f.s. levels of ^{58}Co in Ce-Mg-nitrate, calculated for 2/3 of the Co^{++} -ions in an external magnetic field $H = H_z = 300$ Oe. The values of E are expressed in millidegrees Kelvin and the lowest level E_{10} has been taken as zero point on the energy scale. E and ψ have been calculated from table 2 with the aid of the values of A and B , obtained from paramagnetic resonance data (Tre 53) and from the value for the nuclear magnetic moment of ^{58}Co (4.05 n.m.). A and B are positive for a positive nuclear magnetic moment (see III § 5E and IV. § 5). Also the expectation values $\langle I_z \rangle$ and $\langle I_z^2 \rangle$ are given in the table.

that $B(S_x I_x + S_y I_y)$ causes an only small perturbation on the level splittings $\Delta E = A/2$ for $B = 0$. The energy shift $\delta E(I_z)$ of the level ($S_z = -1/2, I_z$) may then be calculated by perturbation theory, which yields

$$\delta E(I_z) = -[I(I+1) - I_z(I_z - 1)] B^2/4 [g\beta H + (2I_z - 1) A/2] \quad (23)$$

The energy difference between the levels $(-1/2, I_z + 1)$ and $(-1/2, I_z)$ is then approximately $\Delta E(I_z + 1, I_z) = A/2 - 2B^2 I_z/4g\beta H$ and the relative change in $\Delta E(I_z + 1, I_z)$ due to the perturbation is then $-B^2 I_z/Ag\beta H$.

Since $S_z = -1/2$, for the upper levels $I_z/A < 0$ and for the lower levels $I_z/A > 0$, which shows, that the lower levels become more closely spaced and the upper levels more widely spaced than if B were zero. However, the relative change in ΔE is smaller than a few per cent if $B < 0.1 A$, provided again that $g\beta H > 2AI$.

If $B \approx A$, a larger field is needed in order to keep the change in ΔE smaller than a few per cent, namely $g\beta H > 0.1 B$. Since large fields are undesirable, one better allows the level splittings to become appreciably different from $A/2$. The splittings can be calculated to a reasonable accuracy with (23) if $B \leq A/2$. If $B > A/2$ the diagonalization of the Hamiltonian is required if accurate results are wanted, unless $g\beta H > 100 B^2/A$, in which case the ratio B/A becomes irrelevant.

Summarizing one may say, that aiming at maximum polarization, it is not necessary to make H larger than is needed to satisfy the relation $H > B^2 I/2Ag\beta$, since then the level splittings are certainly at least 50% of the values for infinite H . The additional requirement $g\beta H > 2AI$ has always to be fulfilled, because otherwise f_e becomes a limiting factor; this requirement is somewhat weakened if, like in the case of Mn, $S > 1/2$ and a term DS_z^2 in the Hamiltonian helps the magnetic field in pulling the levels $S_z = -S$ and $S_z = -S + 1$ apart.

Two facts should further be mentioned:

a) If $A = 0$, nuclear polarization with a field H in the z -direction is still possible, though being a second order effect. This becomes apparent from table 2 under the simplifying assumption $T = 0$, because then only the degenerate level $E_{8,9}$ is populated.

b) For $A < B$, application of a magnetic field in the x or y -direction may be more successful. This problem may be treated mathematically by adding to the Hamiltonian (21): $g_{\perp}\beta(H_x S_+ + H_x S_-)/2$. However, in this case rotational symmetry may not, even approximately, exist and as will be seen in Chapter III, one should be very careful to use the calculated degree of nuclear polarization as a measure for the magnitude of effects in the radiation from radioactive nuclei.

§ 5. Magnetic h.f.s. alignment.

5. A. General remarks.

Alignment of nuclear spins is caused by anisotropy in the h.f.s. interaction or a preferred direction of the electronic angular momentum. (Ble 51, a, b) No preferred direction for the nuclear spins exists if $A=B$ and if moreover the electronic angular momentum behaves like a free spin; in this case the h.f.s. energy is expressed by:

$$E = (1/2) A \{F(F+1) - I(I+1) - S(S+1)\} \quad (24)$$

where $|\mathbf{F}| = |\mathbf{I} + \mathbf{S}|$ can have values ranging from $|I-S| \leq F \leq |I+S|$; from (24) it can be seen that E does not depend on F_x or I_x .

The anisotropy of the h.f.s. interaction can in the Hamiltonian be expressed, either directly by $A \neq B$, or indirectly, like in the case of Mn^{++} , by a term DS_z^2 leading to a preferred direction for the electronic angular momentum (if $S > 1/2$) and consequently also for the nuclear spins, though A may be equal to B .

If $B = D = 0$, the levels for successive values of I_z are separated by the amount AS_z ; a twofold (spatial) degeneracy remains, because the energies of the levels (S_z, I_z) and $(-S_z, -I_z)$ are equal.

If on the other hand $B = A$ and $D \neq 0$, the calculation of the energy levels is complicated, unless $D \gg A = B$, which is essentially the former case, since the B term may then be neglected and the D -term becomes irrelevant for our discussion at temperatures below 1°K . For small values of S and I the energies may be found by diagonalization of the Hamiltonian, but laborious calculations are required if, for instance, $S = 5/2$ and I larger than 2. Approximate solutions can be given by perturbation calculation, either by applying DS_z^2 as a small perturbation to the coupling ASI , the energies of which are given by (24), or by introducing $B(S_x I_x + S_y I_y)$ as a small perturbation to the coupling $DS_z^2 + AS_z I_z$. These two procedures are successful if, for instance, $D \leq 0.2 A$ and $B = A \leq 0.2 D$ respectively.

It may be further mentioned, that calculation of the energy levels for the case $A \neq 0, B \neq 0$ can be treated in nearly the same way as discussed in section 4. G.

Nuclear alignment is particularly of interest for a number of rare earth ions having large, anisotropic h.f.s. splittings in ethylsulfate single crystals. We take the example of the Ho^{+++} ion with stable ^{165}Ho nuclei, for which $I = 7/2$. In a magnetically dilute Ho -ethylsulfate single crystal the lowest temperatures obtained after adiabatic demagnetization, will be determined by the large h.f.s. splitting, being the main contribution to H_{nat} . It may be interesting to discuss the relation between the entropy S ,

the temperature T and the degree of nuclear alignment, which is expressed by the orientation parameter $f_2 = \langle I_z^2 \rangle / I^2 - (I + 1) / 3I$, mentioned in Chapter III.

The entropy S in a large magnetic field can be calculated from the partition function for energy levels, which are determined by the spin-Hamiltonian $\mathcal{H} = g_z \beta H_z + A_z S_z$ where $S_z = \pm 1/2$, $A/k = 0.48^\circ\text{K}$ and $g_z = 15.36$ (Ble 55).

It is then found that, if we write $S = S_e + S_N$,

$$S_e/R = \ln 2 + \ln \sum x - x \frac{\sum x}{\sum x} \quad (25)$$

$$S_N/R = \ln 2 + \ln \sum \text{Ch } y - \frac{\sum y \text{Sh } y}{\sum \text{Ch } y} \quad (26)$$

where $x = g_z \beta H_z / 2kT$ and $y = A I_z / 2kT$ and the summation has to be carried out over $I_z = 1/2, 3/2, 5/2$ and $7/2$ ($I_z > 0$).

For $T = 0$ both S_e and S_N vanish, except if $H = 0$, in which case S_e approaches $R \ln 2$, representing the remaining spatial degeneracy. S_N represents the contribution of the nuclear moments to the entropy and has been plotted in fig. 15 as a function of T .

The maximum entropy which can be removed by isothermal magnetization is $R \ln 2$; it may

be seen from fig. 15 that after adiabatic demagnetization $T = 0.3^\circ\text{K}$ is a lower limit for the temperature since otherwise the decrease in S_N would be larger than $R \ln 2$.

The parameter f_2 has also been plotted as a function of T in fig. 15. Clearly $f_2 = 0.27$ is the upper limit for the degree of nuclear alignment for the stable Ho nuclei, which can be obtained in this case of internal cooling using one sort of paramagnetic ions (see section 4). If also radioactive Ho nuclei are

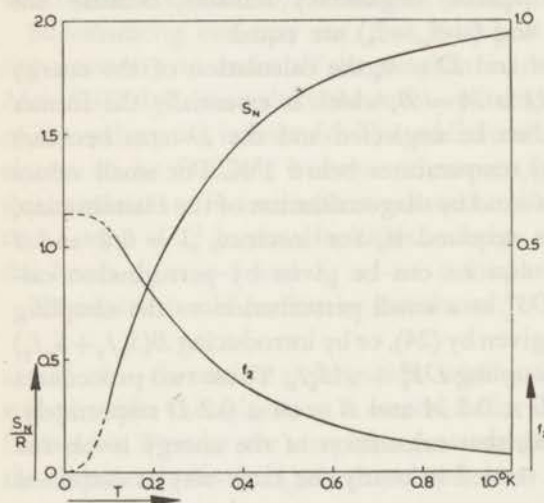


Fig. 15. Entropy S and degree of nuclear alignment f_2 as a function of temperature T for the case of stable ^{165}Ho nuclei ($I = 7/2$) in ethylsulfate single crystals. S_N is the entropy of the nuclear spin system and equals $R \ln(2I + 1)$ at high temperatures. The degree of alignment is given by:

$f_2 = \langle I_z^2 \rangle / I^2 - (I + 1) / 3I$, as is discussed in III, § 1; $f_2 = 0$ at high temperatures and $f_2 = 4/7$ for complete alignment.

incorporated in the crystal, the value of f_2 for these nuclei can be found approximately from the f_2 value for the stable nuclei by a change in scale factor of T , which change is determined by the nuclear gyromagnetic ratios (see also Chapter III, § 1).

5. B. *Advantages of the absence of an external magnetic field.*

H.f.s. alignment is experimentally simpler than h.f.s. polarization, because no external magnetic field is required. The use of a magnetic field has several disadvantages:

a) The major disadvantage is that the temperature of the sample in a polarizing field will be appreciably higher than the temperature in zero field.

b) In order to ensure a homogeneous temperature distribution in a crystal situated in a magnetic field, the field must be homogeneous over the sample volume. This requirement is extremely important for salts like Ce-Mg-nitrate, which have very anisotropic g -values. In such a case, if the field applied in the g_{\parallel} -direction is inhomogeneous, the components of the field in the g_{\perp} -direction will cause a temperature rise, which may be quite different for various parts of the crystal. Experience has shown that the magnetic field should be homogeneous to within about 1% over the sample volume, for the experiments reported herein a cube approximately 3 cm on an edge. If iron core magnets are used to produce the field, then the pole faces must be large because the pole distance cannot be made smaller than the diameter of the cryostat, in our case about 7 cm. A reduction in the diameter of the cryostat can only occur at the expense of the sample diameter.

A homogeneous field of a few hundred Oersteds can be easily obtained with an iron core magnet, but iron cores have some disadvantages as will become clear from the discussion below. A Helmholtz coil can be used to produce very homogeneous fields, but for fields larger than 500 Oe one encounters difficult cooling problems, unless one allows large dimensions for the coils.

c) The material used for producing the magnetic field, gives rise to gamma ray scattering into the detectors. This is particularly serious for iron core magnets, since the iron has to be placed near the source. Moreover the geometry of the arrangement is unfavourably affected. For an iron core magnet it becomes very difficult to measure the intensity of the gamma radiation in the direction of the magnetic field; with Helmholtz-coils a measurement of the intensity for directions making angles of about 45° with the field becomes awkward, but generally such a measurement is not

as desirable as the measurement in the direction of the field. For that reason Helmholtz-coils are often preferred.

d) The magnetic field affects the pulse height and hence the counting rate of the photomultipliers. These should be magnetically shielded and if high field strengths are used, the photomultipliers have to be placed farther from the sample. In the latter case either light pipes are required or the scintillation crystals must be removed from the vicinity of the samples so that smaller solid angles and smaller counting rates have to be accepted.

e) The susceptibility χ_H of the sample in a magnetic field is different from the susceptibility χ_0 in zero field, even if χ_0 and χ_H are measured at the same thermodynamic temperature. In order to know T^\otimes , one must first reduce the measured values of χ_H to χ_0 . The formula for the reduction has been given in section 3.B., but is only valid for spherical samples, so before the transformation from χ_H to χ_0 is applied, χ_H must be first reduced to that for a sphere. Because T^\otimes is found in a less direct manner than in the alignment method, more errors may be introduced.

f) Experimentally, the susceptibility measurements in the presence of a magnetic field, H , are less accurate than in zero field, because vibrations of the cryostat relative to H or variations in H induce currents in the mutual inductance coils. These effects can be reduced by making the field more homogeneous or by adding a compensating coil to the secondary coil.

An additional difficulty is encountered with iron core magnets, since if the magnet is placed around the cryostat the iron causes a shift in the mutual inductance. This shift has to be measured after every run at 1°K, since the shift is not precisely reproducible. Fortunately, this shift is practically independent of the magnetization of the iron, hence also of the magnitude of H .

g) For crystals with very anisotropic g -values the position of the crystals with respect to the direction of H should be well defined and reproducible, otherwise the reduction of χ_H to χ_0 may be in error. This problem is not difficult to solve. The presence of the magnetic field has, on the other hand, the advantage, that the direction of the nuclear spins is defined by the direction of the field and not as in the alignment case, by the crystalline axis. It is obvious that the position of the counters can be more easily defined and reproduced with respect to the magnetic field than with respect to the axis of the crystals in the cryostat.

5. C. *Disadvantages.*

In principle, h.f.s. polarization has some advantages over h.f.s. alignment.

a) If $B = A$ no alignment occurs.

For $B > A$, alignment in a plane will occur, but this is not a very favourable situation for studying the emitted radiations. In these cases h.f.s. polarization is to be preferred.

b) All the effects, which can be observed with oriented nuclei in general, can in particular be observed with polarized nuclei. Aligned nuclei on the other hand do not show some effects which depend on $\langle I_z \rangle / I$ as for example circular polarization of gamma radiation, asymmetry of beta emission, or change in the absorption of polarized neutrons upon reversal of nuclear spin direction.

c) If the values of A or B deviate from the values to be expected on the basis of other evidence, these deviations cannot be simply found from experiments with aligned nuclei. If for instance the observed gamma ray anisotropy is smaller than that to be expected, this may be attributed to many causes. With the h.f.s. polarization method, the validity of the assumptions relative to the degree of nuclear orientation, can be investigated to a certain extent by variation of the polarizing field.

CHAPTER III.

NUCLEAR PHYSICS.

§ 1. Anisotropy of gamma ray intensities.

Nuclear energy levels can, as a consequence of the quantization and the conservation of angular momentum, be characterized by the eigenvalues of their angular momenta, which are expressed in integral or half-integral multiples of \hbar . The conservation law of angular momentum requires that a gamma transition between a nuclear state with angular momentum (spin) \mathbf{I}_i and a state with spin \mathbf{I}_f must carry angular momentum $\mathbf{J} = \mathbf{I}_i - \mathbf{I}_f$, where $|I_i - I_f| \leq |\mathbf{J}| \leq |I_i + I_f|$. Since the transition probability for the gamma transition decreases strongly with increasing J , we will be almost exclusively concerned with $J = 1$ (dipole radiation) and $J = 2$ (quadrupole radiation). Dipole and quadrupole radiation can occur simultaneously between two nuclear levels if $|I_i - I_f| \leq 1$ and $|I_i + I_f| \geq 2$, but we will not consider the case of mixed multipole radiation in any detail because it does not occur in the examples encountered in chapters IV and V, where $I - I_f > 1$.

The wave function of the radiation can be represented by the vector-potential \mathbf{A} of the electromagnetic field. The intensity of a multipole radiation with angular momentum \mathbf{J} is then given by $\mathbf{A}^* \mathbf{A}$, where \mathbf{A} is an eigenvector of \mathbf{J} . The angular dependent part of the intensity can be expressed as a sum of spherical harmonics, which reduces to a sum of even powers of $\cos \vartheta$, where ϑ is the angle with respect to the axis of quantization (z -axis). The expression for the intensity as a function of ϑ is simple in the particular case of dipole radiation ($J = 1$) and $I_i = 1$, $I_f = 0$; this expression, denoted by D_1 , depends of course on the direction of the nuclear spin \mathbf{I}_i with respect to the z -axis. D_1 is in fig. 16 given for the three possibilities $I_z = 1, 0, -1$. The spatial degeneracy of the level $I_i = 1$ has been removed in the fig. by drawing the magnetic sublevels apart. This separation will generally be present only to a very small extent and for a system of unoriented nuclei the populations of the three sublevels will be equal, making the directional distribution $W(\vartheta)$ of the radiation from the system isotropic. This can be seen from the addition

$W(\vartheta) = a_{-1} D_1^{-1}(\vartheta) + a_0 D_1^0(\vartheta) + a_1 D_1^1(\vartheta)$ where $a_1 = a_0 = a_{-1} = 1/3$ are the relative populations of the sublevels. If all nuclear spins \mathbf{I}_i are polarized

in the direction of quantization, $a_1 = 1$ and $a_0 = a_{-1} = 0$ and $W(\theta) = \frac{3}{4}(1 + \cos^2\theta)$; a diagram for $W(\theta)$ was given in fig. 3.

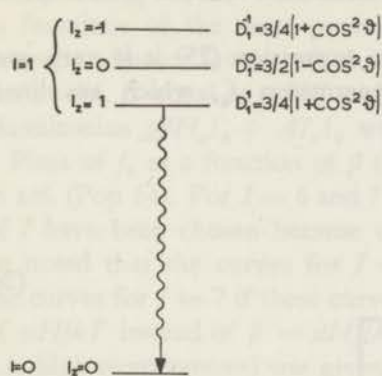


Fig. 16. Directional distributions D_1 of dipole radiation from an initial state $I = 1$ to a final state $I = 0$, given for the three possible values of the z -component of the initial spin. θ is the angle between the direction of emission and the axis of quantization. The magnetic sublevels have been drawn separated; D_1 gives the directional distribution for the case that the nuclear spins are completely polarized along the positive z -axis.

when the first results were reported in Oxford (Dan 51) and Leiden (Gor 51, Pop 52). Theoretical expressions for the directional distributions of the radiations have been given by a number of authors; for references see (Bli 53, 55, 57, Ste 57). We will discuss here in some detail the elegant treatment of COX, TOLHOEK and DE GROOT (Cox 52, Tol 52, 53, Gro 55, Har 55).

If a system of oriented nuclei has an axis of rotational symmetry, as is true in the large majority of cases and if this axis is taken as the axis of quantization, then the directional distribution $W(\theta)$ of the radiation is given by $W(\theta) = \sum_m a_m D_1^m(\theta)$ (25)

Here $m = I_z$ is the magnetic quantum number of the nucleus in its initial state with spin I ; a_m is the relative population of the level with quantum number m ; in case of rotational symmetry the nuclear orientation is completely determined by the values of a_m . Summation over all the magnetic

Though in many cases $J = I_i - I_f$, this is not always true and then different directional distributions occur. In principle one should be able to distinguish between the various radiations $J = 1$ (or $J = 2$), accompanied by a change of 1, 0 or -1 (respectively 2, 1, 0, -1 and -2) units of the nuclear spin, if directional distributions of gamma radiations from oriented nuclei are observed. For instance the sign of the anisotropy ϵ , defined by $\epsilon = [W(\pi/2) - W(0)]/W(\pi/2)$ is negative for a dipole radiation with a spin decrease of 1 and ϵ is positive for a quadrupole radiation with spin decrease 2. Hence measurements of the anisotropy of the intensity of gamma radiation from oriented nuclei may be a useful means for nuclear spectroscopy.

This has been experimentally shown for a dozen of nuclei since 1951,

sublevels gives $\sum_m a_m = 1$. At high temperatures, where the levels will be nearly equally populated, $a_m = 1/(2I + 1)$ for all m . $D_I^m(\theta)$ is the directional distribution of the radiation from the nucleus in the (I, m) state* (here $I = I_0$).

For the mathematical treatment of the expression (25) it is very convenient to introduce the orientation parameters f_k , which are linear functions of the a_m :

$$\begin{aligned} f_1 &= \frac{1}{I} \sum_m m a_m \\ f_2 &= \frac{1}{I^2} \left[\sum_m m^2 a_m - \frac{1}{3} I(I+1) \right] \\ f_3 &= \frac{1}{I^3} \left[\sum_m m^3 a_m - \frac{1}{5} (3I^2 + 3I - 1) \sum_m m a_m \right] \\ f_4 &= \frac{1}{I^4} \left[\sum_m m^4 a_m - \frac{1}{7} (6I^2 + 6I - 5) \sum_m m^2 a_m + \frac{3}{35} I(I-1)(I+1)(I+2) \right] \end{aligned} \quad (26)$$

f_1 can also be written as $\langle I_z \rangle / I$, and is called the nuclear polarization; it is also the magnetization due to the nuclear magnetic moments divided by the saturation magnetization. If $f_1 = 0$, nuclear orientation may still exist. In fact, for systems of oriented nuclei, which are symmetric with respect to reversal of positive and negative directions of the axis of rotational symmetry, all $f_k = 0$ with $k = \text{odd}$. In this case we speak of alignment.

The meaning of f_2 can be understood from the following statements:

- $f_2 = 0$, or $\langle I_z^2 \rangle = (1/3)I(I+1)$ for randomly oriented nuclei;
- $f_2 > 0$ for alignment along the axis of rotational symmetry;
- $f_2 < 0$ for alignment in a plane perpendicular to the rotational axis.

If $f_1 \neq 0$, then usually $f_k \neq 0$ for $k \leq 2I$. In very special cases, however, this may not be so, as for example in the case of ^{60}Co nuclei which show an anisotropic β -emission. If from a number of randomly distributed ^{60}Co -nuclei in particular those nuclei are considered, which emit a β -particle in the direction of the quantization axis, then such a system is characterized by $f_1 \neq 0$ and $f_2 = f_3 = f_4 = 0$. This is related to the fact that in spite of non-conservation of parity in β -decay, no β - γ -directional-correlation has been observed for the allowed β -decay of ^{60}Co .

If the populations a_m are given by the Boltzmann-distribution over equally spaced magnetic sublevels, then the parameter f_k can be written

* The notation D_I^m differs from the notation of COX and TOLHOEK and should also not be confused with the symbol for the rotation group operators.

as a function of temperature T , with I and the level splitting as parameters. f_1 then reduces to the Brillouin-function, as a measure of nuclear magnetization. The f_k for $k > 1$ are more complicated, but all f_k can be expressed as functions of the same parameter $\beta \equiv \Delta/kT$. Here Δ is the splitting between adjacent levels, which, in case of external field polarization of the nuclei, is equal to $\mu H/I$ and for the h.f.s. polarization, defined by a Hamiltonian $g\beta H_x S_x + AI_x S_x$ with $S = 1/2$, equal to $A/2$.

Plots of f_k as a function of β for various spin values I are to be found in ref. (Pop 54). For $I = 6$ and 7 they are shown in fig. 17. These values of I have been chosen because of later applications (chapter V); it may be noted that the curves for $I = 6$ would approximately coincide with the curves for $I = 7$ if these curves would have been plotted as a function of $\mu H/kT$ instead of $\beta = \mu H/IkT$. An approximation of f_1 for small β (i.e. high temperatures) was given in (18). More generally the high temperature approximation for f_k is $f_k \sim T^{-k}$, a result which is of importance in comparing the order of magnitude of nuclear phenomena. Further $f_k = 0$ for $I < k/2$, for instance if $I = 1/2$, only $f_1 \neq 0$, hence the concept of alignment is meaningless for nuclei with spin $1/2$.

After introduction of the orientation parameters, the angular distribution $W(\vartheta)$ can be expressed by the formula:

$$W(\vartheta) = 1 + \sum_{k \text{ even}} b_k f_k P_k(\cos \vartheta) \quad (27)$$

$P_k(\cos \vartheta)$ is a Legendre function and b_k is a parameter, depending on 1) the spin I_i of the initial level; 2) the spin change $\Delta I = I_i - I_f$; and 3) the multipole order J of the gamma transition, $|\Delta I| \leq J$. Further $k \leq 2J$, so that the expansion has only one term for dipole radiation, two terms for quadrupole radiation etc. No higher multipole orders will be considered here. If the gamma transition is of mixed multipole order, the same expression can be used with b_k depending on the mixing ratio δ . Because interference between the two multipole radiations occur, the b_k for a mixed multipole radiation cannot simply be found by a linear combination of the b 's for pure multipole radiations (Har 55). In (Did 57b) an example is given of $W(\vartheta)$ as a function of the mixing ratio δ and from this it may be seen how drastically the b 's are changed by the interference terms. From the foregoing discussion it will be clear, that the terms in the expansion for $W(\vartheta)$ are the product of f_k , determined by the degree of nuclear orientation of the initial nucleus alone, and of $b_k P_k$ which is only determined by the details of the gamma decay. Since we will be almost exclusively concerned with the angular distribution of that quadrupole radiation, called (Q, -2) radiation, which is accompanied by a decrease of the nuclear

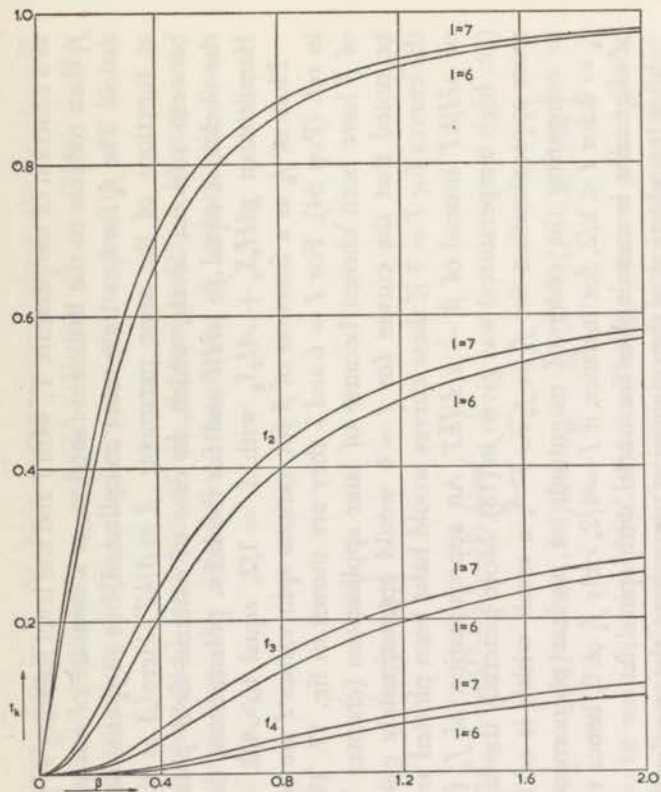


Fig. 17. Orientation parameters f_k for $I = 6$ and $I = 7$ as functions of the parameter $\beta = \Delta/kT$, where Δ is the energy difference between adjacent h.f.s.-levels.

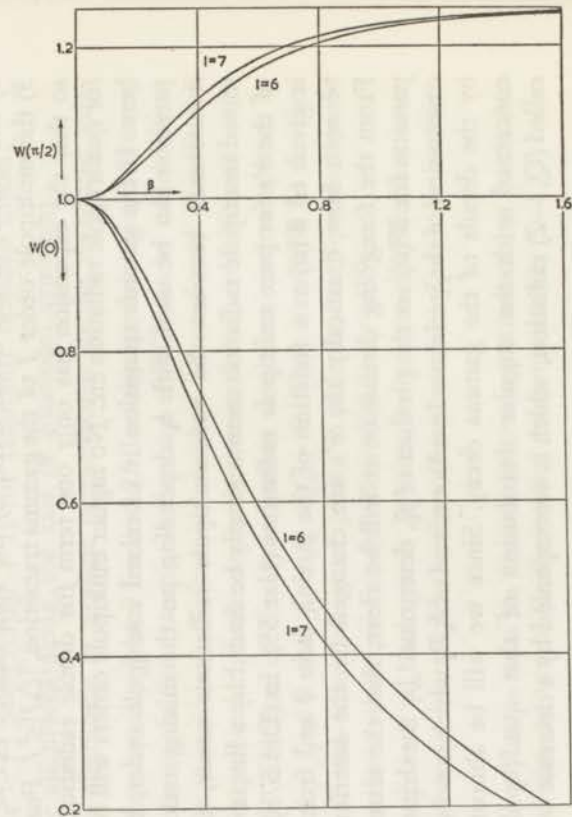


Fig. 18. Intensity W of a quadrupole radiation with a spin decrease of 2, $(Q, -2)$, given as a function of the parameter $\beta = \Delta/kT$ and for the directions $\theta = 0$ and $\theta = \pi/2$ with respect to the axis of nuclear polarization or alignment. W depends also on the spin I of the initial nucleus, except for complete nuclear polarization or alignment. Also the directional distributions $W(\theta, T)$ for successive $(Q, -2)$ radiations in a gamma ray cascade are equal.

spin of two units, the explicit form of formula 27 will be given only for this case (other examples are to be found in Pop 54):

$$W(\vartheta) = 1 - 15/7 N_2 f_2 P_2(\cos \vartheta) - 5 N_4 f_4 P_4(\cos \vartheta) \quad (28)$$

N_2 and N_4 depend on the value of the nuclear spin I_i of the initial level:

$$N_2 = I_i/(2I_i-1) \quad N_4 = I_i^3/(I_i-1)(2I_i-1)(2I_i-3) \quad (29)$$

$W(\vartheta = 0)$ and $W(\vartheta = \pi/2)$ are plotted as a function of β for the cases $I_i = 6$ and $I_i = 7$ in fig. 18.

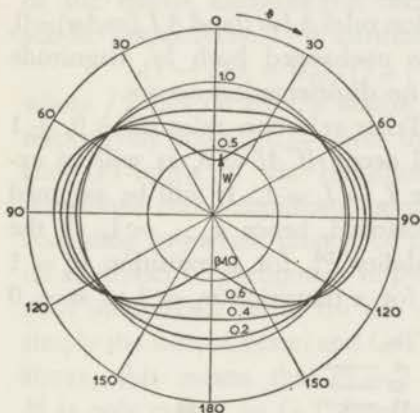


Fig. 19. Directional distribution W of a $(Q, -2)$ radiation as a function of the angle θ of emission with respect to the axis of nuclear polarization. The parameter β depends on temperature according to $\beta = \Delta/kT$, Δ being the energy difference between successive h.f.s. levels. W is only slightly dependent on T for $\theta = 55^\circ$, where $P_2(\cos \theta) = 0$.

W as a function of θ and for a few values of β is shown in fig. 19.

If successive radiations $(Q, -2)$ are considered, like those to be found in the decay of the nuclei ^{60}Co and ^{52}Mn , the nuclear spin decreases during the decay. It is then not necessary to calculate N_k and f_k for each gamma transition separately, since it was shown by COX and TOLHOEK (Cox 53), that in a decay sequence proceeding by $(Q, -2)$ radiations, $N_k f_k$ remains constant. This result signifies that the degree of nuclear orientation is not disturbed by $(Q, -2)$ or more generally, by $(J, \Delta I = -J)$ transitions, consequently the angular distributions of successive $(Q, -2)$ radiations are expected to be equal (see also Fan 57).

§ 2. Disorientation by a preceding beta-transition.

If one wants to study the directional distribution of the intensity of gamma radiation emitted by a system of oriented nuclei, one generally has first a β -decay of the initial nucleus (spin I_0) to an excited state of the residual nucleus (spin I_i), whereafter one or more gamma transitions occur (fig. 20). These gamma transitions proceed usually in a much shorter time than the time required for establishing a Boltzmann distribution over the sublevels of the state I_i , hence the orientation parameters $f_k(I_i)$ are determined by the $f_k(I_0)$ and, possibly, by the influence of the β -transition $I_0 \rightarrow I_i$ ($\Delta I = I_0 - I_i$) on the orientation.

We will see presently, that after β -decay from a system of completely

polarized nuclear spins I_0 , the resultant spins I_i may not be completely polarized.

The disorientation depends on the details of the β -interaction leading to the β -decay, which may be either negaton or positon emission or K-capture. We will consider only allowed β -decay. Although at present fundamental concepts concerning β -interaction are very much questioned, there is no doubt as to the validity of the (phenomenological) distinction between Fermi and Gamow-Teller selection rules and this distinction is all that we need for the following discussion.

For a β -transition obeying Fermi selection rules $\Delta I = 0$ and $\Delta I_z (\equiv \Delta m) = 0$, consequently the nuclear spin remains unchanged both in magnitude and direction, hence $f_k(I_0) = f_k(I_i)$ and no disorientation occurs.

For a β -transition obeying Gamow-Teller selection rules $\Delta I = 0, \pm 1$ and $\Delta m = 0, \pm 1$; a disorientation will occur if $\Delta I = 0$, as will be explained with the aid of fig. (21), where $I_0 = I_i = 1$. It will be assumed that the nuclear spins are completely polarized, hence $a_{m=1} = 1$, all the other a_m 's being zero. Now the probability P_1^1 , for a transition $m_0 = 1$ to $m_i = 1$ relative to the probability P_1^0 , for a transition $m_0 = 1$ to $m = 0$

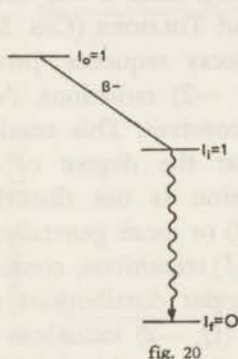


Fig. 20. γ -decay from a state with spin $I_i = 1$ to a state with spin $I_f = 0$, preceded by a β -transition $I_0 = 1 \rightarrow I_i = 1$.

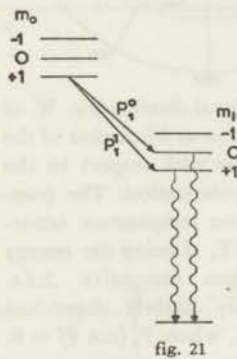


Fig. 21. Disorientation in a system of completely polarized nuclei as a result of a β -decay obeying Gamow-Teller selection rules $\Delta I = 0, \Delta I_z (\equiv \Delta m) = 0, \pm 1$. The fractional transition probabilities P_1^1 for $\Delta m = 0$ and P_1^0 for $\Delta m = -1$ are equal for this case ($I_0 = I_i = 1$, fig. 20).

is given by the ratio $P_1^0/P_1^1 = 1/I = 1$, which ratio is merely determined by geometrical considerations. From this one derives $f_1(I_i) = (\frac{1}{2}) f_1(I_0)$ and more generally for a transition $I_0 = I \rightarrow I_i = I$ (Cox 53)

$$f_k(I_i) = \left[1 - \frac{k(k+1)}{2I_0(I_0+1)} \right] f_k(I_0) \quad (30)$$

However, no disorientation occurs for a GT-transition if $\Delta I = -1$,

since then the nuclear spin changes in magnitude but not in direction; this is mathematically expressed by the relation $N_k(I_o)f_k(I_o) = N_k(I_i)f_k(I_i)$, which can be understood for $k = 1$ and completely polarized nuclei, for which $N_1(I_o) = f_1(I_o) = N_1(I_i) = f_1(I_i) = 1$.

If for a β -transition $\Delta I = 0$, the decay may be caused either by Fermi-interaction or by GT-interaction or by both. Since Fermi-interaction causes no disorientation of the nuclear spins, whereas GT-interaction does, the disorientation for $\Delta I = 0$ depends on the relative magnitude of the matrix elements (i.e. decay probabilities) of GT and Fermi interaction respectively. It is customary to define:

$$(1 - \lambda)/\lambda = C_{GT}^2 |f\sigma|^2 / C_F^2 |f1|^2 \quad (0 \leq \lambda \leq 1) \quad (31)$$

where $f1$ and $f\sigma$ are the matrix elements for Fermi and G.T.-interaction respectively and C_F/C_{GT} gives the relative magnitude of the Fermi terms and GT-terms in the Hamiltonian for the β -interaction. It has to be mentioned that interference between Fermi and GT-interactions might, according to present theory, be possible and could have a profound effect on a number of phenomena in β -decay. In the decay probability, however, such interference terms do not occur and the total decay probability is simply the sum of Fermi and G.T. transition probabilities. For the example above, this means that $P_1^1 = \lambda + (1 - \lambda)I/(I + 1) = \frac{1}{2}(1 + \lambda)$ whereas P_0^0 is only caused by G.T.-interaction: $P_1^0 = (1 - \lambda)/(I + 1) = (1 - \lambda)$.

If one could measure the degree of disorientation actually occurring in an allowed β -transition with $\Delta I = 0$, then the parameter λ might be determined. It is seen that large disorientations can occur only for small values of the nuclear spin (for $I = 1$, even the sign of the anisotropy ϵ of the succeeding gamma transition may be reversed by the disorientation (Did 57a). A nucleus for which a large disorientation may occur is ^{58}Co because of the comparatively small value of $I_o = 2$. Measurements of GRIFFING and WHEATLEY on ^{58}Co , incorporated in a Tutton salt, yielded $\lambda = 0.12 \pm 0.04$ (Gri 56).

We will discuss the example of ^{58}Co in some detail since an accurate determination of λ is of interest for experiments on the asymmetry of β -decay from this nucleus; these experiments (Amb 57, Pos 57b) agree with present theory if $\lambda < 0.03$.

The disorientation results in a smaller anisotropy of the gamma radiation than may be otherwise expected. In order to deduce λ from the observed anisotropy, one has to know the theoretical, undisturbed, anisotropy as a function of T . This requires detailed knowledge about the orientation mechanism. Fortunately most parameters involved are rather accurately known: both the magnetic moment and the spin of the ^{58}Co -nucleus have been determined by paramagnetic resonance absorption to be 4.05 n.m.

and $I_0 = 2$ respectively (Dob 57). From gamma ray anisotropy measurements with aligned nuclei it could be definitively concluded that the spin I_1 of the first level of the daughter nucleus ^{58}Fe is also equal to 2 (Dan 52, Whe 55a, Gri 56), which makes the intensity of a quadrupole transition from that level to the ground state equal to: $W(\theta = 0) = 1 - (10/7)f_2 - (40/3)f_4$. The values of f_2 and f_4 as a function of temperature have been calculated for Co-ions in Ce-Mg-nitrate and a polarizing magnetic field of 300 Oe; for this calculation the results of II, § 4, particularly table 3 were used. $W(0)$ as a function of temperature and of the parameter λ is obtained from f_2 and f_4 with the aid of (30) and the result is shown in fig. 22.

At temperatures $1/T < 20$, f_4 can be neglected and (using 30)

$$f_2(I_i) = \lambda f_2(I_0) + \frac{1}{2}(1 - \lambda) f_2(I_0) = \frac{1}{2}(1 + \lambda) f_2(I_0).$$

If λ is small, then a determination of λ with an absolute accuracy of 0.10 requires the determination of $1 - W(0)$ and of $1/T$ with a relative accuracy of about 10%. It may be estimated, that for instance in Ce-Mg-nitrate f_2 is known with an accuracy of better than 10% if a polarizing field of at least 500 Oe is used, but with this field the temperature determination may not be more accurate than 5–10%. About the same accuracies are estimated for the temperature measurements in salts like Tutton salts

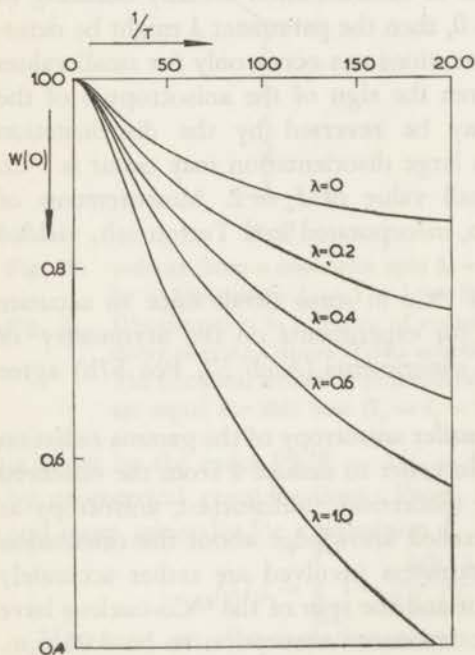


Fig. 22. Influence of a disorientation, due to β -decay, on the gamma ray intensity W as a function of temperature T and of the parameter λ . $W(0)$ is the calculated, normalized intensity of the 0.81 MeV ($Q, -2$) radiation of ^{58}Co , emitted in the preferred direction for the nuclear spins. The calculations have been made for the particular case of Co-ions in Ce-Mg-nitrate and a polarizing field $H = 300$ Oe in the direction of small g -value of the Ce-ions. The h.f.s. splittings and the values of $\langle I_z^2 \rangle$ were given in table 3 for $\frac{2}{3}$ of the Co-ions; for the remaining $\frac{1}{3}$ of the ions equidistant h.f.s. levels may be assumed (Tre 53). λ is the fraction of β -decays caused by Fermi interaction.

and Ni-fluosilicate, in which ^{58}Co nuclei can be aligned. It is seen, that a higher accuracy than 0.10 for λ cannot be easily obtained.

If lower temperatures can be reached the contribution of f_4 also becomes appreciable. A comparison between $W(\vartheta = 0)$ and $W(\vartheta = \pi/2)$ yields:

$$\Lambda \equiv (1/2) \{1 - W(0)\} - \{W(\pi/2) - 1\} = (35/9) (-2 + 5\lambda) f_4.$$

Now the maximum value of f_4 , at $T = 0$, is 0.0214. If for instance $\lambda \approx 0.10$ and again an accuracy of 0.10 is required, one has to determine Λ to within 0.03. This is not difficult from an experimental point of view; but in order to deduce λ from the observed value Λ it is necessary to know f_4 with an accuracy of about 30%. Although T may not be known accurately, this is no serious limitation for the accuracy of f_4 if T is low, since then f_4 is not strongly dependent on T (for *high* T , $f_4 \propto 1/T^4$). However, f_4 can only be reliably calculated from T if the h.f.s. levels are equidistant, which requires a polarizing magnetic field of appreciable magnitude, since f_4 is rather sensitive to small variations in the h.f.s. levels.

The determination of λ is further encumbered by the difficulty, that
 a) in Ce-Mg-nitrate the Co-ions can occur in two different places in the lattice, in which very different h.f.s. splittings occur; $W(0)$ is sensitive to the population distribution of the ^{58}Co -ions over the two lattice positions.
 b) in Tutton salts also two different lattice positions occur; the preferred axes of alignment for the nuclear spins are differently oriented with respect to the tetragonal crystal axis.

The foregoing semi-quantitative discussion and fig. 22 may show that an accurate determination of λ is mainly limited by lack of knowledge about the h.f.s. splittings.

§ 3. Determination of the magnitude of the nuclear magnetic moment.

In view of the experiments described in chapter V it may be useful to discuss concisely how the magnitude of the nuclear magnetic moment of an oriented nucleus may be obtained from the observed anisotropy of the gamma ray intensity from the daughter nucleus. It will be clear from § 1, that for such a determination the parameters involved in the radioactive decay should in principle be known. This requirement is very often fulfilled for at least one gamma transition in the decay; for instance, if the multipole order of that transition has been determined from the sign of the anisotropy and if the transition proceeds to the ground state with zero spin, then the spin and the spin change of the excited level will be known.

From the experimentally observed $W(\vartheta, T)$ one derives $f_2(T, I_i)$ and $f_4(T, I_i)$ for the nuclear level with spin I_i . If that state was fed directly

by a β -transition from the initial nucleus with spin I_0 and if the disorientation caused by the β -transition is known (for instance, for an allowed transition with $I_0 = I_i + 1$), then one can transform $f_k(T, I_i)$ into $f_k(T, I_0)$. However, the additional assumption is required that no reorientation of the nuclear spins occurs during the life time of the excited level with spin I_i .

In practice, problems encountered so far in the discussion, can be reasonably solved for several nuclei belonging to the iron group elements. Sometimes, however, neither I_0 nor the disorientation effects in the β -decay are known, in which case $f_k(T, I_0)$ can only be approximately calculated from $W(\vartheta, T)$. In the nuclei of rare earth ions, mixed transitions and comparatively long life times of the levels often occur, in which case the determination of $f_k(T, I_0)$ becomes difficult, particularly if the mixing ratio δ of the multipole radiations is unknown.

Once $f_k(T, I_0)$ is derived from the experiment, nuclear decay parameters have been eliminated from the problem, which is then reduced to a discussion of the h.f.s. level splittings. For the case of equidistant h.f.s. levels theoretical curves of f_k as a function of Δ/kT were given in section 1, where Δ is the splitting between adjacent levels. The theoretical curve of, for instance, f_2 may be fitted to the experimental f_2 vs T curve by an appropriate choice of the scale factor Δ/k . The comparison yields the value of Δ for the radioactive nucleus; in case the h.f.s. coupling is (solely) determined by $AS_z I_z$, Δ is equal to $|AS_z|$, A being proportional to the nuclear gyromagnetic ratio μ/I_0 .

Suppose that A for a stable nucleus in the same salt has been measured by paramagnetic resonance absorption and that also μ and I are known. Comparison of that A with the A value deduced from the nuclear orientation experiment leads to an evaluation of μ for the radioactive nucleus.

Alternatively, instead of fitting theoretical and experimental f_k vs T curves, also the theoretical W vs Δ/kT and experimental $W(\vartheta)$ vs T curves may be fitted for a definite value of Δ . It should be mentioned that for large I_0 , the value of I_0 is irrelevant for the determination of μ , since for a fixed value of the nuclear magnetic moment μ the theoretical functions $f_k(T)$ and $W(\vartheta, T)$ are approximately independent of the parameter I_0 .

Problems become more difficult if the h.f.s. levels are not equidistantly spaced, because then more parameters are involved in the evaluation of μ from f_2 . In this case the calculation has to be started from the spin-Hamiltonian, taking a reasonable value for the μ of the radioactive nucleus, from which then the h.f.s. constants are obtained by comparison with the known constants for the stable nucleus. From the h.f.s. splittings $f_k(T)$ can be calculated, assuming a Boltzmann distribution over the energy

levels. The calculated $f_k(T)$ or $W(\vartheta, T)$ may be compared with the experimental curves and in successive approximations reasonable agreement can sometimes be obtained for an appropriate choice of μ .

In view of the large number of parameters involved, it is not surprising that a high accuracy for μ cannot always be obtained. The limits to that accuracy are mainly given by:

- 1) the inaccuracy of the temperature determination, which is not predominantly caused by lack of experimental accuracy but by systematic errors in the $T-T^\circ$ relation as a result of insufficient knowledge about the relative magnitude of H_{loc} and H_{ext} .
- 2) lack of precise knowledge about the magnetic environment of each ion and hence of the preferred direction of the nuclear spin for each ion in particular, or alternatively, inaccurate knowledge of the h.f.s. splittings. It should be mentioned that usually the constants in the spin-Hamiltonian are measured for stable nuclei of a paramagnetic ion
 - a) in salts which are magnetically much more diluted than the salts used for the adiabatic demagnetization technique;
 - b) in an external field which is much higher than either the small external magnetic field used in the h.f.s. polarization measurements or the zero external magnetic field in the h.f.s. alignment measurements; and
 - c) at temperatures ranging from 4—20°K, which are much higher than the temperatures used in the nuclear orientation experiments.

It is clear that under such circumstances for instance dipole-dipole coupling between neighbouring ions may be different from the coupling under the conditions of nuclear orientation.

- 3) Inhomogeneity of the temperature distribution in the sample; if the temperature is inhomogeneous, the susceptibility measurement yields an average value of $1/T$, whereas the counting rate is an average value of $W(T)$, which, for instance, at high temperatures is proportional to T^{-2} .

For a number of Co-nuclei the magnetic moments were determined both by nuclear orientation experiments and paramagnetic resonance absorption. Reasonable agreement was found in most cases, though it was also shown that the reliability of the nuclear orientation results is limited to about 10—20%. (Dob. 56, 57).

It was shown by WHEATLEY *et al.* (Whe 55a), that a higher accuracy can be obtained in the comparison of two radioactive nuclei, incorporated in one crystal, if the radiations from these nuclei are simultaneously observed as a function of temperature.

§ 4. Circular polarization of gamma radiation.

Circular polarization has been a well known concept in the theory of light and electromagnetic radiation since the experiments of FRESNEL in 1823 (Fre 23). POYNTING (Poy 09) supposed that circular polarization of light was connected with angular momentum of radiation, and could be expressed by the relation $G = \pm W/\omega$ in which G and W represent the angular momentum and energy per unit volume respectively, and ω is the angular frequency. If we write this relation for a photon with $W = \hbar\omega$, we obtain $G = \pm \hbar$.

The angular momentum per unit volume of a radiation field may be defined by

$$\mathbf{G} = \int \frac{1}{cV} \{ \mathbf{R} \times (\mathbf{E} \times \mathbf{H}) \} d\tau \quad (32)$$

where $(c/4\pi) (\mathbf{E} \times \mathbf{H})$ is the Poynting momentum vector and \mathbf{R} is the radius vector from the origin to the volume element $d\tau$. If one applies this formula to a circularly polarized plane wave, one runs into difficulties (Bro 49). Consider for example the right hand circularly polarized plane wave formally described by

$$\begin{aligned} \mathbf{E} &= \text{Re} (E_x + i E_y) e^{i(\omega t - kz)} \\ \mathbf{H} &= \text{Re} (H_x - i H_y) e^{i(\omega t - kz)} \end{aligned} \quad (33)$$

Re = „real part of“, $|E_x| = |E_y| = |H_x| = |H_y|$. For a right hand coordinate system the z -axis is the direction of propagation and an observer looking in the opposite direction would see a clock-wise rotating electric vector.*

EHRENFEST (Ehr 11) pointed out, that for a wave infinitely extended in the xy -plane, $G_z = 0$, which can be readily seen from the fact that $(\mathbf{E} \times \mathbf{H})_x = (\mathbf{E} \times \mathbf{H})_y = 0$. The values of G_x and G_y depend upon the choice of the origin and are zero if the volume V has rotational symmetry around the z -axis (i.e. cylinder) which will be assumed in the following, because G_x and G_y are irrelevant for the discussion hereafter.

However, if the plane wave has a finite extension in the xy -plane, it can be shown that (32) does not lead to $G_z = 0$. (Hum 43, Bro 49, Hei 54). For example the volume V is a cylinder around the z -axis and the fields \mathbf{E} and \mathbf{B} drop to zero on the wall of the cylinder, then it is found that $G_z = W/\omega$. It is interesting to note that, although G_z arises apparently from the boundary of the wave, G_z is proportional to the energy W and hence to V . It has been discussed by HUMBLET (Hum 43) that G_z can be

* This definition of right and left circular polarization agrees with the optical convention (Bor 33) and differs from the convention followed in (Bla 52).

considered as the z-component of the spin angular momentum of the plane wave.

If a circularly polarized plane wave of finite extension is absorbed, there results a transfer of angular momentum to the absorber, which may start rotating. Such effects were observed in experiments on absorption of polarized light (Bet 36) and microwaves (Car 49).

The description of angular momentum of electromagnetic radiation is more straightforward when using the multipole expansion of the radiation field, which we will discuss here in some detail (see also Ros 55, Moz 55). The Maxwell equation in free space can be replaced by the Helmholtz-equation for the vector potential $\Delta \mathbf{A} + k^2 \mathbf{A} = 0$.

Suppose this were a scalar equation. From the transformation properties of such an equation under rotations in space it follows that solutions exist which possess a definite angular momentum. More properly said: because the equation commutes with the operators \mathbf{L}^2 and L_z , where $\mathbf{L} = -i\mathbf{r} \times \text{grad}$, the solutions can be chosen as eigenfunctions of \mathbf{L}^2 and L_z .

For the vector Helmholtz equation the situation is somewhat more complicated. It is necessary to introduce the operator $\mathbf{J} = \mathbf{L} + \mathbf{S}$, in which \mathbf{L} is again $-i\mathbf{r} \times \text{grad}$ and \mathbf{S} is an operator of spin angular momentum defined by the relations $S_x \mathbf{A} = i \mathbf{e}_x \times \mathbf{A}$ and correspondingly for y and z, $\mathbf{e}_x, \mathbf{e}_y, \mathbf{e}_z$ are unit vectors in x, y, z direction (Moz55). Now the solutions of the vector equations can be chosen as simultaneous eigen vectors of the operators J_z, \mathbf{J}^2 and \mathbf{S}^2 . This can be interpreted as saying that the solutions are characterized by the total angular momentum, \mathbf{J} , the sum of the orbital angular momentum, \mathbf{L} , and spin angular momentum, \mathbf{S} .

The following relations can be proved:

$$J_z \mathbf{A}_{JM} = M \mathbf{A}_{JM} \quad (34)$$

$$\mathbf{J}^2 \mathbf{A}_{JM} = J(J+1) \mathbf{A}_{JM} \quad (35)$$

$$\mathbf{S}^2 \mathbf{A}_{JM} = 2 \mathbf{A}_{JM} \quad (36)$$

It can also be shown that \mathbf{A}_{JM} is not an eigenvector of the operators \mathbf{L}^2, L_z and S_z . From the first two relations it follows that the solutions \mathbf{A}_{JM} , which will be called pure multipole fields, have a total angular momentum \mathbf{J} with component M in the z-direction.

The third relation may be expressed by saying that the vector field has an intrinsic spin 1, which is essentially a consequence of the transformation properties of the vector field under rotations in space.

The solutions \mathbf{A}_{JM} can be separated in divergenceless and irrotational parts, which are called transverse and longitudinal fields respectively. The latter fields are absent in the case of zero scalar potential φ , since then the Lorentz condition $\varphi + \text{div} \mathbf{A} = 0$ reduces to $\text{div} \mathbf{A} = 0$ (transverse fields). Since the operator of space reflection (parity operator) com-

mates with the vector Helmholtz equation, the solutions \mathbf{A}_{JM} can be chosen as having a definite parity; for each pure multipole field (transverse fields, characterized by certain eigenvalues of \mathbf{J}^2, J_z) there arise two linearly independent solutions, one with even and the other with odd parity; the field with parity $(-1)^J$ is called „electric” radiation, the field with parity $(-1)^{J+1}$ „magnetic” radiation.

We mention without further discussion that:

- 1) any solution of the Helmholtz equation can be expanded in the pure multipole fields.
- 2) gamma radiations are in the majority of cases pure multipole fields, either electric or magnetic.

Mixing can occur only between radiations of the same parity and is practically confined to mixtures of magnetic dipole (M1) and electric quadrupole (E2) radiation.

Returning now to the discussion of circular polarization, it can be shown, that a pure multipole radiation with $M > 0$ has the property that the electric vector is rotating clockwise looking along the positive z-axis and is therefore left circularly polarized for an observer looking from $+z$ to $-z$ and right circularly polarized for an observer looking from $-z$ to $+z$ and vice versa for anti-clockwise rotations ($M < 0$) looking along the positive z-axis. Circular polarization is therefore connected with the component of angular momentum in the z-direction, M .

This can also be illustrated for a plane wave, which can be expanded in an infinite sum of pure multipole fields. It turns out, that in the expansion only fields occur with $M = +1, -1$, and are consequently circularly polarized. For a left-circularly polarized plane wave with the positive z-axis as the direction of propagation, all fields in the expansion have $M = +1$. Now a plane wave has no orbital angular momentum for reasons of symmetry, so that the relation $J_z = L_z + S_z$ reduces in this particular case to $J_z = S_z = M = 1$.

In a restricted sense one can therefore say that the circular polarization of the radiation is related to the component of the photon spin in the direction of propagation. The restrictions are the following:

- 1) The whole treatment of multipole fields above has been made in a particular gauge, namely $\text{div } \mathbf{A} = 0$ (no scalar potential). However, if the multipole field solutions of the vector Helmholtz equation were expressed directly in the fields \mathbf{E} and \mathbf{B} , which are observable quantities in contradistinction to \mathbf{A} , then the foregoing discussion remains valid in any gauge.
- 2) The subdivision of J_z into $L_z + S_z$ cannot in general be made in a gauge invariant manner. It can only be proved (Jau 55) that the component of spin angular momentum along the axis of propagation is gauge invariant.

3) Even in a particular gauge L_z and S_z are not, in general, constants of the motion. For a plane wave, with the quantization axis along the direction of propagation, $S_z = M = \pm 1$. It should be mentioned that a linearly polarized wave can be considered as a coherent superposition of two oppositely circularly polarized waves; for such a plane wave the expectation value of S_z is zero, as it is a superposition of equal amounts of $S_z = 1$ and $S_z = -1$ states. One should note that states with $S_z = 0$ do not occur for photons, which is related to the transversality conditions of the electromagnetic field, whereas for particles with spin one and finite rest mass one can have $S_z = 0$ states as well as $S_z = \pm 1$ states.

In connection with the following section it may finally be noted that a multipole field can be approximately a plane wave if at large distances from the origin one considers the multipole field in a specific direction with respect to the quantization axis. The expectation value for the component of angular momentum in the direction of propagation of this plane wave is, in absolute magnitude, smaller than 1 or equal to 1. For the positive z-axis

$\langle S_z \rangle = 1$ in case $M > 0$, whereas $\langle S_z \rangle = -1$ if $M < 0$, irrespective of the values of J and $|M|$, which are related to the directional distribution of the (total) radiation field. The situation for other directions of propagation is discussed in the following section.

§ 5. Polarization of gamma radiation from oriented nuclei.

5. A. Photon polarization.

Before considering the polarization of multipole radiation, we will first discuss how the polarization of plane waves can be formally described (Tol 56).

The polarization of a totally polarized plane wave, represented by a wave function ψ , is determined by the coherent superposition of two basic states ψ_1 and ψ_2 , in which the photon spin is respectively parallel or anti-parallel to the direction of propagation. ψ_1 and ψ_2 represent therefore total left and right circular polarization of a plane wave. ψ can be written as $\psi = c_1\psi_1 + c_2\psi_2$ with the normalization condition $|c_1|^2 + |c_2|^2 = 1$; c_1 and c_2 are complex quantities.

If one writes $c_1/c_2 = \rho e^{i\varphi}$, then ρ and φ completely determine the polarization. For instance for $\rho = 1$ a totally linearly polarized plane wave results; the phase determines the plane of polarization. ρ and φ may be used to define the position of a unit vector ξ , called the polarization vector, in a 3-dimensional coordinate system. The 3 components ξ_1, ξ_2, ξ_3 (Stokes parameters) of ξ then describe adequately the state of polarization of

a completely polarized plane wave. A suitable reference system for ξ is given by the choice of the following 3 unit vectors:

χ_{\parallel} describes a state of linear polarization; the plane of the electric vector can still be arbitrarily chosen and it is convenient in view of further applications, to take the plane through the direction of propagation, \mathbf{k} , and the axis η of rotational symmetry of the nuclear system ($c_1 = c_2 = 1/\sqrt{2}$, $\varrho = 1$, $\varphi = 0$).

$-\chi_{\parallel}$ determines the state of linear polarization with the electric vector perpendicular to the (\mathbf{k}, η) plane ($c_1 = -c_2 = 1/\sqrt{2}$, $\varrho = 1$, $\varphi = \pi$).

χ_{\perp} determines the state of linear polarization with the electric vector rotated over an angle $\pi/4$ with respect to the (\mathbf{k}, η) plane [$c_1 = (1 - i)/2$, $c_2 = (1 + i)/2$, $\varrho = 1$, $\varphi = +\pi/2$].

$-\chi_{\perp}$ determines the state of polarization with the electric vector rotated over an angle $\pi/2$ compared with the former case [$c_1 = (1 + i)/2$, $c_2 = (1 - i)/2$, $\varrho = 1$, $\varphi = -\pi/2$].

$\pm\chi_c$ represent left and right circular polarization respectively ($c_1 = 1$, $c_2 = 1$ respectively).

For this reference system the components of ξ are related to c_1 and c_2 according to

$$\xi = (c_1^*, c_2^*) \sigma \begin{pmatrix} c_1 \\ c_2 \end{pmatrix} \quad (37)$$

where σ_1 , σ_2 and σ_3 are the Pauli spin matrices (usually denoted by σ_x , σ_y , σ_z respectively).

5. B. *Electron polarization.*

The formal description of electron and photon polarization can be developed in very analogous ways in spite of the difference between the electron spin $\frac{1}{2}$ and photon spin 1. This analogy is due to the fact that both photon and electron polarization are described as superpositions of two basic states ψ_1 and ψ_2 . A possible choice for electron polarization is to take for ψ_1 and ψ_2 the states with electron spin parallel or antiparallel to the direction of propagation i.e. complete longitudinal polarization. The linear combinations $\psi_1 + \psi_2$ and $\psi_1 + i\psi_2$ of these two states represent transverse polarization of the electrons along positive x- and y-axis respectively. This is to a certain extent analogous to linear polarization of photons but one cannot speak of the photon spin as pointing in the x- or y-direction if we call the direction of propagation the z-axis.

However, the electron spin can point in any direction in physical space. If we define a polarization vector ξ

$$\xi = (c_1^*, c_2^*) \sigma \begin{pmatrix} c_1 \\ c_2 \end{pmatrix} \quad (38)$$

analogous to (37), then this vector ξ has a more direct meaning than ξ for photons: ξ is the direction of the electron spin (in physical space) in the coordinate system in which the electron is at rest. The vector ξ for the photon gives a characterization of the polarization in a polarization space, for which the meaning of the 1, 2, 3 axes has first to be related with physical space by a suitable convention.

5. C. *Partial photon polarization.*

We return now to photon polarization. So far we have been concerned with complete polarization, either linear, circular or elliptical polarization. As concerns partial polarization, it can be shown, that a beam of partially polarized plane waves can be considered as an incoherent superposition of a beam of completely polarized plane waves and of a beam of unpolarized plane waves. Because of the incoherence, the superposition can be characterized by one single number P , the degree of polarization, which is defined by the ratio of the intensities of the polarized to unpolarized plane waves in the beam, namely $P/(1 - P)$, ($0 \leq P \leq 1$).

The state of polarization of a partially polarized plane wave can be simply described in ξ space by multiplying the unit vector ξ by P . For that reason we will hereafter no longer consider ξ to be a unit vector by definition, but $|\xi|$ may have all values ranging from 0 to 1, corresponding to unpolarized and completely polarized radiation respectively.

Further it can be deduced that the probability W for finding a photon with polarization ξ in a beam of photons, characterized by ξ_0 , is given by $W = (\frac{1}{2})(1 + \xi \cdot \xi_0)$. For the particular cases $\xi = \xi_0$ and $\xi = -\xi_0$ ($|\xi_0| = 1$), this may be easily verified.

5. D. *Polarization of (Q, -2) radiation (completely polarized nuclei).*

The polarization of a multipole field is described by means of the plane wave approximation of a multipole field, considered in a specific direction ϑ with respect to the nuclear spin. The polarization vector ξ_J^M for a pure multipole field with angular momentum J and $M = J_z$ can be decomposed in:

$$\xi_J^M = \xi_1 \chi_{||} + \xi_2 \chi_{\perp} + \xi_3 \chi_c.$$

Because of rotational symmetry ξ_2 will be zero; since the multipole field is completely polarized $\xi_1^2 + \xi_3^2 = 1$. Expressions for ξ_J^M are given in (Tol 53, Cox 53). For a (Q, -2) transition for instance:

$$\xi_{J=2}^{M=-2} = \pm \frac{1 - \cos^2 \vartheta}{1 + \cos^2 \vartheta} \chi_{||} + \frac{2 \cos \vartheta}{1 + \cos^2 \vartheta} \chi_c \quad (39)$$

In (39) the minus sign corresponds to electric quadrupole radiation, the plus sign to magnetic quadrupole radiation. The result for E2-radiation

is shown schematically in fig. 23, and in fig. 24 the values of ξ_1 and ξ_3 are plotted as a function of ϑ . For $\vartheta = 0$ complete left c.p. and for $\vartheta = \pi$ complete right c.p. occurs, but since for these angles the intensity is zero, one better speaks of almost completely circularly polarized radiation for ϑ near 0 or π . For $\vartheta = \pi/2$ there exists complete linear polarization, whereas for intermediate angles the polarization is elliptical.

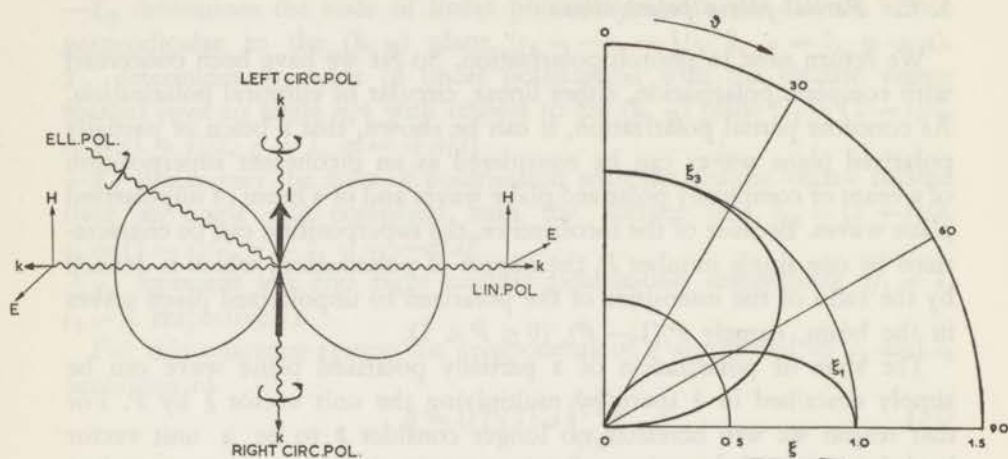


Fig. 23. Polarization of a $(Q, -2)$ radiation. I is the direction of the nuclear spin, or more correctly, the direction of polarization for a system of completely polarized nuclei. \mathbf{k} is the photon momentum; and \mathbf{E} and \mathbf{H} are the directions of polarization of the electric and magnetic vectors for the linearly polarized photons. For the circularly polarized photons the sense of rotation of \mathbf{E} (and \mathbf{H}) are shown in the diagram; the words "left" and "right" refer to clockwise and anti clockwise rotations for an observer looking towards the nucleus.

Fig. 24. Degree of linear polarization, ξ_1 , and of circular polarization, ξ_3 , in case of a $(Q, -2)$ radiation from completely polarized nuclei. θ is the angle of emission of the photons with respect to the axis of nuclear polarization.

It is seen from (39) that the state of linear polarization depends on the electric or magnetic character of the multipole transition, whereas the circular polarization is independent thereof. On the other hand the state of linear polarization is invariant with respect to reversal of the nuclear spin direction (changing ϑ by $\pi - \vartheta$), whereas the sense of circular polarization is reversed. This has two consequences: a) linear polarization can be obtained both from aligned as well as from polarized nuclei and b) by observation of the sense of the circular polarization the direction of the nuclear spin can be determined.

5. E. Circular polarization and sign of nuclear magnetic moment.

In an experiment with polarized nuclei the direction of the nuclear magnetic moment μ is determined by the direction of the magnetic field at the position of the nucleus. If the direction of μ is known and if the sense of circular polarization and hence the direction of \mathbf{I} is experimentally observed, then the relative direction of μ and \mathbf{I} determines the sign of the magnetic moment, which is positive for μ and \mathbf{I} parallel and negative for μ and \mathbf{I} antiparallel. In the case of external field polarization of the nucleus, μ is parallel to \mathbf{H} and no ambiguity can arise; in the h.f.s. polarization method μ may be either parallel or antiparallel to the external polarizing field, depending on the sign of the constant A in the coupling $A \mathbf{I} \cdot \mathbf{S}$. This sign may have been determined experimentally for a stable nucleus, for which also the sign of the magnetic moment is known. This for instance is the case with Mn, where A in Ce-Mg-nitrate is known to be negative for the stable nucleus ^{55}Mn , the μ of which was shown to be positive from a nuclear magnetic resonance experiment. In most other cases, the sign of A can be deduced from theoretical arguments, for instance in the case of Co^{++} the sign of A is given by the sign of the $\mathbf{L} \cdot \mathbf{S}$ -coupling (and of course by the sign of μ).

Determination of the sign of μ is particularly interesting if μ is smaller than about 2 n.m., since otherwise μ may be expected to be positive on basis of the Schmidt model; according to this model values of μ larger than about 2 n.m. are caused by orbital motion of protons, making μ and \mathbf{I} parallel.

Determination of the direction of \mathbf{I} with respect to an external polarizing magnetic field by means of measurement of circular polarization of gamma radiation is also of interest for experiments concerning the asymmetry of beta emission.

5. F. Polarization of various multipole radiations.

In section 5. D. an expression was given for ξ_J^M in case $J = M = 2$, called (Q, -2) radiation. Similar expressions may be derived for other values of J and M (Tol 53); they are listed below for electric radiations:

$$\xi_{J=2}^{M=0} = \xi_{J=1}^{M=0} = \chi_{\parallel} \quad (40)$$

$$\xi_{J=2}^{M=\pm 1} = \frac{1 - 5 \cos^2 \vartheta + 4 \cos^4 \vartheta}{1 - 3 \cos^2 \vartheta + 4 \cos^4 \vartheta} \chi_{\parallel} \pm \frac{-2 \cos \vartheta + 4 \cos^3 \vartheta}{1 - 3 \cos^2 \vartheta + 4 \cos^4 \vartheta} \chi_c \quad (41)$$

$$\xi_{J=2}^{M=\pm 2} = \xi_{J=2}^{M=\pm 1} = -\frac{1 - \cos^2 \vartheta}{1 + \cos^2 \vartheta} \chi_{\parallel} \pm \frac{2 \cos \vartheta}{1 + \cos^2 \vartheta} \chi_c \quad (42)$$

For magnetic radiations the sign of the coefficient of $\chi_{||}$ is reversed. It is seen from the formulae that the sense of circular polarization is determined by the sign of M and is independent of J . No circular polarization occurs for $M = 0$. The situation can be summarized by saying that the spin of the photon, emitted along the axis of the nuclear spin I , is parallel to \mathbf{I} if I is decreased in the transition and antiparallel if I is increased. Conversely, if the direction of the spin of the nucleus is known and the sense of circular polarization is determined, then one can conclude whether the nuclear spin is decreased or increased by the gamma transition.

5. G. Polarization of radiation from partially polarized nuclei.

The radiation emitted from partially polarized nuclei is of course also partially polarized. For instance for an electric dipole radiation, for which the nuclear spin decreases from 1 to 0, the polarization vector is given by:

$$\xi_{J=1}^{M=1} = \frac{\frac{3}{2} f_1 \cos \vartheta \chi_e - \frac{9}{4} f_2 (1 - \cos^2 \vartheta) \chi_{||}}{1 + \frac{3}{4} f_2 (3 \cos^2 \vartheta - 1)} \quad (43)$$

For completely polarized nuclei $f_1 = 1$, $f_2 = 1/3$; the denominator is the intensity of the radiation. At relatively high temperatures $f_1 \propto 1/T$ and $f_2 \propto 1/T^2$ and the denominator becomes practically 1; for $\vartheta = 0$, then the degree of circular polarization is 3/2 times the degree of nuclear polarization $f_1 \propto 1/T$. The degree of linear polarization for $\vartheta = \pi/2$ is equal to $\varepsilon = \{W(\pi/2) - W(0)\}/W(\pi/2)$ and is proportional to $1/T^2$ for small values of $1/T$. It is seen that circular polarization of the radiation is expected to be still considerable at temperatures where the linear polarization and the anisotropy are negligibly small. From (43) it is seen that the experimental determination of the degree of circular polarization yields the value of f_1 as a function of temperature, if also the intensity W or f_2 as a function of temperature are known. It will be shown in Chapters IV and V that ξ_3 and W can be simultaneously observed in one experiment. The comparison between f_1 and f_2 is sometimes of interest as to the spacing of the h.f.s. levels; if the levels are equidistantly spaced, the ratio f_1/f_2 is only determined by $\beta = \mu H / IkT$. For quadrupole radiations the numerator of the formula for ξ_3 contains also a term with f_3 , the denominator of ξ_1 a term with f_4 , whereas also the anisotropy ε is a function of both f_2 and f_4 . In this case the comparison of ξ_3 and W does not lead so simply to a comparison between f_1 and f_2 , unless T is high and hence f_3 and f_4 can be neglected.

§ 6. Detection of polarization of gamma radiation.

The state of polarization of gamma radiation can be analyzed by a Compton scattering process, because the scattering cross section, and

hence the intensity of the scattered radiation depends on the polarization.

For linearly polarized radiation, the differential cross section $d\sigma/d\Omega$ shows a deviation from rotational symmetry about the direction of the incoming photon and this deviation is most pronounced for small photon energies and for a scattering angle of 90 degrees. The linearly polarized photons are preferably scattered in directions perpendicular to the electric vector, which, for the low energy limit, is a well known fact in optics.

For circularly polarized radiation, the differential scattering cross section has rotational symmetry, but the magnitude of $d\sigma/d\Omega$ depends on the relative directions of photon spin and the spin ξ of the scattering electron, which dependence is most pronounced for large photon energies and scattering over 180°. Reversal of the polarization of the electrons results in a change in scattered intensity and therefore polarized electrons can be used for analyzing the degree and sense of the circular polarization (i.e. for determining the quantity ξ_3 of section 5) (Hal 51).

Formulae for $d\sigma/d\Omega$ were derived by several authors (Kle 29, Fra 38, Fan 49). The complete result a was given in a particular useful form by LIPPS and TOLHOEK (Lip 54a, b), of which we shall give here those terms which are relevant for our discussion. The other terms can simply be dropped, unless more complicated phenomena are discussed, for instance if also the polarization of the scattered photon or of the electron in its final state has to be taken into account.

The differential scattering cross section per unit solid angle $d\sigma/d\Omega$ can be written as:

$$\frac{d\sigma}{d\Omega} = \frac{r_0^2}{2} \left(\frac{k}{k_0}\right)^2 \Phi(\mathbf{k}_0, \mathbf{k}, \xi, \xi) \quad (44)$$

where $r_0 = e^2/mc^2$ (the classical electron radius);

\mathbf{k}_0 is the initial momentum of the photon;

\mathbf{k} is the momentum of the scattered (final) photon;

ξ is the polarization vector of the initial photon;

ξ is the polarization vector of the initial electron;

$$\text{and } \Phi = \Phi_0 + \xi_1 \Phi_1 + \xi_3 \Phi_c \quad (45)$$

$$\text{where } \Phi_0 = 1 + \cos^2 \varphi + (k_0 - k)(1 - \cos \varphi) \quad (46)$$

$$\Phi_1 = -\sin^2 \varphi \quad (47)$$

$$\Phi_c = -(1 - \cos \varphi)(\mathbf{k}_0 \cos \varphi + \mathbf{k}) \xi \quad (48)$$

φ is the angle between \mathbf{k} and \mathbf{k}_0 (angle of scattering), which defines the relation between k and k_0 according to:

$$1/k - 1/k_0 = 1 - \cos \varphi \text{ or } k = \frac{k_0}{1 + k_0(1 - \cos \varphi)} \quad (49)$$

The meaning of ξ is defined in such a way, that $\xi_3 = 1$ or -1 represents complete left and right circular polarization respectively, whereas

$\xi_1 = \pm 1$ represents complete linear polarization, the electric vector being in the plane of scattering for $\xi_1 = 1$ and perpendicular to the plane of scattering for $\xi_1 = -1$.*

Φ_0 gives the Compton cross section for unpolarized radiation ($\xi_1 = \xi_3 = 0$), whereas the terms with Φ_l and Φ_c are the polarization dependent parts of the cross section.

We will first consider $d\sigma/d\Omega$ for unpolarized radiation. Moreover we will start neglecting the angular dependence and integrate $d\sigma/d\Omega$ over all angles in order to obtain the total Compton scattering cross section σ . Theoretical expressions (first derived by Klein-Nishina) for σ are plotted for iron in fig. 25. In the graph the cross sections for photoabsorption

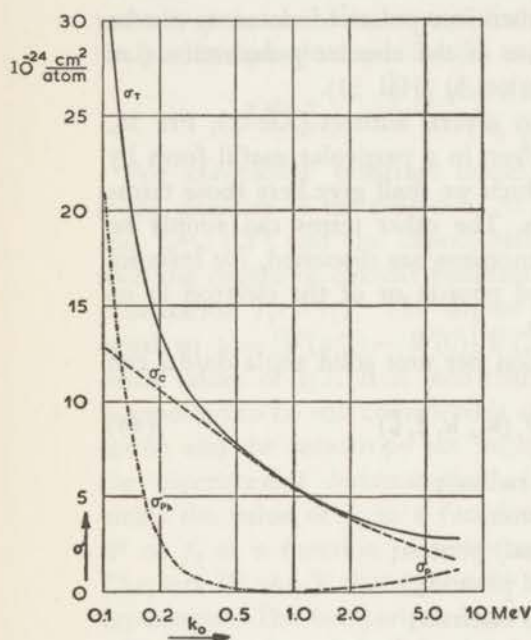


fig. 25

of scattering and $W(\varphi)$ has been normalized to $\int W(\varphi)d\varphi = 1$. The curves A, B and C refer to a photon energy k_0 of respectively $k_0 = 4$, $k_0 = 2$ and $k_0 = 1$ (units $mc^2 = 0.51$ MeV).

and pair creation are also indicated and if added to the Compton-scattering cross section, a total absorption or attenuation cross section is obtained.

* This convention, which differs from (Lip 54 a, b) has been chosen in order to make (45) applicable in chapters IV and V, where the plane of scattering is also the (k, η) plane (except V, § 6).

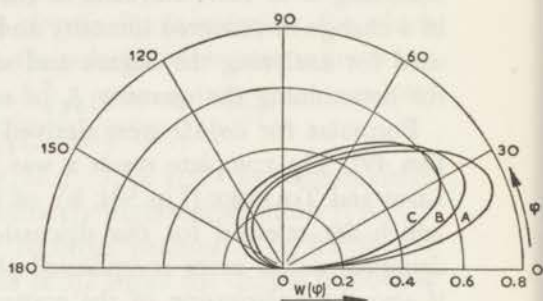


fig. 26

Fig. 25. σ_0 , the theoretical total Compton scattering cross section of iron atoms for unpolarized photons, plotted as a function of the photon energy k_0 . Also the cross sections for photo absorption and pair production, respectively σ_{ph} and σ_p , have been indicated in the diagram (dot and dash curves). The drawn curve represents the total absorption or attenuation cross section $\sigma_T = \sigma_c + \sigma_{ph} + \sigma_p$.

Fig. 26. Angular distribution $W(\varphi)$ of Compton scattered photons. φ is the angle

For a comparison of the theoretical total cross section with experimental results, the reader is referred to (Dav 52, 55); it may be remarked that agreement between theory and experiments is fairly good (e.g. iron).

How the Compton scattering depends on the scattering angle φ is seen from fig. 26, where the angular distribution $W(\varphi)$ of the scattered photons for $k_0 = 1, 2$ and 4 (in units of mc^2) is plotted; $W(\varphi) = (d\sigma/d\Omega) \sin \varphi$, in other words, $W(\varphi)$ is the relative intensity of scattered photons per unit angle and the normalization condition is $\int W(\varphi) d\varphi = 1$. It is seen that for energies of the order of 1 MeV or higher, forward scattering predominates to a large extent.

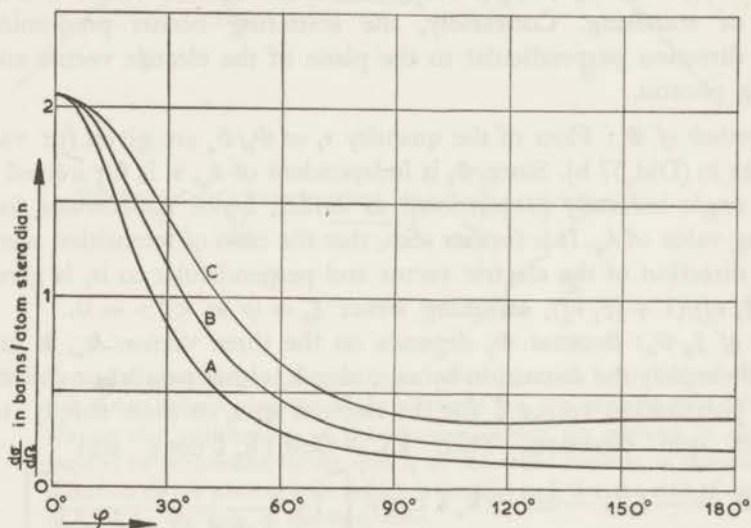


fig. 27

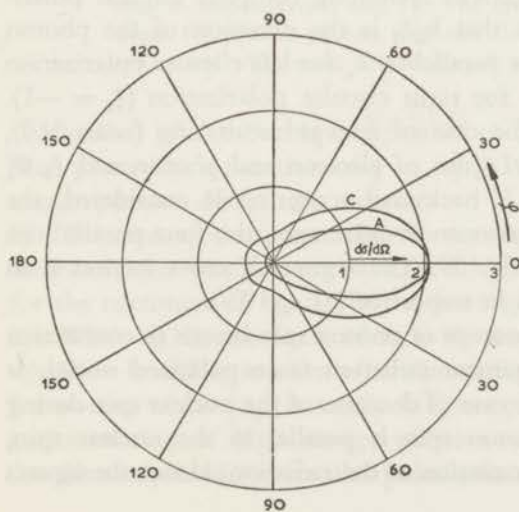


fig. 28

Fig. 27. Differential Compton scattering cross section $d\sigma/d\Omega$ for iron, given in barns/atom steradian and as a function of the angle of scattering, φ . The curves A, B and C correspond to photon energies of $k_0 = 4$, $k_0 = 2$ and $k_0 = 1$ respectively (units mc^2).

Fig. 28. Polar diagram of fig. 27.

Returning again to the quantity $d\sigma/d\Omega$, its values for $k_0/mc^2 = 1, 2$ and 4 are plotted in fig. 27 as functions of the scattering angle φ .

$d\sigma/d\Omega$ for $\varphi = 0$ is independent of the energy of the incoming photon, its value being r_0^2 . A polar diagram of $d\sigma/d\Omega$ is shown in fig. 28.

Sign of $\xi_1 \Phi_l$: since Φ_l is always negative (or zero) it follows from the definition of ξ_1 that $\xi_1 \Phi_l$ is positive if the electric vector is perpendicular to the plane of scattering and $\xi_1 \Phi_l$ is negative if the electric vector lies in the plane of scattering. Since for $\varphi = \pi/2$ and for complete linear polarization $|\Phi_l| = |\xi_1| = 1$ and moreover for small energies $\Phi_0 \approx |\Phi_l|$, $\Phi = \Phi_0 + \Phi_l$ is very small if the electric vector lies in the plane of scattering. Conversely, the scattering occurs predominantly in the direction perpendicular to the plane of the electric vector and incoming photon.

Magnitude of Φ_l : Plots of the quantity $\nu_l \equiv \Phi_l/\Phi_0$ are given for various energies in (Did 57 b). Since Φ_l is independent of k_0 , ν_l is for a fixed scattering angle inversely proportional to $d\sigma/d\Omega$, hence ν_l decreases for increasing value of k_0 . It is further seen, that the ratio of intensities, scattered in the direction of the electric vector and perpendicular to it, is given by $(1 - |\xi_1 \nu_l|)/(1 + |\xi_1 \nu_l|)$, assuming either $\xi_3 = 0$ or $\langle \xi \rangle = 0$.

Sign of $\xi_3 \Phi_c$: Because Φ_c depends on the three vectors \mathbf{k}_0 , \mathbf{k} and ξ , we will simplify the discussion by assuming \mathbf{k}_0 either parallel or antiparallel to the polarization vector ξ for the electron spin, or more simply: to the electron spin direction. Then $\mathbf{k} \xi = (k/k_0) \mathbf{k}_0 \xi \cos \varphi$ and

$$\xi_3 \Phi_c = -\xi_3 (1 - \cos \varphi) \mathbf{k}_0 \xi \cos \varphi \left[1 + \frac{1}{1 + k_0 (1 - \cos \varphi)} \right] \quad (50)$$

hence has the sign of $-\xi_3 \mathbf{k}_0 \xi \cos \varphi$. Assuming complete circular polarization ($|\xi_3| = 1$), one can say that $\mathbf{k}_0 \xi_3$ is the direction of the photon spin, because the photon spin is parallel to \mathbf{k}_0 for left circular polarization ($\xi_3 = 1$) and antiparallel to \mathbf{k}_0 for right circular polarization ($\xi_3 = -1$). From this it is seen that in the case of forward scattering ($\cos \varphi > 0$), $\xi_3 \Phi_c$ is positive for antiparallel spins of electron and photon and $\xi_3 \Phi_c$ is negative for parallel spins. If backward scattering is considered, the sign of $\xi_3 \Phi_c$ is reversed. In order to avoid errors, the four possibilities are schematically indicated in fig. 29. The scattering cross section is in the cases II and III larger than in respectively I and IV.

An advantage of using the concept of photon spin is seen in connection with circular polarization of gamma radiation from polarized nuclei. It was discussed in § 5 that, in the case of decrease of the nuclear spin during the gamma transition, the photon spin is parallel to the nuclear spin, irrespective of the direction of emission of the radiation. Hence the figures

I and III have been connected to II and IV respectively by drawing also the initial and final spin of the gamma emitting nucleus. If the direction of ξ in II is reversed, then the cross sections in I and II are equal and depend only on the relative orientation of \mathbf{I}_i and ξ .

Under reversal of electron spin or of photon spin, but not of both, the scattered intensity will change by a factor $(1 - \xi_3 \nu_c)/(1 + \xi_3 \nu_c)$ where $\nu_c \equiv \Phi_c/\Phi_0$.

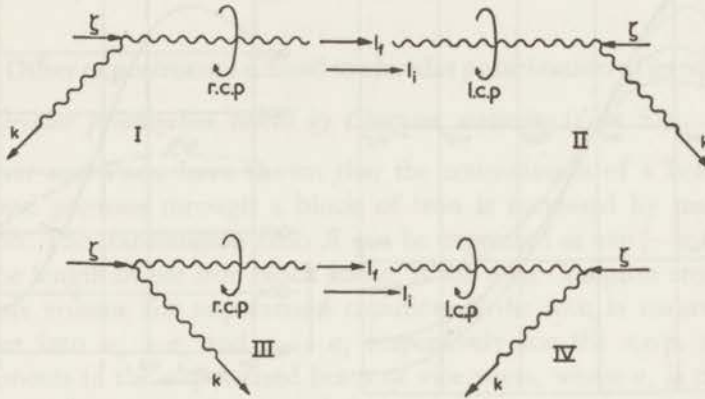


Fig. 29. Compton scattering of circularly polarized photons by polarized electrons. ξ is the polarization vector of the electrons (i.e. the electron spin direction); the circular polarization of the photons, which are emitted in directions parallel or antiparallel to the spin \mathbf{I}_i of the initial nucleus, is defined by the direction of the photon spin, which is parallel to \mathbf{I}_i for the case of a decrease of \mathbf{I}_i to \mathbf{I}_f , the spin of the final state.

The differential scattering cross sections in the cases II and III are larger than in respectively I and IV. The cross section for forward scattering is larger for parallel photon spin and electron spin than it is for antiparallel spins, and vice versa for backward scattering.

Magnitude of Φ_c : For \mathbf{k}_0 antiparallel to ξ , the quantity $\nu_c = \Phi_c/\Phi_0$ has been plotted as a function of φ in fig. 30 for various energies. There are two important differences with ν_i :

- 1) Whereas ν_i decreases with increasing energy, ν_c on the contrary increases; for small energies $k_0 < 1$ MeV and $\varphi = 60^\circ$ (approximately for the maximum of ν_c , fig. 30) ν_c is roughly equal to $(2/5) k_0 (1 - k_0/4)$.
- 2) While ν_i , in the limit of $k_0 = 0$, reaches a maximum for $\varphi = \pi/2$, $\nu_c(\pi/2) = 0$ and ν_c reaches a maximum for φ about $\pi/4$ and a minimum for $\varphi = \pi$, where $|\nu_c|$ is nearly 1. Consequently, as far as ν_c is concerned, backscattering of high energy photons would be a favourable method for the analysis of the circular polarization of the photons.

Particularly for high energy photons, however, the back scattered intensity will be relatively small, since the differential Compton cross section $d\sigma/d\Omega$ for $\varphi > \pi/2$ is small (fig. 27, 28).

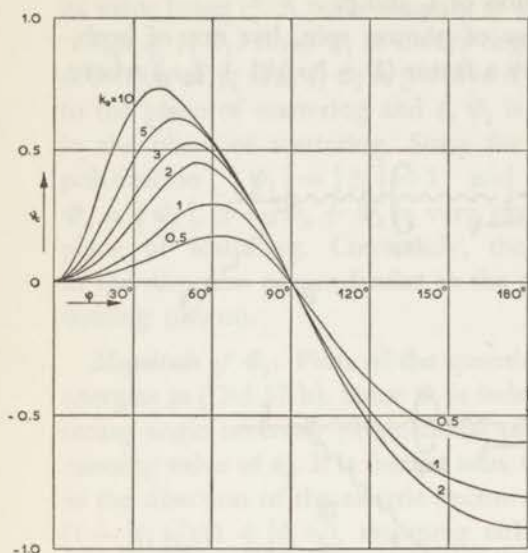


fig. 30

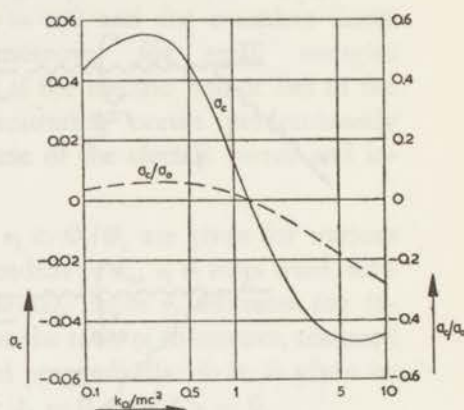


fig. 31

Fig. 30. ν_c , the ratio of the circular polarization sensitive part of the Compton scattering differential cross section to the normal Compton differential cross section, plotted as a function of the scattering angle, φ . k_0 is the photon energy in units mc^2 ; the curves for $k_0 > 2$ and $\varphi > 90^\circ$ are omitted from the diagram as they nearly coincide with the curve for $k_0 = 2$.

Fig. 31. σ_c is that part of the total Compton scattering cross section, which is sensitive to circular polarization of photons and to electron polarization. σ_c is plotted as a function of photon energy and for the case of complete photon and electron polarization and is expressed in units $2\pi r_0^2$ where r_0 is the classical electron radius ($2\pi r_0^2 = 0.50$ barns). The dashed curve gives the ratio of σ_c to σ_0 , where σ_0 is the polarization insensitive total Compton scattering cross section.

Another disadvantage of backscattering ($\varphi > \pi/2$) is, that if incident photons of various k_0 -values are present, the scattered photons have relatively small energy differences (see also fig. 49), hence energy discrimination between various gamma radiations is difficult. Moreover it is of great practical interest to avoid contributions from multiply scattered photons. Clearly in the case of backscattering it will be much more difficult to discriminate against background and multiple scattering.

Integration of $d\sigma/d\Omega$ over the solid angle $d\Omega$ yields the total scattering Compton cross section σ . In case the scattering electrons are polarized, σ

will also depend on the circular polarization of the incoming photons. σ may be written as $\sigma = \sigma_0 + \sigma_c$ where σ_0 is the polarization insensitive part of the total Compton scattering cross section and σ_c is the circular polarization sensitive part of the cross section. σ_c and also the ratio σ_c/σ_0 have been plotted in fig. 31 as a function of k_0 (in units mc^2). It will be seen in § 7 that analysis of the circular polarization of photons can be accomplished by a measurement of the change in absorption cross section of magnetized iron upon reversal of the direction of electron polarization.

§ 7. Other experiments related to circular polarization of gamma rays.

A. Circular polarization caused by Compton scattering (Gun 53).

GUNST and PAGE have shown that the transmission of a beam of unpolarized photons through a block of iron is increased by magnetizing the iron. The transmission ratio R can be expressed as $\exp(-\sigma_0 L)$, where L is the length of the iron block and σ_0 is the total Compton cross section per unit volume for unpolarized radiation. If the iron is magnetized, σ_0 changes into $\sigma_0 + \sigma_c$ and $\sigma_0 - \sigma_c$ respectively for the r.c.p. and l.c.p. components in the unpolarized beam or vice versa, where σ_c is the polarization sensitive part of the total Compton scattering cross section. The transmission ratio R therefore changes into

$R_m = \frac{1}{2} \exp(-\sigma_0 - \sigma_c)L + \frac{1}{2} \exp(-\sigma_0 + \sigma_c)L = \exp(-\sigma_0 L) \cosh \sigma_c L$, giving a gain in intensity by the factor $\cosh \sigma_c L$ compared with the case of unmagnetized iron.

The measured change in counting rate in the experiment of GUNST and PAGE was about 0.6% for 2.62 MeV photons and $L \approx 30$ cm.

It is seen that, depending on the direction of magnetization, either the l.c.p. or r.c.p. photons are preferably scattered, causing the transmitted beam to be circularly polarized. However, this method for polarizing gamma rays is not effective since for obtaining 80% circular polarization the transmission ratio would certainly be smaller than 10^{-12} .

In the forementioned experiment it may be estimated that $R \approx 10^{-4}$ and that a 5–10% circular polarization was obtained.

B. Circular polarization of photons produced by polarized neutron capture (Tru 56).

TRUMPY observed the circular polarization of photons of comparatively large energy (E_γ between 5 and 10 MeV) following capture of polarized thermal neutrons by various targets of unpolarized nuclei. It is easily seen that, in case of a spin decrease in the gamma transition, the photon spin will be parallel to the neutron spin for $I_c = I_i + \frac{1}{2}$ and antiparallel

to the neutron spin for $I_c = I_i - \frac{1}{2}$, where I_i is the spin of the target nucleus and I_c is the spin of the compound nucleus. The sense of the circular polarization therefore determines I_c if I_i is known. In the reported experiment the circular polarization was analyzed by the transmission method, appropriate for high energy photons. Since the neutron polarization was only 20% the fractional change in counting rate upon reversal of the iron magnetization was only a few tenths of a percent. For a number of nuclei the value of I_c was established.

C. β - γ -circular polarization-correlation experiments.

One of the proposals made by YANG and LEE (Lee 56) for testing the validity of parity conservation in weak interactions, was a measurement of a correlation between β -particles and circularly polarized photons emitted from randomly oriented nuclei. This correlation will generally occur for nuclei such as ^{60}Co , which show an asymmetric β -emission and which emit after β -decay one or more photons.

^{60}Co nuclei, which have emitted electrons in the negative z -direction, will have their spins predominantly in the positive z -direction because of the asymmetry of the β -emission. If the nuclei under consideration ($\langle I_z \rangle$ positive) emit subsequently photons in, say the positive z -direction, then these photons will be left circularly polarized i.e. the photon spin will be in the positive z -direction.

For the measurement of this correlation it is essential that coincidences are counted between β -particles and photons which are Compton scattered by magnetized iron. The relative change in coincidence counting rate upon reversal of the field in the magnetized iron is smaller by at least a factor of 3 compared with the case of circular polarization of photons from completely polarized nuclei. Compared with the nuclear polarization experiments the measuring time required for obtaining a certain relative statistical accuracy, of the effect to be measured, is longer by a factor of the order 10^3 . However, low temperatures are unnecessary and, consequently, a greater class of nuclei can be investigated. Further the use of long counting times is not so much of a difficulty at room temperature (it is difficult in a low temperatures experiment).

In the reported experiments the circular polarization of the photons was detected either by the transmission method or the scattering method, which methods are compared later in this section. The results with ^{60}Co , ^{22}Na , ^{95}Zr , ^{124}Sb and ^{46}Sc agree within experimental errors with the so called „two component theory of the neutrino”, which is one of the possible formalisms proposed in connection with the non-conservation of parity in β -decay (Sch 57a, Boe 57a, Lun 57, App 57, Deb 57).

D. *Circular polarization of external bremsstrahlung (Gol 57, Boe 57a).*

The longitudinal polarization of β -particles, which is a consequence of parity non-conservation, may be studied from the circular polarization of bremsstrahlung produced in condensed matter surrounding the source. If the β -particle has relativistic energies, say larger than 2 MeV, then the bremsstrahlung photons are emitted preferentially in a direction parallel to the electron momentum and with the photon spin parallel to the electron spin. The bremsstrahlung photons will therefore be circularly polarized (for β^- emission r.c.p.) and the degree of circular polarization is expected to be large if the photon energy E_γ is nearly equal to the kinetic energy E_e of the β -particle. For instance in the extreme case of 1 MeV photons produced by 1 MeV electrons, the photons which are emitted in the direction of the electron momentum are expected to be 70% circularly polarized (Voy 57 a, b).

If E_γ/E_e decreases from the maximum value of 1 to, say, 0.5 then the degree of circular polarization decreases only slightly (less than 10% for $E_e = 2$ MeV).

For low energy electrons (< 0.5 MeV) the photon polarization will be difficult to observe since:

a) the electron energy will decrease mainly by ionization and only a small part by bremsstrahlung; b) the detection efficiency for circ. pol. photons is small for $E_\gamma < 0.5$ MeV; c) even for $E_\gamma \approx E_e$ and 100% electron polarization, the photon polarization will be smaller than 50% for $E_e < 0.25$ MeV; and d) the longitudinal electron polarization is proportional to v/c .

Results have been reported for 2.24 MeV electrons of ^{90}Y (uniquely forbidden transition, no gammas) and for 0.97 MeV electrons of ^{170}Tm .

E. *Circular polarization of internal bremsstrahlung (Sch 57b).*

Internal bremsstrahlung produced by longitudinally polarized β -particles will also be circularly polarized (Cut 57). Experimental results have been reported by SCHOPPER (Sch 57b) for ^{90}Sr .

F. *Circular polarization of photons produced by „annihilation in flight” of polarized positons (Deu 57, Boe 57b).*

Although positons annihilate mostly after being decelerated to nearly thermal energies, part of the annihilations occur at relativistic positon energies. For $E(\beta^+) > 2.5$ MeV momentum and energy conservation laws require that more than 90% of the total available energy (> 3.5 MeV) is transferred to one photon, which is emitted in a direction making an

angle smaller than 10° with the positron momentum. This fact makes it possible, by means of energy discrimination, to select only the photons originating from annihilations in flight.

For annihilation in flight the photons which are emitted in the direction of the positron momentum, will be circularly polarized in case of longitudinal positron polarization, with the spin of the photon parallel to that of the positron. For completely polarized positons with kinetic energy of more than 1 MeV the circular polarization amounts to at least 80% according to the calculations of PAGE (Pag 57). Conversely, from the measured degree of circular polarization one may infer the degree of longitudinal positron polarization. Such experiments have been recently performed with 3 MeV positons from ^{66}Ga and 1.2 MeV positons from ^{13}N , showing that the longitudinal positron polarization is approximately equal to v/c also for the case of predominantly Fermi-interaction in β -decay. In these experiments background problems have been reduced by selecting high energy positons from the source by means of a β -spectrometer and by having the positons annihilated at a considerable distance from the source.

So far in the discussion it was assumed that the annihilating electron was unpolarized. If the positons are unpolarized and the electrons are, for instance in magnetized iron, partially polarized, then circular polarization may be also observed for the photons emitted in the direction of the positron momentum, as was discussed by PAGE. In this case, however, the degree of circular polarization will be smaller than 8%, since experimentally only a small electron polarization is feasible.

Comparison of transmission method (T.M.) to scattering method (S.M.).

The analysis of the circular polarization of photons by means of magnetized iron may be accomplished either by counting the scattered photons or the unscattered, transmitted photons. Some features of the S.M., particularly the comparison between forward and backward scattering, are discussed in IV, § 1. We will here compare forward scattering and transmission.

- 1) In general energy discrimination is simpler for the transmitted photons than for the scattered photons. The S.M. is disadvantageous in this respect particularly for photons with energies of a few MeV or larger, since pair creation and multiple scattering compete effectively with single scattering.
- 2) The efficiency of the analysis is in the S.M. determined by v_e , whereas for the T.M. the relevant quantity is σ_c/σ_0 , the ratio of the polarization sensitive part of the *total* scattering cross section to the normal *total* scat-

tering cross section. It is seen from fig. 31 that the T.M. is ineffective for $E_\gamma < 0.5$ MeV.

3) The T.M. can be realized with a compact magnet for magnetizing the iron compared with the S.M., where a cylindrical scatterer is most suitable.

4) In the S.M. the direct radiation must be shielded against, which imposes a minimum in the dimensions of the scattering system.

5) With increasing photon energy the maxima, in both the angular distribution (fig. 26) of the scattered radiation and in the quantity ν_c , shift towards smaller scattering angles. As a result the solid angles involved in the S.M. decrease with increasing energy, giving small counting rates.

6) One can show that the fractional change E in counting rate upon reversal of the iron magnetization in the T.M. is given by $2 \xi_3 \tanh(\sigma_c L)$, L and σ_c being defined earlier in this section and ξ_3 is the degree of circular polarization.

For instance $E \approx 0.10$ requires, in the case of 1.2 MeV photons, and $\xi_3 = 1$, that L be approximately 6 times the photon mean free path or $L \approx 12$ cm. This gives a transmission ratio of $e^{-6} \approx 2.5 \times 10^{-3}$; if this number is combined with a solid angle of $2 \cdot 10^{-3} \times 4\pi$ for a 1" NaI crystal, then one finds that one in $2 \cdot 10^5$ of the emitted photons reaches the counter. It will be seen in Chapter IV that in the S.M., $E \approx 0.07$ could also be obtained in the case of $\xi_3 = 1$, completely magnetized iron and 1.2 MeV photons. The number of photons reaching the scintillation crystal (1" diameter) can be estimated from the results, to be 1 per 10^4 .

As far as intensity is concerned, the S.M. is more favourable than the T.M. for photons with an energy of 1 MeV or less. However, it can be shown that for E_γ larger than about 2 MeV the T.M. is to preferred in this respect.

It should be noted that the relative statistical accuracy in E decreases with increasing iron thickness, L .

In the experiments reported under A—F, L varied between 2 and 8 times the photon mean free path.

It may be concluded from the above remarks, particularly 2), 1) and 5) that the S.M. is more favourable than the T.M. for $E_\gamma < 1$ MeV and vice versa for $E_\gamma > 2$ MeV.

CHAPTER IV.

CIRCULAR POLARIZATION OF GAMMA RADIATION EMITTED FROM POLARIZED ^{60}Co NUCLEI.

§ 1. Introduction.

In order to measure circular polarization of gamma radiation from oriented nuclei, it is essential that the nuclei are polarized (instead of aligned), making the orientation parameter $f_1 \neq 0$. We will discuss the values of f_1 which are required for detection of the circular polarization.

The expected degree of circular polarization ξ_3 is roughly equal to $f_1 \cos \vartheta$, where ϑ is the angle of emission of the photon with respect to the nuclear spin.

If the circularly polarized radiation is scattered at polarized electrons, of which the spin direction is reversed, then the scattering cross section is changed by a factor $(1 - \xi_3 \nu_c)/(1 + \xi_3 \nu_c)$, ν_c being defined in chapter III. The fractional change E' in the counting rate is therefore expected to be $2 \xi_3 \nu_c$. Since in magnetized iron, if completely saturated, only about 2 of the 26 electrons are polarized, the relative change is reduced to $2 \xi_3 \nu_c/13$. For forward scattering of ^{60}Co gamma rays the maximum value of ν_c is about 0.5, for backward scattering ν_c may be nearly 1. It is evident, that for completely circularly polarized radiation the effect E' can be at most 8% for forward scattering and about 15% for backward scattering. These numbers, however, represent the ideal case and particularly for backward scattering there are a number of limiting factors. For instance, for a cylindrical scatterer the solid angle in which the radiation is scattered is proportional to $\sin \varphi$ and therefore very small for scattering angles $\varphi \approx 180^\circ$, for which the maximum of $|\nu_c|$ occurs. Moreover, in an experiment at low temperatures the source is surrounded by a relatively large cryostat and a polarizing magnet, which makes scattering under an angle $\varphi \approx 180^\circ$ very awkward. A scattering arrangement for $\varphi = 120-150^\circ$ could be easily realized, but comparison with the case $\varphi \approx 60^\circ$ shows that the scattered intensity per unit solid angle is lower for backscattering by a factor of about 5 for ^{60}Co photons (fig. 27). Consequently for a fixed measuring time the relative statistical accuracy for E' would be somewhat higher in the case of forward scattering.

Backscattering has moreover the disadvantage that the energy of the

photons scattered at the magnetized iron is not appreciably different from the energies of multiply scattered photons and hence a large background of extraneously scattered radiation is to be expected. Since the geometrical arrangement is also less favourable for large φ , forward scattering ($\varphi \approx 60^\circ$) was preferred in spite of the relatively smaller magnitude of the effect.

For $\varphi = 60^\circ$ the maximum value for E' is roughly $0.08 \xi_3$ or $0.08 f_1$. Since an effect of smaller than, say, 0.5% could be easily masked by other effects such as the influence of the magnetic field on the counters, f_1 should be at least 0.1 and larger values would be desirable.

A crystal, which is very suitable for obtaining a large degree of nuclear polarization in twovalent ions is Ce-Mg-nitrate, as was first shown by Ambler *et al.* (Amb 53), who obtained a value for f_1 of roughly 75%. Whereas the Co ion is very favourable for obtaining a large nuclear polarization, the choice of ^{60}Co is on the other hand favoured in view of:

- a) two photons of 1.17 and 1.33 MeV are emitted in cascade, having equal values of ξ_3 and, because of the small energy difference, also nearly equal values of ν_c ; this gives a gain in intensity by a factor 2;
- b) the relative statistical accuracy with which E' can be measured is roughly proportional to $\nu_c (d\sigma/d\Omega)^{1/2}$; this quantity considered as a function of energy and for a fixed scattering angle of $\varphi = 60^\circ$ reaches a maximum for a photon energy of about 1.1 MeV. Though this is not a very sharp maximum ^{60}Co clearly presents a favourable case. Whereas for photons of a hundred keV or less ν_c and E' become unduly small, on the other hand for high energy photons background problems become more serious because of pair creation and the relatively great energy loss by the scattering; and
- c) ^{60}Co has a long half life and can be obtained in high specific activity. No complications arise because of internal conversion, mixed multipolarity, long half life of excited states etc.

§ 2. Apparatus for the detection of the circular polarization.

a. Sample and magnets.

The sample consisted of 6 single crystals of $2\text{Ce}(\text{NO}_3)_3 \cdot 3\text{Mg}(\text{NO}_3)_2 \cdot 24\text{H}_2\text{O}$, weighing 20.74 g. in total and containing 110 μC of ^{60}Co and about 10 mg $\text{Co}(\text{NO}_3)_2 \cdot 6\text{H}_2\text{O}$. They were mounted in a quartz holder with their trigonal axes horizontal. The holder was supported by a pressed cylinder of chrome alum, which in its turn was fixed to the glass vessel in the helium bath by a thin walled glass foot (Pop 55).

The magnetizing field was 22000 Oe for the sample and about 17000 Oe

for the alum. The temperature measurements were made in the usual way by measuring ballistically the susceptibility perpendicular to the trigonal axis by means of two coils around the sample and a mutual inductance bridge.

After adiabatic demagnetization the cryostat was pulled out of the magnet and the apparatus used for the scattering experiment was raised around the cryostat by means of a hydraulic lift. This apparatus is drawn schematically in fig. 32. It consists mainly of two magnets, called M_s and M_p hereafter. M_s is intended to magnetize the scattering iron. The energizing coils W for M_s each contained about 4000 windings of 2 mm Povin insulated copper wire and were fed by a current of 3 amperes. Holes of 6 cm diameter

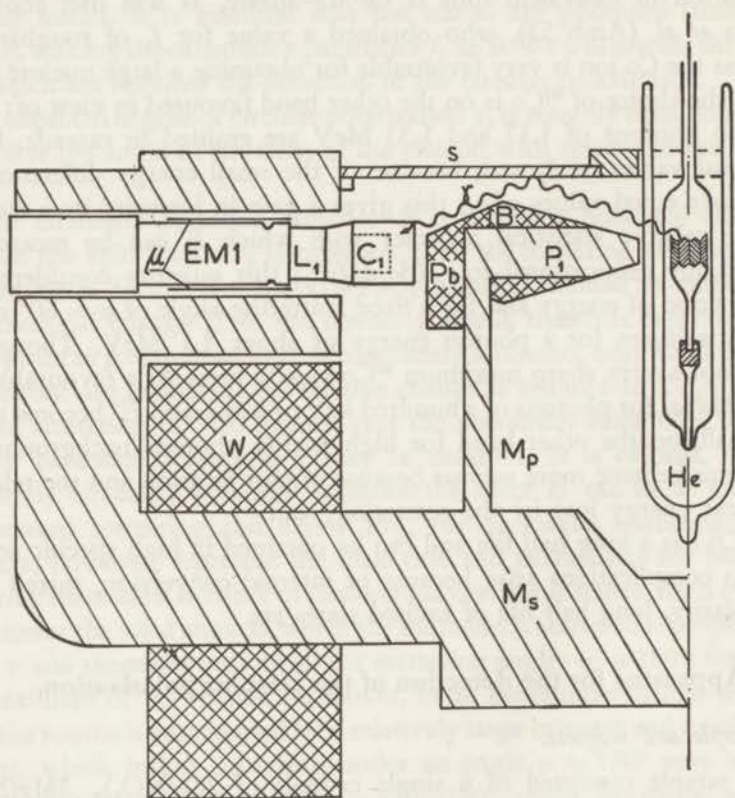


Fig. 32. Schematic diagram of the apparatus for producing and measuring circularly polarized γ -rays.

W and B are the magnetizing coils for, respectively, the saturating magnet M_s and the polarizing magnet M_p . The γ -ray detectors consist of NaI (Tl) crystal C , lightpipe L , and photomultiplier EMI . S is the scattering Armco-iron.

were bored in the poles for the detectors. The overall length of M_s was 104 cm.

The scattering iron consists of 2 sets of 9 Armco-iron plates, the size of each plate being 0.8—3.8—20 cm. One side of each set is connected to a big pole shoe and the other side to the central piece of iron around the cryostat. This central piece is made of 2 cm thick iron, and has a relatively small magnetic resistance. The nine strips encircle the poles P of M_p and the counters from three sides. Only the side of one strip is drawn in fig. 32, the others are mounted behind and before the plane of the drawing.

The division of the scattering iron in 9 separate strips was preferred above the use of 3 single plates because it was hoped that the lines of force would be more parallel to the axis of the arrangement, *i.e.* the polarization direction of the electron spins in the iron would be better defined.

M_p , the polarizing magnet, served for the polarization of the ^{60}Co nuclei. The field axis of M_p lays along the trigonal axis of the Ce-Mg-nitrate crystals. The yoke of M_p was also part of the magnetic circuit for M_p .

The polarizing coils B were wound directly on the poles P with 1.2 mm diameter Povin insulated copper wire and with the special form shown to provide angular definition for the γ -rays. There was a shunting of polarizing field flux by the surrounding iron so that a current of 5.00 amperes was necessary to produce a field of 263 oersteds in the centre of the gap when the polarizing field and field in the iron were antiparallel, while a current of 3.60 amperes was necessary to produce the same field when the two fields were parallel. There was no measurable effect of the polarizing field on the degree of saturation of the iron plates. The field between the poles was not quite homogeneous, but varied somewhat over the area of the Ce-Mg-nitrate crystals. The field in the center was 263 Oe, whereas an average value of 280 Oe had to be taken over the stack of crystals.

b. Scintillation counters.

The counters consisted of NaI (Tl) cylindrical crystals C placed in front of the iron poles and optically connected to EMI photomultipliers type 6260 by means of lucite light pipes L 5 cm long. These EMI tubes proved far superior to the RCA type tube in terms of magnetic field independence of the pulse height. The photomultiplier tubes were mounted inside the iron poles to reduce to a minimum the effects of reversing the polarizing field. Tube I was further shielded by two concentric Mu-metal shields μ , figure 32, while only one Mu-metal shield was available for tube II. In addition, the magnetizing coils W for the scattering plates were placed on the lower yoke to reduce the magnetic field at the position of the photo-

multiplier. This gave poor efficiency for saturating the iron, and it is quite possible that the photomultipliers would have operated well enough with the magnetizing coils mounted on the poles. In any event, the actual effect on the counting rate of reversing the 280 Oe polarizing field was $0.13 \pm .13\%$ for counter I and $0.30 \pm .08\%$ for counter II for the pulse height discrimination used in the experiments. Though the EMI tubes were mounted in a region of the hollow pole where the stray field was only a few oersteds, the influence on the counters of the magnetic field of M_s was not negligible. Therefore the current through the coils of M_s was kept constant within 1% during the experiments.

c. *Background.*

In an apparatus to detect scattered γ -rays, the detectors must be shielded against not only the direct radiation from the source but also the extraneously scattered radiation from all parts of the apparatus as well as from the walls and floor of the laboratory. The effects of background from extraneously scattered radiation are usually extremely large in that energy region which corresponds to degraded Compton radiation, namely the energy region up to 300 keV.

In attempting to reduce extraneous background one can either use a "closed" geometry where a very large amount of lead shielding is used, or an "open" geometry where the only scattering material near by is just that whose purpose is to scatter the γ -rays. An open geometry is possible in the case of forward scattering and leads to excellent results.

As may be seen in figure 32 almost all the heavy scattering material was located behind the scintillation crystals so that extraneously scattered radiation would have scattering angles greater than 90° . In practice, scattering angles from 45° to 70° were accepted so that scattering from the base was not serious. The angle of the accepted radiation from the axis of the polarizing field was designed for a range from 15° to 30° . This design gave sufficient volume in the inner cone for the polarizing magnet. Most of the shielding against direct radiation was done by the polarizing magnet (iron and copper), although a small amount of lead, Pb, fig. 32, was placed just behind the polarizing magnet for extra shielding. The 18 Armco-iron scattering plates could be easily removed to measure the background. The results of the background measurements for counter I are shown in the form of pulse height distributions in fig. 33. The pulse height selector during the measurements selected recoil electron energies in the detector crystals from about 500 keV to 700 keV, using the ^{137}Cs 662 keV γ rays as calibration.

By graphical integration the areas under the two pulse height distributions were obtained between the discriminator limits and compared to find the background fraction f_B of the counting rate in the absence of nuclear polarization. f_B is 13.2% for counter I and 11.7% for counter II. The difference in these numbers probably arises from the fact that detector I

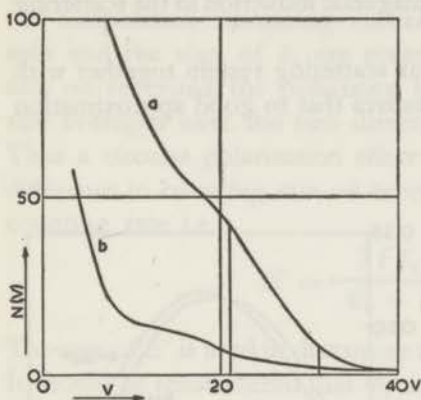


Fig. 33. Pulse height distributions in counter I. Curve *a* with the Armco-iron scattering plates. Curve *b* without scattering plates. The 662 keV ^{137}Cs peak is at $V = 29$ volts. The discriminator during the experiment accepted pulses between 21 and 31 volts, as is indicated by vertical lines.

was a large ($2\frac{1}{2}$ cm radius, 5 cm high) NaI crystal while II was much smaller ($1\frac{1}{2}$ cm radius, $2\frac{1}{2}$ cm high). The counting rates in the two crystals were not very different since all parts of the big crystal were not equally exposed to the radiation.

The low background justifies the relatively complicated design of the magnets. The more simple arrangements recently used for measuring β - γ -polarization-correlation (Boe 57a, Sch 57a, Deb 57) work equally well for the detection of circular polarization, but the background contribution cannot be as reliably determined. On the other hand, in those arrangements the stray field of the magnetized iron is confined to a smaller area, so that magnetic influences on the counters can be kept smaller than in our case. It was found that, even if the light pipes L were lengthened to about 50 cm, a large amount of magnetic shielding was required to make the change in counting rate smaller than 0.5% if the M_s -field was reversed. Since reversal of the M_s -field is essential in a β - γ -polarization-correlation experiment, our arrangement is not very favourable for the detection of circular polarization in such an experiment.

For the experiment described here, however, only the polarizing field is reversed and this has an effect on the counting rate which is small compared to E . These circumstances make a precise knowledge of the background desirable if E should be measured with an accuracy of, say, better than 10%.

§ 3. Magnitude of the effect.

The formula for the differential cross section $d\sigma/d\Omega$ for Compton

scattering of polarized radiation by free electrons was given in section 6 of Chapter III. For the case of scattering by iron atoms it may be assumed that for $E\gamma > 1$ MeV the Compton cross section is for all 26 electrons the same and equal to the free electron value.

The fraction of polarized electrons per Fe atom will be called f and, as will be discussed later, depends on the magnetic induction in the scattering iron strips.

The almost cylindrical symmetry of our scattering system together with the large size of the scattering magnet ensures that to good approximation

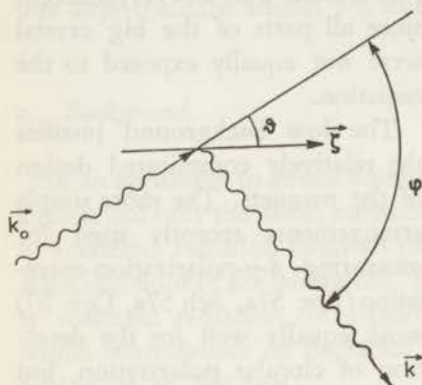


Fig. 34

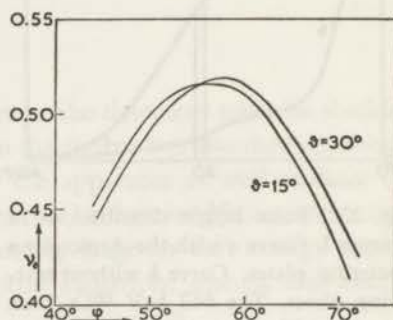


Fig. 35

Fig. 34. Pictorial representation of the scattering of the photon k_0 by an electron with spin direction ζ . ϑ is equal to the angle of emission of k_0 with respect to the axis of nuclear polarization.

Fig. 35. Variation of ν_c with scattering angle φ and for the two limits of the angle of emission ϑ . ν_c is the ratio of the circular polarization sensitive part of the differential Compton cross section to the normal differential Compton cross section.

the axis of the polarizing field, the incident quantum k_0 , the scattered quantum k and the electron spin direction ζ all lie in a plane. The angles between k_0 , k and ζ are defined pictorially in fig. 34. Since ζ is nearly parallel or antiparallel to the polarizing magnetic field and hence to the nuclear spin, ϑ (or $\pi - \vartheta$) is also the angle of emission of k_0 with respect to the nuclear spin.

Now $d\sigma/d\Omega$ may be written (Lip 54):

$$\begin{aligned} \frac{d\sigma}{d\Omega} &= 26 \frac{r_0^2}{2} \left(\frac{k}{k_0}\right)^2 \left(\Phi_0 + \xi_1 \Phi_1 + f \xi_3 \Phi_c\right) = & (51) \\ &= 13 r_0^2 (k/k_0)^2 \{[(1 + \cos^2\varphi) + (k_0 - k)(1 - \cos\varphi)] - \xi_1 \sin^2\varphi \\ &\quad - f \xi_3 (1 - \cos\varphi) [(k + k_0) \cos\varphi \cos\vartheta + k \sin\varphi \sin\vartheta]\} \end{aligned}$$

Since the counting rate is proportional to the differential cross section we will, for the purpose of our discussion, omit the proportionality constants altogether and then the counting rate may be written as:

$$\Phi = \Phi_0 + \xi_1 \Phi_l + f \xi_3 \Phi_c. \quad (52)$$

When the polarizing field is reversed without changing its magnitude, the temperature remaining constant, only the direction of the nuclear spin and the sign of ξ_3 are reversed. Hence the difference in counting rate on reversing the polarizing field is given by $2f\xi_3\Phi_c$. The counting rate averaged over the two directions of the nuclear spin is $\Phi_0 + \xi_1\Phi_l$. Thus a circular polarization effect E' may be defined by the ratio of the difference in counting rate on reversing the polarizing field to the average counting rate i.e.

$$E' = \frac{2f\xi_3\Phi_c}{\Phi_0 + \xi_1\Phi_l} = \frac{2f\xi_3\nu_c}{1 + \xi_1\nu_l} \quad (53)$$

The sign of E' is used to determine the sign of the nuclear magnetic moment. It should be remembered that Φ_l and ν_l are negative and that for an electric quadrupole transition with a spin decrease of two units ($Q, -2$), ξ_1 is negative, irrespective of the direction of \mathbf{I} .

In practice, the effect is averaged over the finite geometry of the apparatus. However, in spite of the wide range of angles accepted, the ratios of the cross sections vary so slowly with the angle in the region of interest that their averages may be estimated fairly accurately. The angle of emission ϑ between \mathbf{k}_0 and the axis of the polarizing field was designed for a variation from 15° to 30° . If the scattering electron has equal distances to source and counter, the geometrical arrangement makes the scattering angle φ equal to 45° , which corresponds to $\vartheta = 22\frac{1}{2}^\circ$.

All other rays have angles of scattering greater than 45° in the ideal case. The discriminators accept pulse heights corresponding to recoil electrons in the detectors from 480 to 710 keV. This energy range corresponds to a range in scattering angle of 44° to 68° for the 1.17 MeV radiation and 48° to 71° for the 1.33 MeV radiation. The discriminator cut-off at low energies was made in part to reduce extraneous scattering background but mostly to stay near the maximum of the curve of ν_c vs φ .

The ratio ν_c in the case of the 1.17 MeV γ -ray is shown in fig. 35 for the above region of scattering angles and for the two limiting values of ϑ . The broad maximum and relatively small dependence on ϑ make possible a rather accurate determination of the average value of the ratio. In determining the average, it is assumed that the weight to be assigned to any given value of φ is determined by the height of the pulse height curve (less the background), figure 33, at the energy which corresponds to φ ,

as calculated by the formula (III, 49). This assumption is valid for those quanta which are completely absorbed in the counting crystal. Since the Compton edge for 710 keV γ -rays is already as low as 520 keV, probably very few of the accepted counts corresponded to γ -rays which were not completely absorbed. The averages for both counters obtained with this weighing scheme and an angular range from 45° to 69° corresponding to an average of the two γ -ray energies are shown in Table 4. The dependence on θ is slight.

TABLE 4

| Average over scattering angle φ from 45° to 68° of the cross-section ratios for both energies of incident γ -rays and for both counters. | | | | | |
|---|----------|---------------------------|------------------------------|---------------------------|------------------------------|
| E_γ | θ | $\langle \nu_c^I \rangle$ | $\langle \nu_c^{II} \rangle$ | $\langle \nu_l^I \rangle$ | $\langle \nu_l^{II} \rangle$ |
| 1.33 | 15° | 0.516 | 0.517 | — 0.364 | — 0.361 |
| 1.33 | 30° | 0.518 | 0.518 | | |
| 1.17 | 15° | 0.497 | 0.498 | — 0.389 | — 0.386 |
| 1.17 | 30° | 0.500 | 0.500 | | |

In order to obtain a final average the cross section averages must be weighed and averaged according to the fractions of the scattered counting rate which come from each of the two incident γ -ray energies present. The ratio of the polarization insensitive cross sections is nearly constant and equal to $\Phi_0^{1.33}/\Phi_0^{1.17} = 0.925$.

This gives a weight of 0.48 to the higher energy averages and 0.52 to those for the lower energy. Accordingly, for a negligible background, the following equations are obtained for the magnitude of the effect in each of the two counters.

$$\text{Counter I.} \quad E' = 2f\xi_3 \frac{0.507}{1 - 0.377\xi_1}, \quad (54)$$

$$\text{Counter II.} \quad E' = 2f\xi_3 \frac{0.508}{1 - 0.368\xi_1}. \quad (55)$$

The quantity f may be determined by measurement of the magnetic induction in the scattering plates. The magnetic induction B and f , the fraction of polarized electrons per atom, are related by the equation

$$B = H + 4\pi[26f\beta N_0], \quad (56)$$

$\beta = 0.927 \times 10^{-20}$ gauss cm³; $N_0 = 8.46 \times 10^{22}$ cm⁻³. H was of the order of magnitude 50 Oe when B was 16.000 gauss. B was measured by winding a few turns around a scattering plate and observing the deflection of a fluxmeter when the magnetizing current was reversed. The fluxmeter was

calibrated by reversing a known current through a calibrated mutual inductance. B varied about 10% over the length of a plate, figure 36, and was rather constant at the same position from plate to plate. The value of f for the experiment was taken to be 0.060. An orbital contribution to B of 3% was taken into account (Arg 53).

The effect of background is to reduce the magnitude of the observed effect E from the E' given in equation (54, 55):

$$E = E' [1 - (W_B/\bar{W})] \quad (57)$$

where W_B is the background counting rate and \bar{W} is the average of the actual counting rates for the two relative orientations of the polarizing field and the field in the iron. If it is assumed that W_B is independent of temperature but that $\bar{W} = \bar{W}_0 \bar{I}(1/T)$, then

$$E = E' [1 - \{f_B \bar{I}(1/T)\}]. \quad (58)$$

$\bar{I}(1/T)$ is the average fractional counting rate as function of $1/T$ normalized at 1°K. \bar{W}_0 is the average counting rate at high temperatures; consequently, $f_B = W_B/\bar{W}_0$ is just the background fraction of the high temperature counting rate.

It should be noted that both detectors give the same sign for the effect.

The reason for this is that the sign of $\xi_3 \Phi_c$ in the cross-section formula depends physically not on the direction of \mathbf{k}_0 but on the relative senses of the rotations of the electric vector of \mathbf{k}_0 and the electron spin (see also Chapter III section 6). For a given relative orientation of polarizing field and field in the iron, this relative sense is the same for the forward scattering detected by both counters. Consequently each counter gives an independent value for the sign and magnitude of the circular polarization effect.

§ 4. Experiment.

In preliminary experiments the anisotropy of the emitted γ -radiation was measured as a function of $1/T^*$ in various polarizing fields. The values for $\varepsilon = [W(\pi/2) - W(0)]/W(\pi/2)$ obtained at the lowest temperatures were 0.45, using a polarizing field of 200 Oe. No increase in anisotropy was found when bigger fields up to 800 Oe were used. A polarizing field

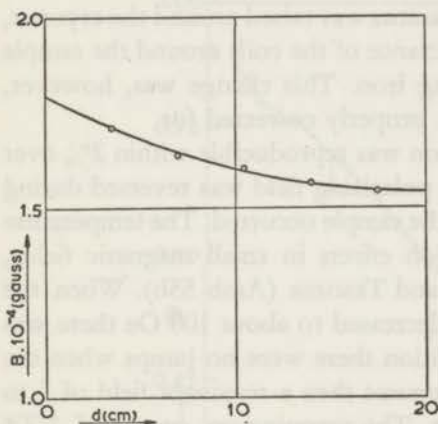


Fig. 36. Variation of magnetic induction B in a scattering plate with distance d from the pole.

of 280 Oe was therefore considered to be sufficient for the actual scattering experiments. During these experiments the polarizing field was kept constant within 1% and by reversal of the field the change in absolute magnitude was certainly smaller than 1%. Therefore no measurable change in anisotropy due to reversal of the polarizing field could occur. Starting 40 sec after each demagnetization the radiation was counted during 3 min intervals, which yielded about 35,000 counts in counter I and about 25,000 in counter II. The total measuring time was about 40 minutes, during which the pill warmed up to about 0.1°K.

Simultaneously χ , the magnetic susceptibility of the sample, was measured, giving $1/T^*$. When the scattering apparatus was raised around the cryostat, there was a change in the mutual inductance of the coils around the sample due to inductance of the neighbouring iron. This change was, however, constant for all the runs and could be properly corrected for.

The magnetic thermometer calibration was reproducible within 2% over the several measuring days. When the polarizing field was reversed during the run, a considerable warming up of the sample occurred. The temperature jumps were probably due to relaxation effects in small magnetic fields, reported also by AMBLER, HUDSON and TEMMER (Amb 55b). When the magnitude of the reversing field was decreased to about 100 Oe there was no change in heat production. In addition there were no jumps when the field was simply switched off, but of course then a remanent field of 5 to 10 Oe from the iron was still present. The warming-up curves of $1/T^*$ versus time never showed a nearly flat part at the lowest temperatures, as reported by DANIELS and ROBINSON (Dan 53). In view of the fact that the warming up rate was small, the heat leak being very small and the specific radioactivity low, it is impossible that the flat part was already passed during the time which elapsed between the start of the demagnetization and the first $1/T^*$ measurements.

It is probable that the relatively large amount of Co in the sample is responsible for different thermal properties in comparison with the pure salt.

Because of the unknown composition and shape of the crystals it was impossible to obtain the Curie-Weiss θ either by comparison with the data of DANIELS and ROBINSON, by entropy measurements, or by calculation. The magnitude of θ is probably in the region of 1 millidegree, requiring a correction of -10 to -15% to the quoted values of $1/T^*$ at the lowest temperatures, the correction being negligible at higher temperatures. Because of the uncertainty in θ , this correction has not been applied to the quoted results. The values of $1/T^*$ were corrected, however, for the decrease in susceptibility caused by the polarizing field according to the formula:

$$\left(\frac{1}{T^*}\right)_H = \left(\frac{1}{T^*}\right)_O \frac{\tanh(g_{||} \beta H / 2kT)}{g_{||} \beta H / 2kT}.$$

A typical curve for the change of counting rate with temperature and with field reversal may be found in fig. 37. In the scattering experiment counting rates were measured alternately with the polarizing field parallel to the field in the iron plates (counting rate W_p , marked by circles in the graph) and with polarizing field anti-parallel (W_a , marked by crosses). A value for $E = (W_p - W_a) / \frac{1}{2}(W_p + W_a)$ at a definite temperature was obtained from three adjacent points at different temperatures as follows

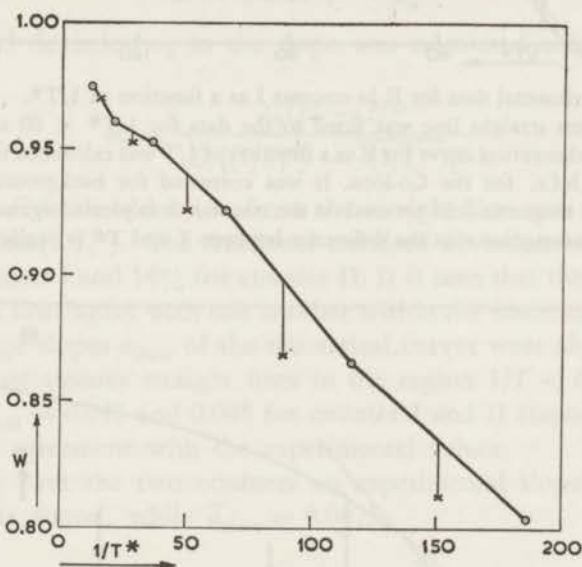


Fig. 37. Experimental curve for counter I of variation of counting rate W with $1/T^*$ and field reversal. The circles correspond to the polarizing field and induction in the iron parallel, while the crosses correspond to the two fields anti-parallel. — The statistical error in each point was 0.55%.

and as indicated on fig. 37. If the lowest temperature point were a circle, subsequent circles were connected by straight lines. $W_p - W_a$ was then given by the vertical distance between a cross and a circle, the temperature corresponding to that of the cross. This procedure avoided errors due to long time drifts in the apparatus.

The experimental results for counters I en II are shown, respectively, in figures 38 and 39. The vertical lines associated with each point give the statistical standard deviation. Each point represents the average of the results from several runs.

It will be shown in the following section that the effect should have the

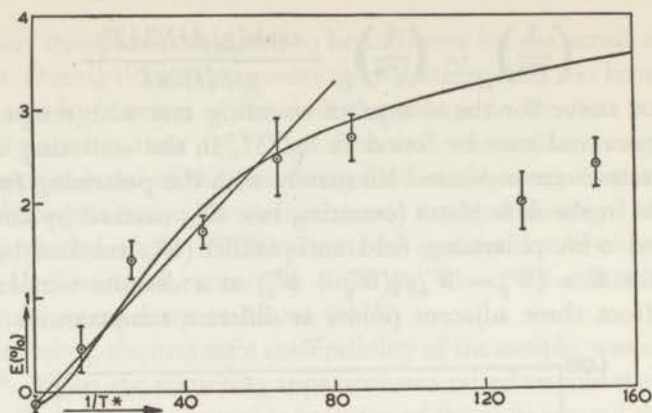


Fig. 38*. Experimental data for E in counter I as a function of $1/T^*$.

A least squares straight line was fitted to the data for $1/T^* < 60$ and is given in the graph. The theoretical curve for E as a function of $1/T$ was calculated from TRENAM'S data for the h.f.s. for the Co-ions. It was corrected for background and for the influence of the magnetic field reversal on the counter. It is plotted against $1/T^*$ under the assumption that the difference between T and T^* is negligible.

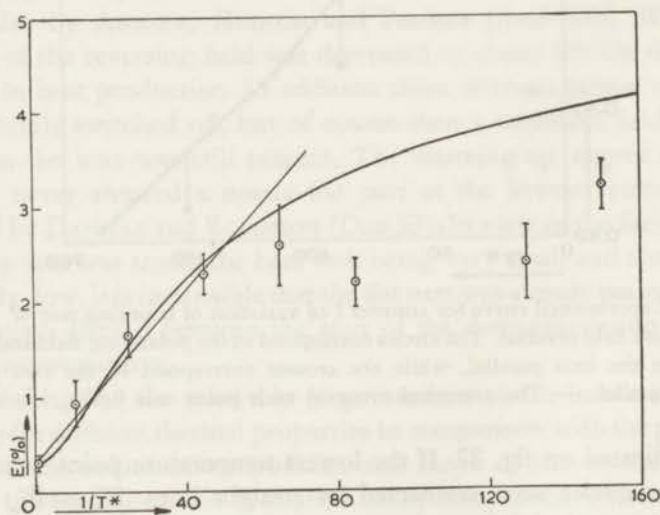


Fig. 39*. Experimental data for counter II. See caption of fig. 6.

- * Fig. 38 and 39 differ from the corresponding figures in (Whe 55b) with respect to:
- 1) a small difference in the theoretical curve, since in the calculations different values of μ and of the ion ratio were used.
 - 2) The standard deviations in the E-points, as given in (Whe 55b), were calculated from the total number of counts involved, which calculations were partly in error. The statistical errors in fig. 38 and 39 are the standard deviations in the spread in E over the various runs.

form indicated by the curve in figures 38 and 39. In the region below $1/T^* = 60$ this curve has a rather definite average slope. In order to check this average slope, least squares straight lines were calculated for all experimental points below $1/T^* = 60$, the points being weighted according to their statistical accuracy. The results for both counters expressed in per cent are

$$\text{Counter I:} \quad E = -0.16 + \frac{0.0435}{T^*}$$

$$\text{Counter II:} \quad E = +0.26 + \frac{0.0473}{T^*}$$

The standard deviation σ_b in the slope was calculated according to the formula

$$\sigma_b = \frac{\sum_i (E_i - E)^2}{\sum_i [(1/T_i^*) - \overline{(1/T^*)}]^2}$$

where $E_i - E$ is the deviation from the straight line and $\overline{(1/T^*)}$ is the average of the $(1/T_i^*)$. The fractional standard deviations obtained were 13% for counter I and 14% for counter II. It is seen that the slopes of the experimental lines agree with one another within the statistical accuracy.

The average slopes a_{theor} of the theoretical curves were also determined by fitting least squares straight lines in the region $1/T < 60$. This gave values of $a_{\text{theor}} = 0.047$ and 0.048 for counter I and II respectively, which are in good agreement with the experimental values.

Averaging over the two counters an experimental slope $\bar{a}_{\text{exp}} = 0.045$ ($\pm 10\%$) was found, while $\bar{a}_{\text{theor}} = 0.0475$.

§ 5. Discussion of the experimental results.

a. Sign of the nuclear magnetic moment.

It was found that the forward scattered counting rate for a given value if $1/T$ was greater when the polarizing field \mathbf{H}_p and the induction in the iron \mathbf{B}_i were parallel than when they were anti-parallel. The same effect was found in both counters.

In order to deduce the sign of the nuclear moment, the relative orientations of \mathbf{H}_p and the magnetic field \mathbf{H}_N acting on the nucleus must first be determined in the case of low temperatures. This relative orientation depends on the spin-orbit coupling in Co^{++} and on the interaction of the effective Co^{++} spin moment \mathbf{S} and \mathbf{H}_p .

$S = \frac{1}{2}$ for Co^{++} in this salt. The interaction of \mathbf{S} with \mathbf{H}_p is given by

$$H_E = g\beta H_p S_z$$

β is the Bohr magneton and g the spectroscopic splitting factor. There are

two energy levels corresponding to $S_z = \pm \frac{1}{2}$. The state with $S_z = -\frac{1}{2}$ lies lowest so that at low temperatures \mathbf{S} is opposite in direction to \mathbf{H}_p . The magnetic field at the nucleus comes mostly from orbital circulation of the electrons (section 2.B, chapter II), the direction of the orbital motion relative to the spin being determined by the sign of the constant λ in the spin-orbit coupling $\lambda\mathbf{L}\cdot\mathbf{S}$.

For Co^{++} , $\lambda = -180 \text{ cm}^{-1}$ so in the lowest energy state \mathbf{L} and \mathbf{S} are parallel. Thus \mathbf{L} is also oppositely directed from \mathbf{H}_p . However, \mathbf{L} corresponds to a circulation of negative charge; consequently the field at the nucleus, \mathbf{H}_N , is parallel to \mathbf{H}_p . The interaction of the nuclear moment with \mathbf{H}_N is given by

$$H_N = -(\mu/I)H_N I_z.$$

Thus for $\mu > 0$ the nuclear states with $m = I_z > 0$ lie lowest while for $\mu < 0$ the nuclear states with $m < 0$ lie lowest.

In the case of the ^{60}Ni cascade following β -decay in ^{60}Co the total spin decreases in the γ -ray transitions. If Δm is negative for a transition, corresponding to the states with $m > 0$ lying lowest, then the radiation emitted in the directions parallel and antiparallel to \mathbf{H}_p is respectively, l.c.p. and r.c.p. On the other hand, if Δm is positive for a transition, corresponding to the states with $m < 0$ lying lowest, the radiation emitted in the directions parallel and antiparallel to \mathbf{H}_p is respectively, r.c.p. and l.c.p. Consequently the photon spin is parallel to \mathbf{H}_p .

Since the electron moment is negative, the magnetization vector of the iron is antiparallel to the spins of the electrons producing the magnetization. Thus \mathbf{B}_I and $\boldsymbol{\xi}$ are antiparallel, where $\boldsymbol{\xi}$ is the polarization vector for the electrons.

When μ is positive and \mathbf{H}_p and \mathbf{B}_I are parallel then according to the preceding paragraphs the photon spin is antiparallel to $\boldsymbol{\xi}$. For forward scattering the counting rate is larger for the photon spin antiparallel to than for the case of the photon spin parallel to $\boldsymbol{\xi}$. Hence for positive μ the counting rate for both counters should be larger for \mathbf{H}_p and \mathbf{B}_I parallel than for \mathbf{H}_p and \mathbf{B}_I antiparallel. Since this was actually observed, one must conclude that ^{60}Co has a positive nuclear magnetic moment.

A positive moment for ^{60}Co is to be expected on a purely empirical basis since all measured magnetic moments of magnitude greater than 3 n.m., for which the signs have also been measured, have proved to be positive. This conclusion has considerable theoretical basis from the single particle model for the case of high spin. Then the large moments arise mostly from the orbital circulation of protons and are, therefore, positive.

The shell model of the nucleus predicts that the ground state configuration for the protons is $(f_{7/2})^7$ while that for the neutrons is $(f_{7/2})^8(f_{5/2})^2(p_{3/2})^3$. The

magnetic moment of the $(f_{7/2})^7$ protons in ^{59}Co is + 4.6 n.m. while the magnetic moments of neighbouring nuclei having odd $p_{3/2}$ neutrons are all less in absolute value than 0.5 n.m. Consequently, it is expected that the magnetic moment of ^{60}Co results mainly from the $f_{7/2}$ protons and is positive.

b. *Absolute magnitude of the effect.*

The absolute magnitude of the effect is given by equations (54, 55, 57) where the only unknown quantities are the degree of circular polarization ξ_3 and the degree of linear polarization ξ_1 . Expressions for ξ_1 and ξ_3 have been given by Tolhoek and Cox for E2 radiation with $I_t = I_1 - 2$, such as occurs in the ^{60}Ni cascade. Their results are

$$\xi_3 = \frac{2N_1 f_1 \cos \vartheta + 5N_3 f_3 (-5 \cos^3 \vartheta + 3 \cos \vartheta)}{2[1 - \frac{15}{7} N_2 f_2 P_2(\cos \vartheta) - 5N_4 f_4 P_4(\cos \vartheta)]} \quad (59)$$

$$\xi_1 = - \frac{\frac{45}{7} N_2 f_2 (1 - \cos^2 \vartheta) + \frac{25}{4} N_4 f_4 (7 \cos^4 \vartheta - 8 \cos^2 \vartheta + 1)}{2[1 - \frac{15}{7} N_2 f_2 P_2(\cos \vartheta) - 5N_4 f_4 P_4(\cos \vartheta)]} \quad (60)$$

For ^{60}Co with $I = 5$, $N_1 = 1$, $N_2 = 5/9$, $N_3 = 25/36$, and $N_4 = 125/252$.

ϑ is the angle of \mathbf{k}_0 with \mathbf{H}_p . The ξ 's must be calculated for an average ϑ which was taken to be that for the symmetrical ray, 23° . However, ξ_3 is very insensitive to ϑ in this region so that an error in ϑ of 5° gives an error in ξ_3 of only about $1\frac{1}{2}\%$ at $1/T = 100$, ξ_3 increasing as ϑ decreases.

The calculation of the orientation parameters f requires a knowledge of the energy levels of the nucleus in the combined polarizing and ionic field.

The energy levels of Co^{++} in the isomorphous salt Bi-Mg-nitrate were measured by Trenam (Tre 53); his values for the h.f.s. splitting constants A and B refer to the ^{59}Co nucleus with $I = 7/2$ and $\mu = 4.648$ n.m. For ^{60}Co the measured values $\mu = 3.80$ n.m. and $I = 5$ were used to calculate the constants A and B from the corresponding values for ^{59}Co . The result is that for $\frac{1}{3}$ of the Co-ions:

$$g_{||} = 7.29, g_{\perp} = 2.34, A/k = 0.0234^\circ\text{K}, B/k < 0.00008^\circ\text{K},$$

while for $\frac{2}{3}$ of the ions the constants are:

$$g_{||} = 4.11, g_{\perp} = 4.38, A/k = 0.00706^\circ\text{K}, B/k = 0.00853^\circ\text{K}.$$

In a preceding publication (Whe 55b) it was assumed that $\mu = 3.5$ n.m. and that the two types of ions occurred in the ratio 3 : 5, as these parameters fitted rather well to results of anisotropy measurements with polarized ^{60}Co nuclei, and since at that time a more accurate value for μ was not available. It can be shown that the theoretical anisotropy of gamma ray intensities in the temperature region of interest ($T > 0.005^\circ\text{K}$) is not noticeably changed if the parameters $\mu = 3.80$ n.m. and an ion

ratio 1 : 2 are used instead of $\mu = 3.5$ n.m. and an ion ratio of 3 : 5. For this reason the ratio 1 : 2 is adopted here, which ratio was also obtained from the paramagnetic resonance data (Tre 53).

The energy levels are calculated for $H = H_z = 280$ Oe according to section 4.G. of Chapter II, and are partly shown in fig. 40. The lowest levels have $I_z > 0$, corresponding with positive values of A and B or to \mathbf{I} and \mathbf{S} parallel. According to a) this refers to parallel \mathbf{H}_p and \mathbf{I} or to a positive value of μ . The numbers indicated for S_z and I_z refer to the case of complete Paschen-Back effect, whereas in fact a mixture of the wave functions $|S_z, I_z\rangle$ and $|S_z + 1, I_z - 1\rangle$ occurs.

However, when $H = 280$ oersteds the mixture is so small that for $1/T < 150$ it changes the degree of polarization by only one or two per cent from that which is calculated assuming that each level corresponds to a definite value for $m = I_z$. This last assumption has been made in the calculations.

The probability of a level being occupied was assumed to be proportional

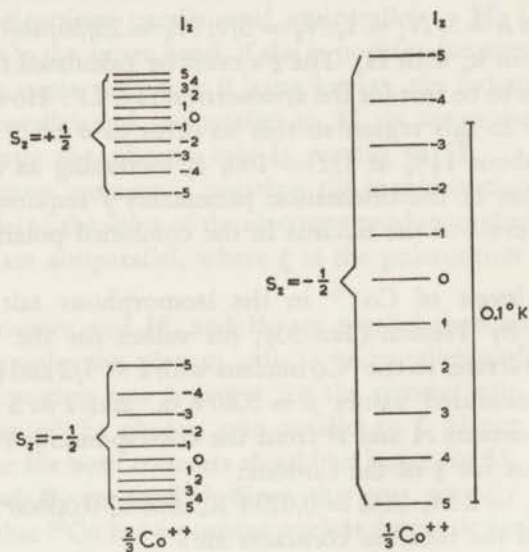


Fig. 40. Energy levels for the two types of Co^{++} ions in cerium magnesium nitrate with a polarizing field of 280 Oe in the direction of the trigonal axis, as calculated from TRENAM'S data (Tre 53).

to the Boltzmann factor $\exp(-W/kT)$. The orientation parameters f , equation (26), were calculated by summing over all 22 levels for both types of ions in regions where simplifying numerical assumptions could not be made. The resultant values for ξ were weighted according to the

1 : 2 ratio and substituted into equations (54, 55, 58) to give the theoretical estimate for the effect. The theoretical curves are drawn in figures 38 and 39 where the influence of the magnetic field on the counters has been included. The influence of the linear polarization was at maximum about 4%.

The agreement of the theoretical curve with the experimental data is rather good in the region below $1/T = 60$. As mentioned earlier there is good agreement for both counters between the slopes of the least squares lines fitted to the theoretical curves and those fitted to the experimental data.

However, at lower temperatures there is a marked discrepancy with the theoretical curve, which is well outside the statistical errors in the points. At lower temperatures the degree of polarization is far more sensitive to the exact details of the energy level splitting than at higher temperatures, since in the former case only a few of the lowest levels are appreciably populated.

Probably the interaction between the Ce^{+++} -ions and Co-ions has a considerable influence on the h.f.s. energy levels; moreover the h.f.s. constants for Co in Ce-Mg-nitrate may be somewhat different from the constants measured in Bi-Mg-nitrate. It may be mentioned that similar discrepancies were encountered in anisotropy measurements of Mn-nuclei in the same salt (Gra 54, Hui 56, 57). Very recently it was shown (Kur 57) that when the Ce-ions are replaced by diamagnetic La-ions and the crystal is cooled externally, there exists good agreement between the theoretically calculated anisotropy of the gamma ray intensity and the experimental data.

The agreement between theory and experiment at relatively high temperatures makes it probable that the assumptions on which the calculations of the degree of circular polarization and of the efficiency of the analyzer are essentially correct. Inversely, it may be concluded that in favourable cases the degree of circular polarization and also f_1 can be measured to an accuracy of 10%, a number which could probably be improved by taking more experimental data.

CHAPTER V.

ANISOTROPY AND POLARIZATION OF GAMMA RAYS EMITTED FROM ORIENTED ^{52}Mn NUCLEI.

§ 1. Introduction.

It was suggested in Chapter II, § 4, that a considerable orientation of Mn nuclei can be obtained in Ce-Mg-nitrate both by h.f.s. polarization and h.f.s. alignment. It will be recalled here that Mn ions, incorporated in Ce-Mg-nitrate, can occupy two different lattice positions, which have very different values of the crystalline field splitting parameter D . Fortunately, however, both the g -values and the h.f.s. splitting parameter A are for the two lattice positions the same: $g = 2$ and $A/k = 0.0234^\circ\text{K}$ per unit gyromagnetic ratio. This circumstance makes quantitative interpretation of h.f.s. polarization measurements somewhat simpler than in the analogous case of Co^{++} in Ce-Mg-nitrate.

In the absence of an external magnetic field, the electronic angular momentum \mathbf{S} of the Mn-ion will be aligned along the crystalline c -axis at low temperatures. The levels $S_z = \pm 5/2$ lie lower than the levels $S_z = \pm 3/2$ by the energy amount $4D$, which, for $2/3$ of the ions, corresponds to 0.046°K . The overall h.f.s. splitting is, according to table 1, roughly 0.05°K per nuclear magneton. Consequently at temperatures of, say, 0.01°K or lower, a considerable degree of nuclear alignment may be expected.

Both in case of polarization and of alignment the nuclear spins will be preferably parallel to the crystalline c -axis (see II, § 4).

It should further be mentioned that, according to (Kle 56), the temperature T^\otimes obtained from the susceptibility measurements does not differ from T by more than a few per cent for $T > 0.004^\circ\text{K}$ (Dan 53).

Two series of experiments were carried out. The first series (I) was devoted to an investigation of the anisotropy of the gamma ray intensity and the results, though inaccurate, led to a spin assignment for various nuclear levels (§ 3). After some improvements in the experimental techniques the experiments were resumed with a stronger radioactive source. This experiment (II) yielded information about the magnitude of the nuclear magnetic moment of ^{52}Mn (§ 4). The main purpose of experiment II was

to measure the circular and linear polarization of the Mn-radiations (§ 5 and 6).

Both in experiment I and II measurements were also carried out with aligned nuclei (§ 7).

§ 2. Decay scheme.

^{52}Mn (5.7 days) decays by β^+ -emission (33%) or K-capture (67%), succeeded by a cascade of 3 gamma rays of 0.73 MeV, 0.94 MeV and 1.46 MeV to the ground state of ^{52}Cr (fig. 41, Pea 46, Goo 46, Seh 54).

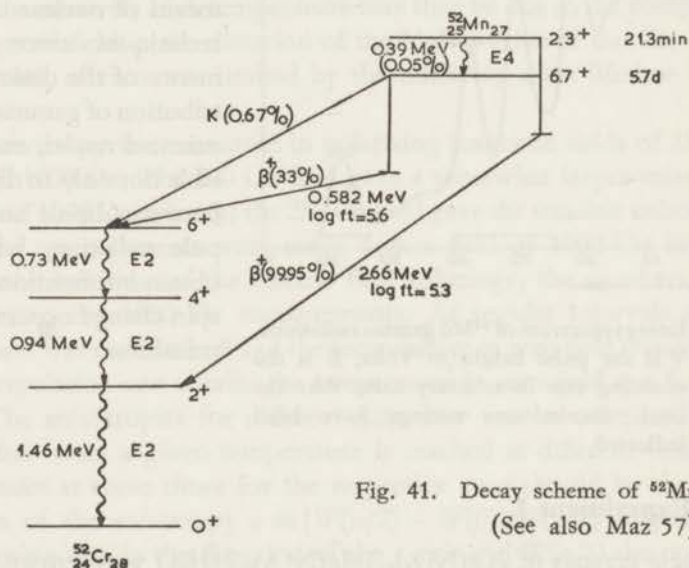


Fig. 41. Decay scheme of ^{52}Mn .
(See also Maz 57).

The order of the 0.73 and 0.94 MeV radiations is not known. Measurements (Kei 54) of the internal conversion coefficients α for these three radiations yielded the values $\alpha(0.73) = 3.0 \times 10^{-4}$, $\alpha(0.94) = 1.8 \times 10^{-4}$ and $\alpha(1.46) = 7.2 \times 10^{-5}$. The theoretical values for E2 radiations are respectively 3.60×10^{-4} , 1.75×10^{-4} and 6.9×10^{-5} . These radiations are, therefore, probably E2, but M1 cannot definitively be excluded. This means that no parity changes occur during the γ -transitions.

^{52}Mn has an excited state with a half life of 21.3 min. which has two possible modes of decay: β^+ -emission (99.95%) to the first excited state of ^{52}Cr and decay to the ground state of ^{52}Mn by a 0.39 MeV γ -ray (0.05%).

Conversion electrons corresponding to a 0.39 MeV gamma transition were observed (Osby 46) with an intensity of 5×10^{-4} electrons per 2.66 MeV positron. Since no gamma rays of 0.39 MeV were observed, one

must conclude that the 0.39 MeV gamma radiation is strongly converted. According to the Weisskopf-formula for the gamma transition probability, the 0.39 MeV radiation is E4 or M4, though E5 is also possible.

Although these data can be most simply fitted to the spin sequence $I = 6^+, 4^+, 2^+$ for the excited states of ^{52}Cr , unequivocal proof that this spin assignment is correct was not given.

It was thought worth while to investigate this problem by means of nuclear orientation techniques since measurements of the directional distribution of gamma rays from oriented nuclei, make it possible not only to discriminate between dipole and quadrupole radiation, but also to obtain information about the spin change occurring in the transition.

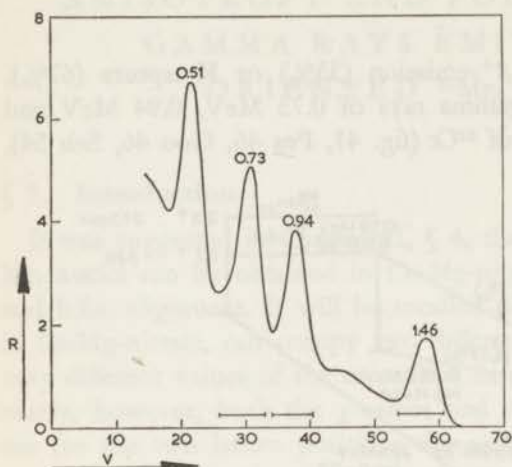


Fig. 42. Energyspectrum of ^{52}Mn gamma radiations. V is the pulse height in Volts, R is the counting rate in arbitrary units. Also the used discriminator settings have been indicated.

§ 3. Experiment I.

5 single crystals of $2\text{Ce}(\text{NO}_3)_3 \cdot 3\text{Mg}(\text{NO}_3)_2 \cdot 24\text{H}_2\text{O}$ were grown, weighing 6.2 g in total, which, at the start of the experiments contained about $15 \mu\text{C}$ of ^{52}Mn and less than 0.5 mg stable ^{55}Mn . They were mounted with parallel axes in the usual way, suitable for the adiabatic demagnetization technique (Gor. 51, Pop 55).

A field of 22 kOe was applied in the direction of higher g value (fig. 13), i.e. perpendicular to the c -axis of the crystals, at a temperature of 1°K , leading to a zero field temperature of about 0.003°K .

One counter was placed along the c -axis of the crystals and the other counter in a direction perpendicular to the c -axis. The counters consisted of $1\frac{3}{4}$ " diameter NaI-crystals mounted directly on the face of EMI multipliers and were magnetically shielded by concentric iron tubes and permalloy sheets. The counting equipment accepted pulses, corresponding to the photo peaks of the scintillation crystal. The energy spectrum of the ^{52}Mn radiations, as observed by our equipment, is shown in fig. 42.

The susceptibility was measured in a direction perpendicular to the *c*-axis. The quoted $1/T^*$ values have not been corrected for the demagnetizing factors, which were unknown.

For the measurements with polarized nuclei, magnetic fields up to 1000 Oe were applied along the *c*-axis of the crystals. In fields of 1000 Oe it was impossible to measure the susceptibility because the vibrations of the cryostat gave rise to varying inductions in the mutual inductance coils. The lowest temperatures obtained in fields of 400 Oe were about 0.025°K. The field was somewhat inhomogeneous because the counter arrangement made it preferable to place the cryostat at the end of a magnetized, straight iron bar. The relatively high temperature may then be due to the component of the magnetic field in the direction of the high *g*-value of the Ce.

The number of runs was limited by the relatively short lifetime of the nucleus.

The γ -anisotropy was measured in polarizing magnetic fields of 250 Oe, 400 Oe and 1000 Oe. The 400 Oe field gave a somewhat larger anisotropy than a field of 1000 Oe, whereas the 250 Oe field gave the smallest anisotropy. Most of the measurements were made with a field of 1000 Oe in order to swamp the influence of the electric field splittings; the numbers given below refer to the 1000 Oe measurements. At regular intervals during a run the field was switched off and the temperature in zero field was measured. By interpolation one obtains the temperature in zero field as a function of time. The anisotropies for different runs now can be compared using the fact, that when a given temperature is reached at different times, the counting rates at these times for the respective runs should be the same.

The sign of the anisotropy $\varepsilon \equiv \{W(\pi/2) - W(0)\}/W(\pi/2)$ (where $W(0)$ is the counting rate in the direction of the *c*-axis and $W(\pi/2)$ the counting rate perpendicular to the *c*-axis) was positive for all three γ -rays. The sign of ε leaves only the following three possibilities for the multipolarity of the radiations:

- a) Dipole radiation with no spin change (D, 0)
- b) Quadrupole radiation with a spin increase of two units (Q, +2)
- c) Quadrupole radiation with a spin decrease of two units (Q, -2).

Neither the statistical accuracy nor the accuracy of the T^* determination was high enough as to discriminate between the 3 cases for every gamma ray separately.

There was experimentally no systematic difference in magnitude of ε for the 3 γ -energies; for all the runs ε at the lowest temperatures remained between the limits $\varepsilon = 0.42 \pm 0.05$.

Therefore, no appreciable disorientation occurred during the γ -decay.

Such a disorientation would have caused a decrease of the anisotropy of the 1.46 MeV gamma ray relative to the anisotropy of at least one of the other gamma rays, which decrease was not observed.

Since the spin of the ground state of the even-even nucleus ^{52}Cr is 0, the 1.46 MeV radiation can only be (Q, -2) and thus the spin of the 1.46 MeV level must be 2.

The radiation between the first and second excited state of ^{52}Cr is also (Q, -2) because the other two possibilities have to be rejected. (Q, +2) would give to the second excited state spin 0 and would cause a complete loss of anisotropy of the 1.46 MeV radiation and its preceding transition. (D, 0) would decrease the anisotropy ϵ for the 1.46 MeV radiation at the lowest temperatures with 55% relative to the ϵ for the other γ -rays and this was not observed. The spin of the second excited state therefore must be 4.

If the radiation between the second and third excited state were (D, 0) or (Q, +2), the spin of the third excited state would be 4 and 2 respectively. A quadrupole transition with a spin increase from 2 to 4 would have an anisotropy which is, at the lowest temperatures, 50 per cent higher than the ϵ for the succeeding γ -rays. This possibility can be ruled out by the experimental results and is moreover improbable in view of the absence of a direct transition to the ground state. A (D, 0) transition between two levels with spin 4 would make ϵ at the lowest temperatures 18% higher than ϵ for the following (Q, -2) transitions. Though this is not definitely outside the experimental error in ϵ , analysis of the data shows that it is very improbable that the anisotropy of the 1.46 MeV radiation is smaller than the anisotropy for the other gamma rays.

The experimental results show therefore that all radiations are (Q, -2) radiations and that the spin assignment for the ^{52}Cr levels is 6, 4, 2, 0. This conclusion is corroborated by the results of experiment II, as is discussed in § 4. From the foregoing discussion it may be seen, however, that a high accuracy for ϵ vs T is not always necessary for determining the spins of the levels in the decay scheme.

Because the anisotropy for the 3 γ -rays is apparently the same, the counting rates for all the runs and the 3 gamma energies were averaged separately for the 2 counters and are shown plotted in fig. 43 as a function of $1/T^*$ in zero field.

The temperatures in the field of 1000 Oe (T_{1000}^*) were unknown, but it must be expected, that the value of $T_{1000}^* - T_0^*$ is approximately constant.

The indicated errors in the plotted points are the weighted averages of the statistical errors in the counting rate and do not represent the errors in the temperature measurements of the different runs.

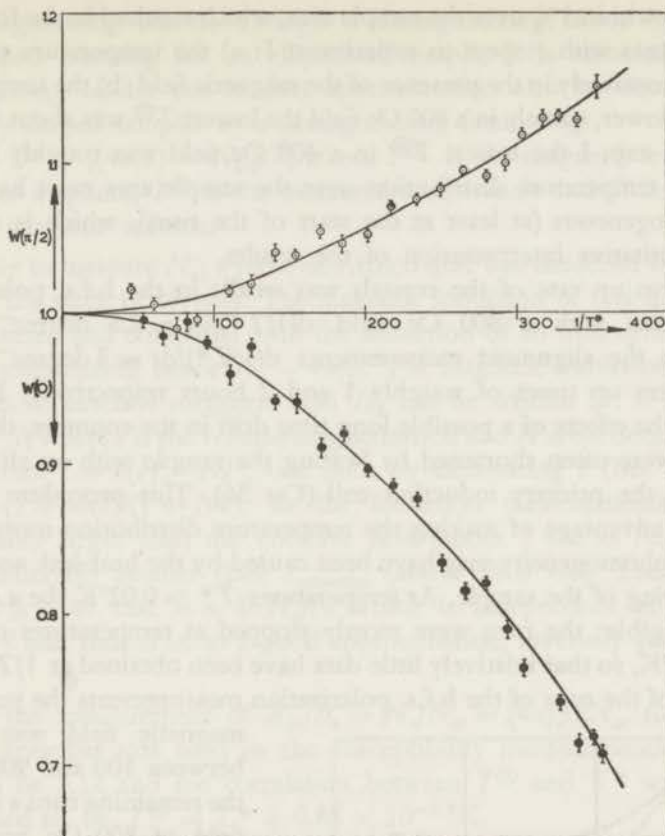


Fig. 43. Intensity of the gamma radiation, emitted by ^{52}Mn nuclei, which were polarized in an external magnetic field of 1000 Oe. $W(0)$ is the intensity of the radiation in the direction of the c-axis of the crystals, which is also the axis of the magnetic field. $W(\pi/2)$ is the intensity perpendicular to the c-axis. Both $W(0)$ and $W(\pi/2)$ have been normalized to unity for high temperatures. For the significance of $1/T^*$, the temperature in zero magnetic field, see the text.

§ 4. Experiment II.

4. A. Experimental part.

In this experiment 4 single crystals of Ce-Mg-nitrate were used, which weighed 13 g in total and which contained at the start of the experiment about $150 \mu\text{C}$ of ^{52}Mn .

The h.f.s. polarization measurements were carried out with a polarizing magnetic field produced by two water cooled, ironless coils (1.3 kW), which gave a maximum field strength of 1000 Oe. The field was homo-

geneous to within 1% over the sample area, which resulted in the following improvements with respect to experiment I: a) the temperature could be measured accurately in the presence of the magnetic field; b) the temperature was much lower, namely in a 800 Oe field the lowest T^{\otimes} was about 0.007°K whereas in exp. I the lowest T^{\otimes} in a 400 Oe field was roughly 0.02°K ; and c) the temperature distribution over the sample area must have been fairly homogeneous (at least at the start of the runs), which is essential for a quantitative interpretation of the results.

The warm up rate of the crystals was small: in the h.f.s. polarization measurements with a 800 Oe field $d(1/T^*)/dt \approx 2.5 \text{ degree}^{-1}\text{min}^{-1}$, whereas in the alignment measurements $d(1/T^*)/dt \approx 3 \text{ degree}^{-1}\text{min}^{-1}$, giving warm up times of roughly 1 and 2 hours respectively. In order to reduce the effects of a possible long time drift in the counters, the warm up times were often shortened by heating the sample with an alternating current in the primary induction coil (Cas 36). This procedure has the additional advantage of making the temperature distribution more homogeneous; inhomogeneity may have been caused by the heat leak and radioactive heating of the sample. At temperatures $T^* > 0.02^{\circ}\text{K}$ the a.c. losses were negligible; the runs were mostly stopped at temperatures of a few times 0.01°K , so that relatively little data have been obtained at $1/T^* < 50$.

In part of the runs of the h.f.s. polarization measurements the polarizing magnetic field was varied between 100 and 900 Oe. In the remaining runs a constant field of 800 Oe was used. Some results for polarizing fields of 100, 300 and 900 Oe are plotted in fig. 44. For comparison also the results for zero magnetic field are indicated, which results are more extensively discussed in section 7.

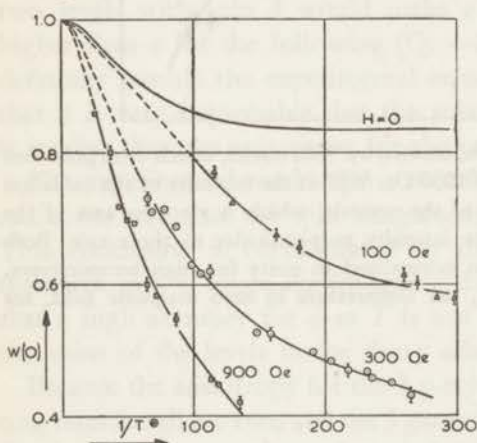


Fig. 44. Normalized intensity W of the 0.94 MeV gamma radiation in the direction ($\vartheta = 0$) of the polarizing magnetic field as a function of $1/T^{\otimes}$ and for various field strengths H . The curves are drawn with the purpose of connecting the experimental points and are extrapolated to $1/T^{\otimes} = 0$. The curve for $H = 0$ is deduced from the results of § 7.

4. B. Treatment of the data.

The anisotropy for the 3 gamma rays was measured for nuclei oriented by h.f.s. polarization in an external magnetic field of 800 Oe. The T^* -values were corrected for:

a. Demagnetizing effects. Though a demagnetizing factor has only a well defined meaning for an ellipsoidal sample, it is assumed that the demagnetizing effects can in first approximation also be described for arbitrarily shaped samples by a demagnetizing factor N_{cr} :

$T^{\otimes} = T^* + [(4\pi/3) - N_{cr}]C'$, where T^{\otimes} is the magnetic temperature reduced to a sphere, T^{\otimes} is the measured temperature and C' is the Curie constant per unit volume.

In order to measure N_{cr} a piece of Armco iron was modelled to the same shape as the stack of crystals. The magnetic induction of this iron sample was measured and compared with the induction of an iron sphere, which has a demagnetizing factor $N_s = 4\pi/3$. The magnetic induction B of the sample in an external magnetic field H_e can be written as: $B = H_e + (4\pi - N)I$, where I is the volume magnetization and N is the demagnetizing factor. Since $I = \chi(H_e - NI)$, one finds by eliminating I (Bec 39):

$B/H_e = (1 + 4\pi\chi)/(1 + N\chi)$. In the induction measurements H_e was considerably larger than the coercive field (about 1 Oe in Armco iron) and considerably smaller than $I_{saturation}$ (about 1800 Oe). Then $N\chi \gg 1$ and $4\pi\chi \gg 1$ so that $B \approx 4\pi H_e/N$ which is independent of the exact value of χ and thus B is, to a good approximation, inversely proportional to N .

From the measurement of $B_{cr}/B_s = N_s/N_{cr} = (4\pi/3)/N_{cr}$ follows N_{cr} for the principal axis used in the susceptibility measurements. N_{cr} was found to be 3.12 and the correlation between T^{\otimes} and T^* was thereby determined to be $T^{\otimes} = T^* + 0.85 \times 10^{-3} \text{ }^\circ\text{K}$.

b. Influence of the magnetic field on the susceptibility. The susceptibility was measured in a direction (called the y-axis hereafter) perpendicular to the crystalline c-axis, whereas the polarizing magnetic field was in the direction of the c-axis (z-axis, see also fig. 13). In order to find T^{\otimes} , one must reduce the susceptibility χ_H , measured in the presence of the magnetic field, to the susceptibility χ_0 which would have been measured if the magnetic field were isothermally removed. This reduction depends on the g -values.

Paramagnetic resonance measurements (Coo 53) at 4°K have shown that $g_x = g_y = 1.84$ and $g_z = 0.25 \pm 0.05$. However, after our measurements were finished, results of susceptibility measurements below 1°K were published (Whe 56), which give a much smaller value for g_z , namely $g_z < 0.03$. Consequently a field $H_z = 800$ Oe should give a temperature rise of only a few percent. But in the present experiments with 3 runs at different magnetic fields, ranging from 100 Oe to 900 Oe, the temperature rise was much larger and agreed with $g_z = 0.25$; this value was derived

from the temperature rise with the aid of the known (Dan 53, Coe 53) specific heat $c/R = 7.5 \times 10^{-6}/T^2$.

Part of the discrepancy may be due to inhomogeneities in the magnetic field, geometrical imperfections in the crystal growth, and particularly to misalignment of the crystals in the magnetic field. It should be mentioned that the lowest measured temperatures in a field of 800 Oe were for all runs the same to within 3%. Because of the uncertainty in the g_z -value in our crystals and in the precise direction of the magnetic field relative to the crystalline c-axis, the reduction of χ_H to χ_0 is based on the measured rise in T^\otimes , in a magnetic field of 800 Oe.

When a magnetic field $H_z = 800$ Oe was adiabatically applied, the measured T^\otimes increased from $T_i^\otimes = 0.003$ to $T_f^\otimes = 0.009$. As a first approximation it is supposed that the measured T^\otimes is equal to the thermodynamic temperature $T(T_i = T_i^\otimes, T_f = T_f^\otimes)$. From the isentropic temperature rise due to application of a field in an arbitrarily chosen direction and from the specific heat, one can calculate the Boltzmann factor $a = (\beta/2kT) \sqrt{(g_x^2 H_x^2 + g_y^2 H_y^2 + g_z^2 H_z^2)}$ in which β is the Bohr magneton and H_x, H_y, H_z are the components of the field along the axes. From the magnitude of a one can find the reduction from χ_H to χ_0 according to the formula (13):

$$\chi_H/\chi_0 = (\tanh a)/a - \{[\tanh a - (a/\cosh^2 a)]/a^2\} \cdot g_y^2 H_y^2 / (g_x^2 H_x^2 + g_y^2 H_y^2 + g_z^2 H_z^2).$$

For $T_i = 0.003^\circ\text{K}$ and $T_f = 0.009^\circ\text{K}$, $a = 1.10$ and this makes $(\tanh a)/a = 0.73$ and $[\tanh a - (a/\cosh^2 a)]/a^2 = 0.37$. If $g_z = 0.25$, then the second term in (13) may be omitted, because H_y is so much smaller than H_z . This is no longer true if $g_z = 0$; in view of the geometrical arrangement in the experiment H_y must have been considerably smaller than H_x and then $g_y^2 H_y^2 / (g_x^2 H_x^2 + g_y^2 H_y^2 + g_z^2 H_z^2)$ becomes of the order of 0.1.

If $\chi_H/\chi_0 = 0.73$, then T_f^\otimes in a field of 800 Oe would have been 0.0066 instead of the first approximated value of 0.009. From $T_f = 0.0066^\circ\text{K}$ as a second approximation one deduces $a = 1.00$ and $\chi_H/\chi_0 = 0.76$, which gives $T_f^\otimes = 0.0069$.

The numbers given here apply only to the lowest temperatures obtained, but similar calculations lead to reductions for all measured susceptibilities. At $1/T^\otimes = 80$ the correction given by the $(\tanh a)/a$ term is about 8%, at $1/T^\otimes = 40$ about 2%. Because the second term in (13) is neglected, the real $1/T^\otimes$ values for $1/T^\otimes < 80$ may be a few percent higher still. For $1/T^\otimes > 80$ the plotted $1/T^\otimes$ values may be up to 10% too low. Because of this uncertainty the quantitative discussion of the results is confined to the region $1/T^\otimes < 80$. It should be remarked that in the experiments of section 5 and 6, where fields lower than 800 Oe were used, χ_H/χ_0 reached also values of

about 0.75 at the lowest temperatures ($1/T^{\otimes} \approx 250$).

The intensity $W(\vartheta)$ of the quadrupole radiation for polarized nuclei has a minimum in the direction of the axis of the magnetic field ($\vartheta = 0$). The counting rates $W(0)$, normalized to unity for high temperatures were a few percent higher for the 0.73 MeV and 0.94 MeV gamma radiation than for the 1.46 MeV gamma rays. This is due to the fact that 1.46 MeV gamma rays

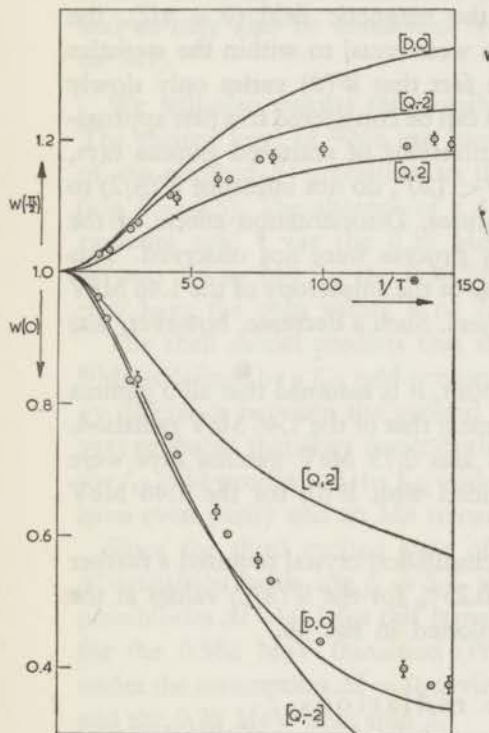


fig. 45

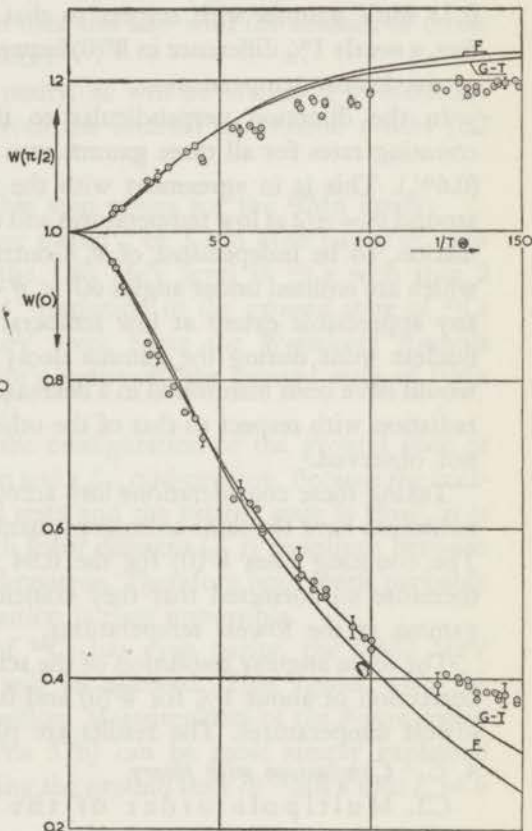


fig. 46

Fig. 45. Experimental points of $W(0)$ and $W(\pi/2)$ for the 1.46 MeV radiation compared with three theoretical curves (see § 3) as a function of $1/T^{\otimes}$, calculated for a nuclear magnetic moment of 2.6 n.m. and assuming $T = T^{\otimes}$.

Fig. 46. Intensities of the gamma radiation of ^{52}Mn -nuclei, polarized in an external magnetic field of 800 Oe, as a function of $1/T^{\otimes}$. For a number of arbitrarily chosen points the statistical errors are indicated in the graph.

The theoretical curve, indicated with G-T, has been calculated under the assumption that only the G-T-interaction in the β^+ -decay has a non-zero matrix element and for $\mu = 2.8 \mu_N$. Curve F is calculated for $\mu = 2.6 \mu_N$ and assuming a non-zero matrix element only for the Fermi-interaction.

can scatter at the polarizing magnet into the scintillation crystal and contribute to the measured intensity of the lower energy gamma rays, whereas the scattered radiation has a smaller temperature dependence. The influence of the 1.46 MeV radiation on the results for the 0.94 and 0.73 MeV gamma rays is roughly the same. Scattering of the 0.94 MeV gammas in the cryostat may give an additional increase to the counting rate of the 0.73 MeV gamma with respect to that of the 0.94 MeV gamma ray. In fact, a nearly 1% difference in $W(0)$ between the two radiations was observed at the lowest temperatures.

In the direction perpendicular to the magnetic field ($\vartheta = \pi/2$), the counting rates for all three gamma rays were equal to within the statistics (0.6%). This is in agreement with the fact that $W(\vartheta)$ varies only slowly around $\vartheta = \pi/2$ at low temperatures and can be considered to a first approximation, to be independent of ϑ . Contributions of scattered gamma rays, which are emitted under angles $60^\circ < \vartheta < 120^\circ$, do not influence $W(\pi/2)$ to any appreciable extent at low temperatures. Disorientation effects of the nuclear spins during the gamma decay process were not observed. This would have been manifested in a decrease of the anisotropy of the 1.46 MeV radiation with respect to that of the others. Such a decrease, however, was not observed.

Taking these considerations into account, it is assumed that all 3 gamma radiations have the same anisotropy, namely that of the 1.46 MeV radiation. The counting rates $W(0)$ for the 0.94 and 0.73 MeV gamma rays were therefore so corrected that they coincided with $W(0)$ for the 1.46 MeV gamma at the lowest temperatures.

The finite angular resolution of the scintillation crystal required a further correction of about 1% for $W(0)$ and 0.25% for the $W(\pi/2)$ values at the lowest temperatures. The results are plotted in fig. 46.

4. C. Comparison with theory.

C.I. Multipole order of the radiations.

In § 3 it was concluded from the apparent absence of disorientation of nuclear spins that all 3 radiations of ^{52}Mn were (Q, -2) transitions. For completeness we will compare the results of experiment II for the 1.46 MeV radiation with the three possibilities (Q, -2), (Q, +2) and (D, 0), which give a positive value of the anisotropy ε (§ 3).

In fig. 45 the theoretical curves for $W(0)$ and $W(\pi/2)$ have been plotted for the three possibilities under the assumption that $I_0 = 6$ and that the parameter $\beta = \mu H / I k T$ is equal to 1 for $1/T = 100$ ($\mu \approx 2.6 \mu_N$)*. It is seen that the curves for (D, 0) cannot be fitted to the experimental points for any choice of the horizontal scale factor i.e. for the nuclear

*) μ_N is 1 nuclear magneton (n.m.) or 5.05×10^{-24} erg/gaus.

magnetic moment. ($Q, +2$) is also to be rejected since the lower limit for $W(0)$, being approximately 0.5, is higher than the lowest experimental values of $W(0)$.

Since the experimental points for the 0.94 MeV and the 0.73 MeV radiations do not differ from the points for the 1.46 MeV radiations by more than a few percent, all radiations must be ($Q, -2$). This conclusion agrees with the internal conversion data and also with the absence of cross-over transitions in the gamma decay.

The levels of ^{52}Cr have even parity, as will be discussed in section 6 and as may also be concluded from the internal conversion results (E2 or M1).

We will also discuss the possible spin values for the ^{52}Mn levels:

The excited level of ^{52}Mn can have a spin 2 or 3 and even parity in view of the allowed β^+ -transition to the 1.46 MeV level in ^{52}Cr with spin 2 ($\log ft = 5.3$). The absence of a β^+ -transition to the ground state of ^{52}Cr excludes spin 1 for the 0.39 MeV level. Since the Weisskopf formula favours E4 or M4 for the 0.39 MeV radiation, the ground state of ^{52}Mn may have the spin values 6 or 7.

The shell model predicts that the configuration of the ground state of ^{52}Mn is defined by a $f_{7/2}$ odd-proton and a $f_{7/2}$ odd-neutron. Because the energy difference between the ground state and the excited state is small, it is very probable that they result both from different (j, i) couplings between the $f_{7/2}$ odd-proton and the $f_{7/2}$ odd-neutron. Therefore both levels probably have even parity and an M4 transition is then impossible.

Since the third excited state of ^{52}Cr has even parity, the 0.582 MeV β^+ -transition with $\log ft = 5.6$ will be allowed. This agrees with the possibilities $\Delta I = 0, 1$ for this transition. Measurements of the β -asymmetry for the 0.582 MeV transition (Pos 57b) can be most simply explained under the assumption $\Delta I = 0$, giving the ground state of ^{52}Mn a spin $I_0 = 6$ and the 0.39 MeV state spin 2.

C. II. Nuclear magnetic moment.

The spacing of the h.f.s. levels for different values of the nuclear magnetic moment of ^{52}Mn was calculated with the aid of the spin-Hamiltonian (Ble 54, Tre 53).

$$H = \beta(g_x H_x S_x + g_y H_y S_y + g_z H_z S_z) + D(S_z^2 - 35/12) + A.S.I. \quad (61)$$

The levels (for H in the direction of the crystalline c -axis) are given in the first approximation by:

$$\begin{aligned} & \pm \frac{5}{2} g_z \beta H_z + \frac{10}{3} D \pm \frac{5}{2} A I_z \\ & \pm \frac{3}{2} g_z \beta H_z - \frac{2}{3} D \pm \frac{3}{2} A I_z \\ & \pm \frac{1}{2} g_z \beta H_z - \frac{8}{3} D \pm \frac{1}{2} A I_z. \end{aligned} \quad (62)$$

Then the effect of the term $A(S_x I_x + S_y I_y)$ on this level scheme was calculated by first order perturbation theory; the mixing of states with different I_z , due to this term, was not taken into account, because the theoretical anisotropy ε was not affected by it by more than 1%.

One can then calculate the orientation parameters (III, §1) f_2 and f_4 , for various temperatures and from this derive $W(0)$ and $W(\pi/2)$ for a $(Q, -2)$ radiation as a function of $1/T$. (See formula 28).

In the calculations, the spin I_0 of ^{52}Mn was taken to be 6. In view of the decay scheme $I_0 = 7$ is also possible, but less probable. It should be noticed, that the theoretical anisotropy ε for a fixed value of the nuclear magnetic moment μ increases only about 3% if one changes I_0 from 6 to 7. The form of the curve of ε vs $1/T$ is nearly unmodified (fig. 18) and in our experiment it was thus impossible to distinguish between $I_0 = 6$ and $I_0 = 7$. The estimated value of μ is only 5% too low if I_0 were 7 instead of 6.

A change in the orientation parameters may be caused during the β^+ -transition. Suppose the matrix-element $|\langle 1 | \mathbf{1} | \rangle|^2$, describing the Fermi part of the interaction in the Hamiltonian for the β^+ -decay, is zero. Then the β -transition, which is probably allowed, will be caused by the Gamow-Teller part of the interaction only and this will be called simply "pure G-T-interaction" hereafter, whereas the case $|\langle \sigma | \mathbf{1} | \rangle|^2 = 0$ will be referred to as "pure F-interaction". The formulae of COX and TOLHOEK give for pure G-T-interaction in the decay of ^{52}Mn with $I_0 = 6$ to the third excited state of ^{52}Cr with spin $I_i = 6$: $f_2(I_i) = 39/42 f_2(I_0)$ and $f_4(I_i) = 32/42 f_4(I_0)$. No such change occurs for complete F-interaction or in the case of an allowed β -transition from $I_0 = 7$ to $I_i = 6$.

As mentioned before, the discussion will be divided in two parts: the "high" temperature region and the low temperature region.

a. *The temperature region $1/T^\circ < 80$.*

There is reasonable agreement between theory and experiment for $\mu = 2.8 \mu_N$ if one assumes complete G-T-interaction for the allowed β -transition from $I_0 = 6$ to $I_i = 6$; agreement is also achieved for $\mu = 2.6 \mu_N$ and pure F-interaction. An upper limit for μ can be found if one examines the causes which may have systematically decreased the anisotropy. The two most apparent are:

1. the disorientation due to the β -decay. This disorientation is largest for pure G-T-interaction.

2. The fact that for a given overall h.f.s. splitting the anisotropy decreases from its value for equidistant spacings if the lower levels lie closer together than the upper levels. An unequal spacing of the h.f.s. levels can occur due to: a) an incomplete Paschen-Back effect since the external magnetic field is only finite b) crystalline electric field splittings

and other possible interactions on the Mn-ion in the crystal such as, for instance, a spin-spin coupling between the Mn^{++} and Ce^{+++} -ions. The results of measurements of the anisotropy in the absence of a magnetic field (section 7) show that at low temperatures there is an overall alignment of nuclear spins along the c-axis of the crystal. Consequently the interactions, averaged over all the Mn-ions, help the external magnetic field to make the Paschen-Back effect more complete. It is therefore considered to be a rather safe assumption, that, on the average for all ions, the h.f.s. levels in a field of 800 Oe are at least as well equally spaced as if there were only the incomplete Paschen-Back effect. The spacing of the h.f.s. levels was therefore approximately calculated by perturbation theory with different values for the nuclear magnetic moment, assuming $D = 0$ in the spin-Hamiltonian. It is then found that for $\mu = 3.6 \mu_N$ there is definite disagreement with the experimental results.

A lower limit for μ is given by the following considerations. For a given value of μ the maximum anisotropy possible is obtained if a) the h.f.s. levels are equidistant, and b) if the β -transition does not disorient the nuclear spins, which is the case with a pure Fermi-interaction. For $\mu = 2.3 \mu_N$ the differences between the calculated values and experimental points of $W(0)$ and $W(\pi/2)$ are already beyond the statistical errors.

The magnitude of μ is therefore taken to be $2.8 \mu_N$ with a lower limit of $2.3 \mu_N$ and an upper limit of $3.6 \mu_N$. The value of $\mu = 2.8 \mu_N$ is supposed to be more probable than $\mu = 2.6 \mu_N$ obtained with pure Fermi-interaction in the β -decay, because it will be seen that in the region $1/T^* > 80$ experimental results favour the G-T-interaction. No definite answer can be given, however, as to the question whether the matrix-element $|\int \sigma|^2$ had a substantial magnitude. Agreement between theory and experiment in both $1/T^*$ regions can for instance also be obtained for pure Fermi-interaction under the assumption that 10% of the nuclei did not take part in the orientation process; this would have led to the conclusion that $\mu = 2.8 \mu_N$ instead of $\mu = 2.6 \mu_N$.*

A rather crude discussion of this result is given here in terms of the Schmidt model for the nuclear magnetic moment.

For ${}^{52}_{25}Mn_{27}$ both odd-proton and odd-neutron are in $f_{7/2}$ states.

* Recently measurements of the h.f.s. splitting constant A by means of paramagnetic resonance experiments were reported (by Jeffries), which yielded a gyromagnetic ratio $\mu/I_0 = 0.514$. Since I_0 is very probably equal to 6, the value of μ is then $\mu = 3.1$ n.m., which is in reasonable agreement with our result. This shows that in external magnetic fields of 800 Oe or larger the h.f.s. splittings do not deviate more than 10% from the theoretical estimates.

If the magnetic moment could be understood from the (j, j) coupling between one odd proton with $j_p = 7/2$ and one odd neutron with $j_n = 7/2$ to a nuclear spin $I_o = 6$ or 7 , one should observe a magnetic moment $\mu = \frac{1}{2} I_o (g_p + g_n) \mu_N$ (g_p and g_n are the gyromagnetic ratios of proton and neutron respectively in their specific (l, j) -states.)

We shall take experimental g -values from the neighbouring nuclei $^{53}\text{Mn}_{28}$ with $\mu = 5.05 \mu_N$ (Dob 56) and $I_o = 7/2$ and $^{49}\text{Ti}_{27}$ with $\mu = -1.10 \mu_N$ and $I_o = 7/2$, providing $g_p = 1.44$ and $g_n = -0.315$. With these g -values one obtains for the magnetic moment of ^{52}Mn $\mu = 3.30 \mu_N$ if $I_o = 6$. For $I_o = 7$ the calculated value $\mu = 3.85 \mu_N$ would not be compatible with the experimental results.

b. *The temperature region $1/T^* > 80$.*

If μ is given a value in order to fit the theoretical curves with the data from $1/T^* < 80$, then there is no agreement in the region $1/T^* > 80$, as may be seen in fig. 46. The deviation is most significant for the $W(\pi/2)$ counting rates, because both theoretical and experimental values are relatively independent of $1/T^*$ at low temperatures. Consequently the discrepancy between theory and experiment probably is not due to inaccuracies in the T^* -measurements or to deviations of the h.f.s. levels from the theoretical calculations. This discrepancy can be partly explained if one assumes a still stronger disorientation of the nuclear spins during the β -decay than was the case for pure G-T-interaction in the transition from $I_o = 6$ to $I_i = 6$. A stronger disorientation can be caused for a transition between $I_o = 5$ to $I_i = 6$ or in case of a forbidden transition, but these cases are improbable in view of the decay scheme and calculations show, that they do not give complete agreement with experiment either.

For $W(0)$ the discrepancy between the experimental points and the curves of fig. 46 is likely to be due to the uncertainty in T^* and the spacing of the hyperfine structure levels. Measurements of the anisotropy in magnetic fields ranging up to 700 Oe showed, that the experimental results cannot be properly described by theory based on the mentioned spin-Hamiltonian. An unknown interaction on the Mn-ions will affect the theoretical curve particularly in the low temperature region, whereas the overall h.f.s. splitting will be relatively unaffected. The overall splitting determines in first order the anisotropy in the high temperature region, on which the discussion of the magnitude of μ is based.

In connection with the discussions in section 7 it is remarked here, that comparison between the measured $W(0)$ and $W(\pi/2)$ at the lowest temperatures ($1/T^* = 140$), gives $f_2 = 0.42 \pm 0.005$ and $f_4 = 0.059 \pm 0.003$.

§ 5. Circular polarization.

5. A. Experiment.

The same experimental arrangement as described in Chapter IV was used for the measurement of the circular polarization of the emitted gamma rays. The field of the magnet for the polarization of the nuclei was made more homogeneous by fixing two thin circular iron plates on top of the pole pieces. It should be remarked that when a magnetic field applied in the $g_{||}$ direction is inhomogeneous, the field components in the g_{\perp} direction will cause a temperature rise and affect the susceptibility measurements.

Counter I accepted photons between 450 and 650 keV, counter II photons between 400 and 700 keV. The background for counter I was 20% and for counter II 26%.

The results for E' , as defined in chapter IV, and averaged over successive temperature regions $\Delta 1/T^* = 50$, are:

| | Counter I | Average | Counter II | Average |
|-----------------------|----------------------|-----------------|----------------------|-----------------|
| $1/T^{\otimes} = 250$ | $E' = 3.7 \pm 0.4\%$ | | $E' = 3.9 \pm 0.5\%$ | |
| $1/T^{\otimes} = 200$ | $E' = 4.1 \pm 0.3\%$ | $3.9 \pm 0.2\%$ | $E' = 4.0 \pm 0.3\%$ | $3.8 \pm 0.2\%$ |
| $1/T^{\otimes} = 150$ | $E' = 3.8 \pm 0.3\%$ | | $E' = 3.5 \pm 0.1\%$ | |

These results have to be corrected for a) the influence of the magnetic field reversal on the counters, respectively $-0.2 \pm 0.2\%$ and $+0.3 \pm 0.3\%$; b) the background, which correction was treated in chapter IV. As will be seen from fig. 47 the intensity W is not very temperature dependent in the region $1/T^* \approx 200$ and therefore the average (normalized) values $W = 0.77$ and $W = 0.80$ have been taken for counters I and II respectively. The magnitude of the effect E , corrected for background, is then calculated from $E = (1 - 0.20/0.77)^{-1} E' = 1.35E'$ and $E = (1 - 0.25/0.80)^{-1} E' = 1.45E'$. This, combined with the correction for magnetic field reversal, gives for counter I: $E = 5.5 \pm 0.3\%$ and for counter II: $E = 5.1 \pm 0.4\%$. The quoted errors represent the statistical errors deduced from the spread in the measured values of E' and do not include systematic errors.

5. B. Sign of the magnetic moment.

There is no doubt as to the sign of the effect, as may be seen from fig. 47. It was found, that the counting rates, obtained when the external magnetic field H_p for the polarization of the nuclei was parallel to the magnetic field H_s for the magnetization of the scattering iron, were lower than in case of antiparallel orientation of the two magnetic fields. Let us call the spins of the polarized nuclei I and the spins of the electrons in the magnetized

iron ξ_{iron} . If now the nuclear spin is decreased during the gamma transition and if the gamma ray is scattered by the electron in a forward direction, as was the case in this experiment, than theory says that the Compton cross section is lower for parallel \mathbf{I} and ξ_{iron} than for \mathbf{I} and ξ_{iron} antiparallel. (Fig. 29).

Therefore \mathbf{I} and ξ_{iron} were parallel for parallel orientation of \mathbf{H}_p and \mathbf{H}_s . In the iron ξ_{iron} is antiparallel to \mathbf{H}_s and therefore the experimental result is that at low temperatures \mathbf{I} was antiparallel to \mathbf{H}_p .

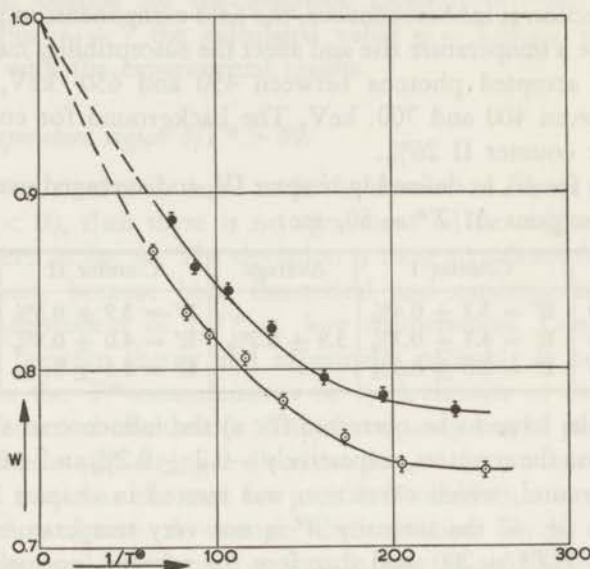


Fig. 47. Circular polarization of gamma rays, emitted from ^{55}Mn -nuclei, which were polarized at low temperatures by an external magnetic field of 300 Oe. W is the counting rate for one counter, normalized to unity at $T = 1^\circ\text{K}$. The open circles correspond to polarizing field and induction in the scattering iron parallel, while the closed circles correspond to antiparallel fields.

The spin \mathbf{S} of the Mn-ions is at low temperatures antiparallel to \mathbf{H}_p . The direction of the magnetic field \mathbf{H}_N , acting on the nucleus and mostly due to orbital motions of the electrons, cannot be deduced from the sign of the $\mathbf{L}\cdot\mathbf{S}$ -coupling in the case of Mn, because $L = 0$ and H_N , though of the order 6×10^5 Oe, is caused by the influence of excited states of the ion. It is known however, that for the positive nuclear magnetic moment of ^{55}Mn , the constant A in the h.f.s. coupling $A\mathbf{S}\cdot\mathbf{I}$ is negative in most salts and in particular in the isomorphous Mg-Bi-nitrate (Tre 53). A negative sign of A means, that for a positive nuclear magnetic moment \mathbf{S} , \mathbf{I} and $\boldsymbol{\mu}$ are antiparallel to \mathbf{H}_p at low temperatures. This situation obtained also in

the case of ^{52}Mn and its nuclear magnetic moment has therefore the positive sign.

For a nuclear magnetic moment of about $3 \mu_N$ a positive sign is to be expected on basis of the Schmidt model.

5. C. *Magnitude of the effect.*

A theoretical evaluation of the magnitude of the circular polarization effect for ^{52}Mn is more difficult than in the case of ^{60}Co because:

a) The spread in the energies of the three gamma radiations is much larger than for the two gamma rays of ^{60}Co . Since the efficiency of the analyzer for the detection of circular polarization depends on the photon energy, calculation of the average efficiency requires knowledge about the relative contributions of the three gamma radiations to the intensity of the scattered radiation accepted by the counter.

b) For an accurate calculation of the degree of circular polarization as a function of temperature, the values of the orientation parameters f_1, f_2, f_3 and f_4 are all required. Now apart from the fact that it is already difficult to calculate the h.f.s. splittings exactly, it was moreover shown in § 4, that deviations from theory occur particularly for a polarizing field as low as 300 Oe.

However, in spite of these complications, a reasonable estimate can still be obtained for this particular case, as will be seen in the subsections C I, C II and C III.

5. C. I. *Efficiency of the analyzer.*

a) The values of $\nu_c \equiv \Phi_c/\Phi_0$ as a function of the scattering angle φ are plotted in fig. 48 for the three gamma radiations of ^{52}Mn . By means of fig. 49 one can easily convert fig. 48 into a graph of ν_c as a function of the energy k of the scattered photon. The result is to be found in fig. 50. In order to obtain a weighted average of ν_c , called $\bar{\nu}_c$, it is necessary to decompose the energy spectrum of the scattered radiation in the relative contributions from the 1.46 MeV, 0.94 MeV and 0.73 MeV radiations. This decomposition can be estimated with the aid of the spectrum of the scattered radiation from the two gamma rays of ^{60}Co under the same experimental conditions. Since the energies of these two γ -rays, namely 1.17 MeV and 1.33 MeV, are not very different, for our purposes the scattered spectrum (fig. 33) can be considered to arise from a single gamma radiation of energy $k_0 = 1.25$ MeV. The intensity spectrum $R(k, k_0)$ can be expressed as:

$$R(k, k_0) = A \frac{dG(\varphi)}{d\varphi} \varepsilon(k) \frac{d\sigma(k_0, \varphi)}{d\Omega} \quad (63)$$

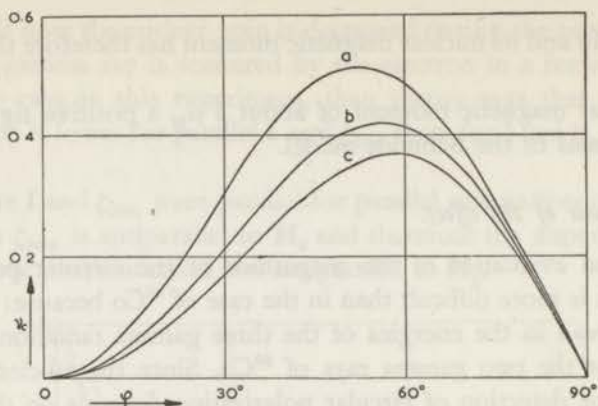


fig. 48 Fig. 48. ν_c , the ratio of the differential Compton scattering cross section, sensitive to circular polarization of the photons and to electron polarization, and the polarization insensitive differential cross section, given as a function of the angle of scattering, φ . a, b and c refer to the energies of the three ^{52}Mn radiations, respectively 1.46 MeV, 0.94 MeV and 0.73 MeV.

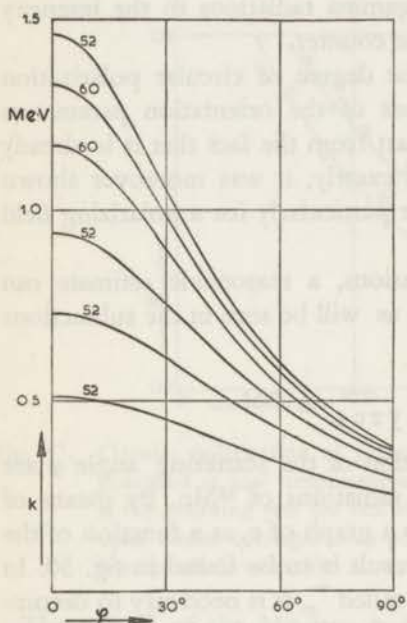


fig. 49

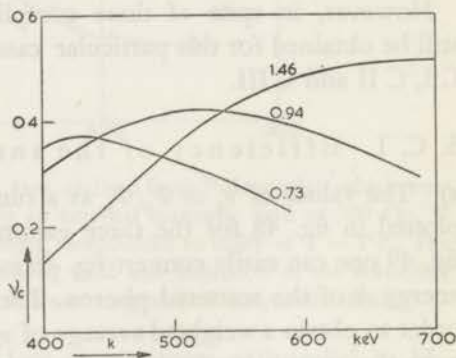


fig. 50

Fig. 49. Energy spectrum of Compton scattered photons as a function of the angle of scattering, φ . k denotes the energy of the scattered photon in MeV. The curves denoted by 52 refer to the three gamma radiations and the annihilation radiation of ^{52}Mn , the curves denoted by 60 refer to the 1.33 MeV and 1.17 MeV radiations of ^{60}Co .

Fig. 50. ν_c as a function of the energy k of the scattered photon. ν_c has been plotted for the three gamma radiations of ^{52}Mn separately.

R is here written as a function of k , since this corresponds with the experimental plots like fig. 33, but because of the relation $1/k - 1/k_0 = 1 - \cos \varphi$,

R can also be expressed as a function of φ ; vice versa $d\sigma/d\Omega$ can be written as a function of k and k_0 . The most important factor on the right hand side of the equation is the unknown geometrical factor $dG(\varphi)/d\varphi$, which is determined by the solid angles involved in a scattering process of a photon with energy k_0 , scattered over the angle φ . $\varepsilon(k)$, the efficiency of the scintillation counter and $d\sigma/d\Omega$, the differential cross section per unit solid angle for the Compton scattering, vary as a function of k in the region of interest (400—700 keV) by a factor of two whereas it can be shown that $dG/d\varphi$ varies as a function of φ in the region from 40° — 70° by more than a factor 10; A is a proportionality constant. Now the followed procedure for the decomposition of the ^{52}Mn scattered intensity spectrum is essentially this: from the observed values of $R(k, k_0 = 2.5)$ one can deduce R for other values k'_0, k''_0 etc. by the transformation $1/k' - 1/k'_0 = 1/k'' - 1/k''_0 = \dots = 1 - \cos \varphi$. Neglecting in first order the factors ε and $d\sigma/d\Omega$, and plotting R as a function of $1/k$ instead of k , this transformation reduces simply to a shift of the spectrum by the amount $1/k_0 - 1/k'_0$ etc. along the $1/k$ -axis.

In a more precise treatment the factors $\varepsilon(k)$ and $d\sigma/d\Omega$ may easily be taken into account. $\varepsilon(k)$ is practically equal to the photo efficiency of the scintillation crystal, since the Compton effect in a 2" NaI(Tl) crystal is small for gamma rays with energy between 400 and 700 keV. $\varepsilon(k)$ varies smoothly from about 0.45 for 400 keV to about 0.30 for 700 keV; $d\sigma(k_0, \varphi)/d\Omega$ was shown in fig. 27 for $k_0 = 1, 2$ and 4 (units mc^2).

The result of the calculations for counter I is shown in fig. 51, where the relative contributions of the three radiations to the total scattered intensity are shown. The sum of the three spectra, derived from the ^{60}Co -spectrum, should be equal to the experimentally observed spectrum of ^{52}Mn , which is a check for the validity of the calculation. The agreement is satisfactory.

The required quantity is:

$$\bar{\nu}_c = \sum_{k_0} \frac{\int_{k=0.9}^{1.3} \nu_c(k, k_0) R(k, k_0) dk}{\int_{k=0.9}^{1.3} R(k, k_0) dk} \quad (64)$$

Graphical integration gives $\bar{\nu}_c = 0.39$. If the integration is performed over only one gamma ray, the result is: $\bar{\nu}_c(1.46) = 0.40$, $\bar{\nu}_c(0.94) = 0.41$, $\bar{\nu}_c(0.73) = 0.33$.

Hence the adopted value for $\bar{\nu}_c$ is not very sensitive for changes in the magnitude of the contributions of the three γ -radiations to the total intensity of the scattered radiation. This justifies the approximate calculation of

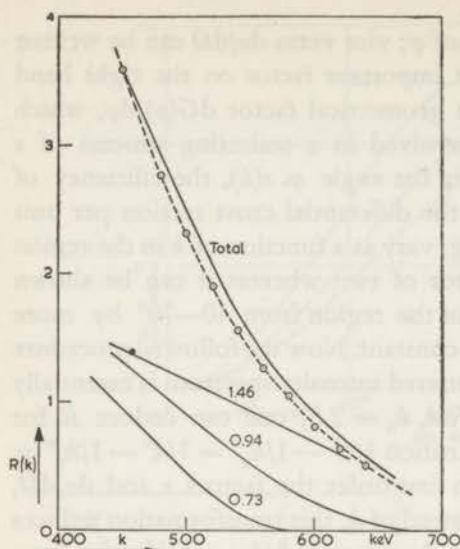


Fig. 51. Energy spectrum of the scattered radiation, accepted by counter I. R is the counting rate in arbitrary units and k is the energy of the scattered photons. The dotted curve is the experimentally observed intensity, corrected for the background radiation, as measured after removal of the scattering iron plates. The curves denoted by 1.46, 0.94 and 0.73 are the estimated contributions of the three ^{82}Mn radiations separately. The sum of these estimated contributions which are deduced from fig. 33, is indicated by the drawn „Total” curve.

$\bar{\nu}_c$ and an error, larger than 10% in the final result, cannot easily have been made.

The plotted values of ν_c in fig. 48 and 50 refer to formula 50 (III, § 6), hence it is assumed that the direction of the electron spin is precisely parallel (or antiparallel) to the direction of the incoming photon, whereas in the experiment the angle between the two directions is, on the average, nearly 30° . It is found, that, using formula (51) instead of (50), the values of ν_c are enlarged by about 10% for the 1.46 MeV photons and by 18% for the 0.73 MeV photons. Taking this into account the weighted average of ν_c becomes: $\bar{\nu}_c = 0.44 \pm 0.04$.

b) The results of the preceding paragraphs, combined with fig. III, 2.2 of ref (Did 57b), may be used to calculate also the weighted average of $\nu_l \equiv \Phi_l / \Phi_o$. The result is: $\bar{\nu}_l = -0.40 \pm 0.05$.

Combination of a) and b) gives for the magnitude of the circular polarization effect*:

$$E = \frac{2f\xi_3\bar{\nu}_c}{1-\xi_1\bar{\nu}_l} = \frac{0.053\xi_3}{1-0.4\xi_1}$$

The value of f , the fraction of polarized electrons per Fe-atom, was equal to 0.060 (Chapter IV, § 3).

5. C. II. Estimates of ξ_3 and ξ_1 .

The formulae for ξ_3 , the degree of circular polarization, and ξ_1 , the degree of linear polarization, for the case of a (Q, -2) gamma radiation, were given in Chapter III, § 5.

* The meaning of E and E' are interchanged with respect to Chapter IV (added in proof).

In the cascade of γ -rays in ^{52}Mn , no nuclear disorientation occurs, and consequently the value of ξ_3 is the same for all three radiations. A nuclear disorientation due to G.T.-interaction in the preceding β -transition may have occurred; from the relation $f_k(I_i) = [1 - k(k+1)/2I_0(I_0+1)] f_k(I_0)$ it is found that the maximum possible changes in f_1 , f_2 , f_3 and f_4 are respectively 2%, 7%, 14% and 24%, if $I_i = I_0 = 6$. Since the magnitude of f_3 and f_4 are smaller than respectively f_1 and f_2 , and also since the effect in ξ_3 , arising from the reduction of f_1 and f_2 , is opposite to the effect of a reduction of f_3 , one can estimate the influence on ξ_3 to be smaller than 5% under the actual circumstances.

We will neglect the possibility of a nuclear disorientation due to the preceding β -transition, since other uncertainties in the calculation of ξ_3 are comparatively larger.

a) Circular polarization.

The observed values of $W(\theta = 0)$, the intensity of the gamma radiation from nuclei polarized in a magnetic field of 300 Oe, can be used to estimate f_1 and ξ_3 . Since W is determined by f_2 and, to a smaller extent, also by f_4 , f_1 can only be calculated from W if the h.f.s. levels are equidistant and the energy differences between the levels are the same for all ions. The latter requirement is approximately fulfilled.

For $1/T^\otimes = 200$, $W(0) = 0.50$ (fig. 44) and the value of $\beta = \mu H / IkT$ must have been approximately 0.7. For ξ_3 , measured in directions between 15° and 30° with respect to the orientation axis, a value of $\xi_3 = 0.85$ is then calculated. A large degree of nuclear orientation ($f_1 \approx 0.8$) must have existed and only a few of the lowest h.f.s. levels will have been appreciably populated.

More experimental values of W are found from the circular polarization experiment itself. For angles between 20 and 30° , $W(\theta)$ dropped from a normalized value of 1 at $T^\otimes = 1$ to about 0.75 at $1/T^\otimes = 200$. Taking a temperature independent background radiation of 20% into account, roughly the same values of β , f_1 and ξ_3 are obtained (0.6, 80% and 81% respectively).

A theoretical estimate of ξ_3 may also start from calculated values of the h.f.s. levels, deduced from the spin-Hamiltonian. Since for $T^\otimes = 0.005^\circ\text{K}$ the degree of nuclear orientation is large, only the energies of a few lower levels are required. We will consider the spin-Hamiltonian

$$H = g\beta\mathbf{H}\cdot\mathbf{S} + D(S_z^2 - 35/12) + AS_xI_z$$

and calculate the h.f.s. levels for $S_z = -5/2$ and $S_z = -3/2$. Then the term

$$A(S_xI_x + S_yI_y) = \frac{A}{2}(S_+I_- + S_-I_+)$$

will be introduced as a perturbation, which mixes states ($S_z = -5/2, I_z$) with ($S_z = -3/2, I_z - 1$). The energy shift of the level ($S_z = -5/2, I_z$) is then given in first order by:

$$\delta E = - \frac{A^2 \langle -5/2, I_z | S_- I_+ | -3/2, I_z - 1 \rangle^2}{4 \{ E_{(-3/2, I_z - 1)} - E_{(-5/2, I_z)} \}}$$

Assuming $I = 6$ and for the nuclear magnetic moment the value $\mu = +2.8$ n.m., gives $(5/2)(52A/k) = 0.0108^\circ\text{K}$, which is the h.f.s. level splitting in the unperturbed scheme for $S_z = -5/2$. A difference between the two groups of Mn-ions in Ce-Mg-nitrate arises because of different values of D . It is found for instance that $\delta E(I_z = -5) = -0.0016^\circ\text{K}$ and -0.0028°K for one third and two thirds of the ions respectively. This gives for the spacing between the lowest levels $I_z = -6$ and $I_z = -5$, respectively for 1/3 and 2/3 of the ions: 0.0092°K and 0.0080°K . If also a few higher spacings are calculated and from that f_1 at $T = 0.005^\circ\text{K}$, we find $f_1(1/3) = 0.97$ and $f_1(2/3) = 0.96$. Generally from such high values of f_1 a nearly 100% circularly polarized radiation is to be expected in the direction $\vartheta = 0$, and more than 95% in the direction $\vartheta = 20^\circ - 30^\circ$.

The purpose of this calculation was to show that theoretically a very high degree of nuclear polarization is predicted. Even if the level splittings were lower by a factor of two, more than 85% circular polarization is estimated to occur for $20^\circ < \vartheta < 30^\circ$. This shows, that the details of the nuclear orientation process are of relatively little importance for the calculation of ξ_3 at $1/T^\circ = 200$, and also ξ_3 is expected to be nearly independent of T° in this temperature region. On the other hand, practically no information about the h.f.s. levels can be inferred from measured ξ_3 -values at these temperatures.

In connection with discussions in § 4 A, § 6 and § 7 C it should be mentioned, that, on basis of the calculations above, a very small value of the γ -ray intensity $W(0)$ could be expected at the lowest temperatures in fields of 100 and 300 Oe ($W(0) < 0.2$). This is, particularly for the 100 Oe field, in disagreement with experimental results (fig. 44).

b) Linear polarization.

$|\xi_1|$, the degree of linear polarization, depends on the values of f_2 and f_4 , which also determine the anisotropy ϵ . From the values of $W(\vartheta = 0)$ at $1/T^\circ = 200$, obtained with a polarizing field of 300 Oe, it is estimated that $|\xi_1|$ for $\vartheta = 25^\circ$ ($\xi_1 < 0$) was approximately 0.10.

5. C. III Comparison with experiment.

From the preceding discussion it is concluded, that the theoretically estimated value of E is:

$E = (0.053 \pm 0.005) \xi_3 / (1 - 0.4 \xi_1) = (0.051 \pm 0.005) \xi_3$
 which gives $E \approx 4.5$ to 5% . The experimental value for counter I was:

$$E = 5.5 \pm 0.3\%$$

The comparison between theory and experiment makes it probable, that ξ_3 was nearly 100% since the experimental value is already larger than the theoretical estimate for $\xi_3 = 100\%$. It is possible, that the background correction, which gives $E = 1.35 E'$, is too large, as the assumption of a temperature independent background radiation is incorrect. Assuming for the background intensity the same temperature dependence as for the total scattered intensity, one obtains $E = 1.25 E'$ and then $E_{\text{exp}} = 5.1 \pm 0.3\%$.

The conclusion of a nearly 100% circular polarization is also obtained from the results mentioned in § 5 A, if the statistical errors in E' are neglected. Then apparently E' changes by less than 10% if T^\otimes changes by a factor 1.7 and this requires $\xi_3 > 90\%$.

§ 6. Linear polarization.

The linear polarization of the 3 gamma rays was measured with the nuclei polarized in an external magnetic field of 400 Oe. The Compton polarimeter was described elsewhere (Did 57, a, b).

Two facts should be mentioned here:

1. For completely polarized nuclei, the gamma radiation, emitted in the $\vartheta = \pi/2$ direction is completely linearly polarized. For these gamma rays the electric vector is parallel to the nuclear spin in case of a magnetic (Q, -2) transition, whereas it is perpendicular to the nuclear spin in case of an electric (Q, -2) transition.

2. Linearly polarized gamma rays are predominantly scattered in a direction perpendicular to the electric vector.

From this it follows that, if one considers gamma rays, emitted in the $\vartheta = \pi/2$ direction, and compares the intensities of the radiation scattered in directions parallel and perpendicular to the nuclear spin, one may determine whether the (Q, -2) transition was an electric or a magnetic transition. From the results with ^{52}Mn it was concluded, that the 3 quadrupole transitions were all electric transitions, therefore no parity changes occur in the gamma decay.

As to the comparison of the magnitude of the linear polarization with theory, one makes use of the formula (Fan 49):

$$N_{\perp} / N_{\parallel} = (1 + \xi_1 Q) / (1 - \xi_1 Q). \quad (66)$$

N_{\perp} is the number of gamma rays scattered in a direction perpendicular to the plane of the incident gamma rays and nuclear spin.

$N_{||}$ is the number of gamma rays scattered in a direction perpendicular to the incident gamma rays and parallel to the nuclear spin.

ξ_1 is the degree of linear polarization ($0 < |\xi_1| < 1$). One finds from STEENBERG'S formulae (Ste 53) for the linear polarization of pure multipole radiation, emitted by oriented nuclei: $\xi_1 = -\varepsilon$ and $+\varepsilon$ for electric and magnetic quadrupole radiation respectively, where

$\varepsilon = \{W(\pi/2) - W(0)\} / W(\pi/2)$ is the anisotropy of the gamma radiation.

Q^* is the quality of the Compton polarimeter for the detection of the linear polarization. Q is a number between 0 and 1 and its meaning may be seen by putting $\xi_1 = 1$ in the formula. Q can be exactly calculated for a certain scattering angle from the theoretical Compton cross section for completely polarized radiation (Lip 54 a, b). Q has to be integrated over the scattering angles accepted by the polarimeter, which makes the calculation of Q necessarily inaccurate. It has to be remarked, that in the experiment the gamma rays were Compton scattered, not under an angle of 90° but under an average angle of 75° with an angular spread of about $\pm 15^\circ$. The energy resolution of the Compton polarimeter for gamma radiation of ^{52}Mn is shown in fig. 52. The calculated values of Q for infinite angular resolution

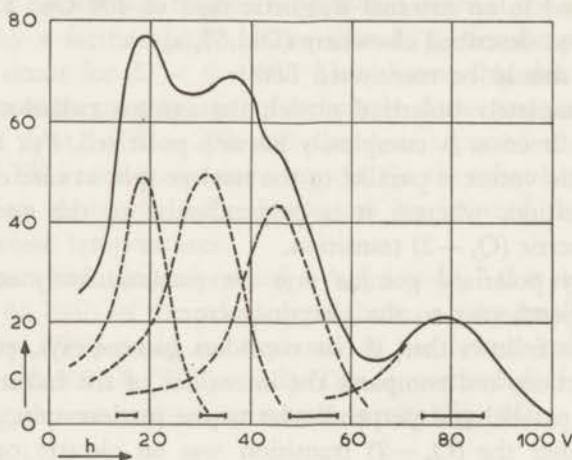


Fig. 52. Coincidence spectrum of the gamma radiations of ^{52}Mn . Coincidence counting rate, due to gamma rays scattered at the (central) plastic scintillator over 75° into the (side) NaI scintillator, as a function of the pulse height (in volts) in the plastic scintillator. The contributions from the 0.511, 0.73, 0.94 and 1.46 MeV radiations are shown together with the discriminator settings, used in the measurement of the linear polarization.

are to be found in column 3 of table 5, whereas the estimated values of Q for the experimental conditions are shown in column 4.

* Q is equal to $-\nu_l$ (III, § 6 and IV, § 3).

TABLE 5

| 1 | 2 | 3 | 4 | 5 | 6 | 7 | 8 | 9 |
|------------|------------------|-------------|------------|----------|---|-------------------------|-------------------------------------|---|
| γ | Energy in MeV | Q_{ideal} | Q_{corr} | $Q\xi_1$ | Contributions from other γ 's | $\sum_i g_i(\xi_1 Q)_i$ | Theor. N_{\perp}/N_{\parallel} | Experimental N_{\perp}/N_{\parallel} |
| γ_0 | 0.511 | — | — | — | 20% γ_1 , 7% γ_2 | -0.08 ^s | 0.84 | 0.78 ± 0.03 |
| γ_1 | 0.73 | 0.575 | 0.52 | -0.33 | 5% γ_0 , 20% γ_2 | -0.30 | 0.53 ^s | $0.52^s \pm 0.01$ |
| γ_2 | 0.94 | 0.506 | 0.46 | -0.29 | 17% γ_3 | -0.28 | 0.56 ^s | 0.57 ± 0.01 |
| γ_3 | 1.46 | 0.374 | 0.35 | -0.22 | — | -0.22 | 0.64 | 0.63 ± 0.01^s |

The anisotropy ε of the gamma radiation was measured in separate experiments in fields of 300 Oe and 500 Oe. The anisotropies in a field of 400 Oe were found by interpolation. In the temperature region $150 < 1/T^{\otimes} < 250$, where N_{\perp}/N_{\parallel} was actually measured, ε changes only slowly with $1/T^{\otimes}$: $\varepsilon = 0.65, 0.63$ and 0.57 for $1/T^{\otimes} = 250, 200$ and 150 respectively. For this reason ε was averaged over the temperature region $150 < 1/T^{\otimes} < 250$ and $\xi_1 Q$ is calculated and shown in column 5.

In the next column (6) one finds the estimated contribution of other gamma rays to the part of the pulse spectrum, accepted by the coincidence analyzer in a setting for the gamma ray in the horizontal row (taken from fig. 53). A weighted average of these contributions to $\xi_1 Q$ is given in column 7, from which the expected N_{\perp}/N_{\parallel} is then calculated by means of (66) (column 8). These values may be compared with the experimentally observed ratio of counting rates N_{\perp}/N_{\parallel} , when normalized to 1 for high temperatures (column 9). For one particular run the counting rates

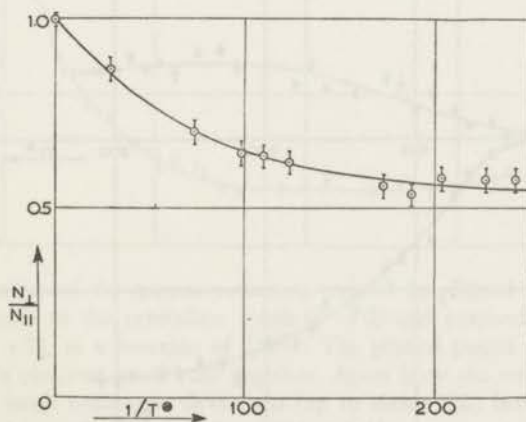


Fig. 53. Linear polarization of the 0.94 MeV gamma radiation, emitted by ^{52}Mn nuclei, which were polarized in a magnetic field of 400 Oe. The circles correspond to measured values of N_{\perp}/N_{\parallel} , normalized to unity at high temperatures. The curve represents N_{\perp}/N_{\parallel} as a function of $1/T^{\otimes}$, calculated from measured values of the anisotropy ε in small magnetic fields.

were also measured for $1/T^{\otimes} < 150$ and the experimental N_{\perp}/N_{\parallel} values for the 0.94 MeV radiation are plotted as a function of $1/T^{\otimes}$ in fig. 53. The expected values of N_{\perp}/N_{\parallel} , calculated for a number of temperatures by the forementioned method, are also plotted in the same graph. The agreement is satisfactory.

Because $|\xi_1| = |\varepsilon|$ it is of course not surprising that linear polarization measurements are consistent with the anisotropy measurements in fields of a few hundred oersted, though the anisotropy as a function of $1/T^{\otimes}$ does not agree with theoretical expectations on basis of the spin-Hamiltonian for Mn in Ce-Mg-nitrate. However the agreement shows to a certain extent that the calculations of Q are correct.

§ 7. Alignment measurements.

7. A. Experiment I.

The results of the anisotropy measurements in zero external magnetic field, obtained in experiment I, are given as a function of temperature T^* in fig. 54. The plotted points are averages of a number of runs for the 1.46 MeV and 0.94 MeV radiation. Again no systematic difference was observed between the anisotropies of the two radiations, all the runs giving values of ε between 0.19 and 0.22 at the lowest temperatures ($1/T^* = 300$).

Two facts are to be mentioned:

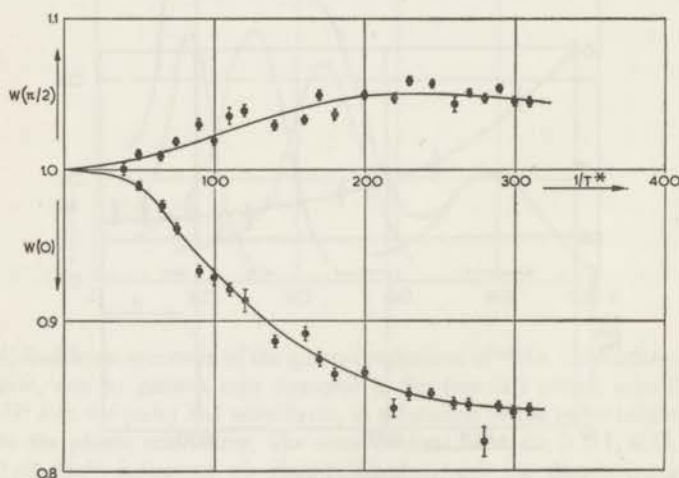


Fig. 54. Intensity of the gamma radiation of aligned nuclei as a function of $1/T^*$. $W(0)$ is the intensity along the c-axis of the crystals, whereas $W(\pi/2)$ is the intensity perpendicular to the c-axis. Both $W(0)$ and $W(\pi/2)$ have been normalized to unity for $T^* = 1$.

- a) the forementioned values of ε are appreciably lower than the values obtained with polarized nuclei in spite of the much lower temperatures in the alignment measurements.
- b) the form of the curves $W(0)$ and $W(\pi/2)$ deviate considerably from the theoretical curve, as for instance given in fig. 18 and fig. 46. This deviation will be still more pronounced in experiment II.

7 B. Experiment II.

Also in experiment II measurements were carried out with aligned nuclei in zero external magnetic field.

The counting rates $W(0)$ and $W(\pi/2)$ have been plotted as a function of $1/T^\otimes$ in fig. 55. At about $1/T^\otimes = 100$ the (W , $1/T^\otimes$) curves show a remarkable bend and for $1/T^\otimes > 100$ the counting rates are nearly constant. The flat part of the curves is much more pronounced than in fig. 54, but the maximum of the anisotropy, obtained at the lowest temperatures, is the same in both experiments.

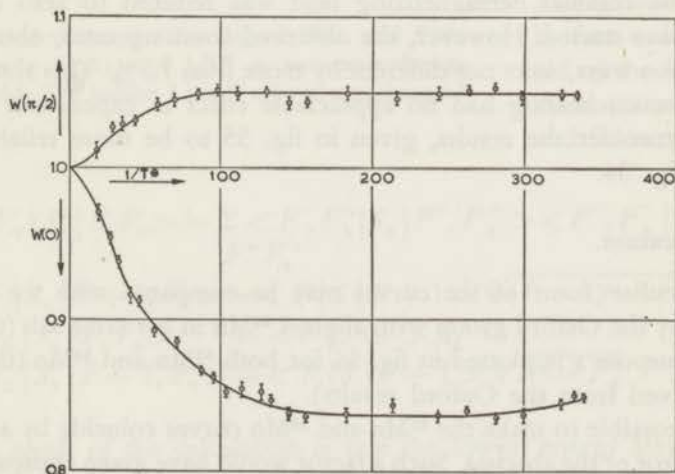


Fig. 55. Intensities of the gamma-radiation, emitted by aligned ^{52}Mn nuclei, in the direction of the crystalline c-axis ($\vartheta = 0$) and perpendicular to the c-axis ($\vartheta = \pi/2$), as a function of $1/T^\otimes$. The plotted points are averages of the points obtained in all runs together. Apart from the statistical errors, there were small systematic deviations (up to about 1%) between the runs, due to the use of various demagnetizing fields.

The reason of the discrepancy between the later measurements and those of exp. I is not fully understood, but could be due to the fact that the warm-up time of the crystals used in the former experiment was 5 times as short

as in exp. II. It is known that at the lowest temperatures obtained (0.003°K) heat conductivity is very bad and it is quite possible that some time after demagnetization heat leaks have caused an inhomogeneous temperature distribution in the crystals. This effect would change the relation between the counting rates and $1/T^{\otimes}$, except when the counting rates are linear functions of $1/T^{\otimes}$. A reduction of temperature inhomogeneity was achieved by alternating current heating during a run, because mainly the coldest parts of the crystals are heated by such a procedure.

Demagnetizations from smaller magnetic fields of 11000 Oe, 7500 Oe and 4500 Oe led to temperatures of about 0.006, 0.010, and 0.020°K respectively at the start of the counting. One may assume that the temperature at the start of the experiment is homogeneous and then the true counting rates are measured. As a further precaution, the demagnetization was sometimes carried out in two stages. In the first stage the temperature was lowered to about 0.1°K ; the heat produced at the crystal surface by condensation of the He exchange gas can be conducted throughout the crystal in a short time at that relatively high temperature. After a few minutes the residual demagnetizing field was reduced to zero and the counting was started. However, the observed counting rates, obtained in these various ways, were not different by more than 1.5%. This shows that inhomogeneous heating had no appreciable effect in experiment II. We therefore consider the results, given in fig. 55 to be more reliable than those of fig. 54.

7 C. Discussion.

The peculiar form of the curves may be compared with the results, obtained by the Oxford group with aligned ^{54}Mn in the same salt (Gra 54). For this purpose ϵ is plotted in fig. 56 for both ^{52}Mn and ^{54}Mn (the latter being derived from the Oxford results).

It is impossible to make the ^{52}Mn and ^{54}Mn curves coincide by a change in scale factor of the abscissa. Such a factor would have given approximately the ratio of the magnetic moments of the two nuclei. A procedure such as this, however, would only be justified if the hyperfine energy levels for the nuclei in this salt were equidistant.

These energy levels in zero magnetic field are given by $H = D(S_z^2 - 35/12) + A \mathbf{S} \cdot \mathbf{I}$. As can be seen from the values for A and D , the electric field splittings, in particular for 2/3 of the ions, are not (as in the investigated Co-salts: Gor 51, Pop 55, Whe 55b) large in comparison with the hyperfine splittings, and the level scheme may then be complicated. In principle, it is possible to calculate the energy levels for different values of A exactly

and from this the anisotropy as a function of $1/T$, but the elaborate calculations required did not look promising in view of the possibility that

D for Ce-Mg-nitrate might be different from the D for Bi-Mg-nitrate.

A perturbation calculation was carried out for $2/3$ of the ions, starting with the energy levels given by $AS \cdot I$ i.e. the (F, F_z) representation was used ($F = I + S$). The removal of the $2F + 1$ fold degeneracy of the levels by the term $D(S_z^2 - 35/12)$ was calculated in first order with the aid of the formulae (in the notation of CONDON and SHORTLEY):

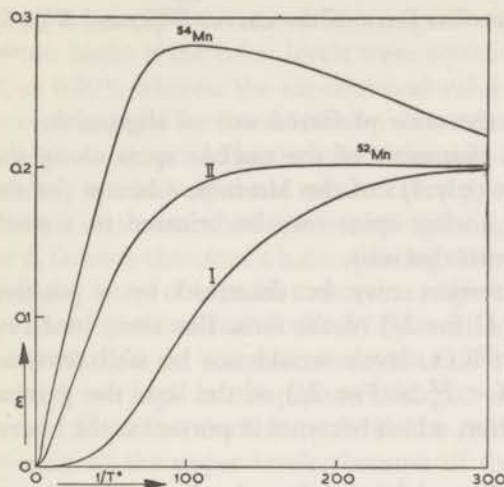


Fig. 56. Anisotropy ϵ for aligned ^{52}Mn and ^{54}Mn nuclei as a function of $1/T^*$ in zero external magnetic field. The indices I and II refer to experiments I and II.

$$\langle F', F_z' | S_z^2 | F, F_z \rangle = \sum_{F'', F_z''} \langle F', F_z' | S_z | F'', F_z'' \rangle \langle F'', F_z'' | S_z | F, F_z \rangle$$

$$\langle F, F_z | S_z | F + 1, F_z \rangle = \langle F | S | F + 1 \rangle \sqrt{(F + 1)^2 - F_z^2}$$

$$\langle F, F_z | S_z | F, F_z \rangle = \langle F | S | F \rangle F_z$$

$$\langle F, F_z | S_z | F - 1, F_z \rangle = \langle F | S | F - 1 \rangle \sqrt{F^2 - F_z^2}$$

The result of the calculation is that the lowest energy levels are well resolved and have high expectation values of I_z^2 . For instance, the level splitting between the two lowest levels with respectively $\langle I_z^2 \rangle = 36$ and $\langle I_z^2 \rangle = 28.2$ would be approximately 0.013°K . The energies of these two levels can also be calculated exactly by solving partly the secular equation for $D(S_z^2 - 35/12)$ in the (F, F_z) representation, which yields a splitting of 0.006°K . Consequently one would expect a high anisotropy (ϵ at least 0.5 for $1/T = 300$) for $2/3$ of the ions; the same conclusion holds for $1/3$ of the ions, for which the energy levels were calculated starting with the (S, S_z) representation and considering $A \cdot I \cdot S$ as a perturbation. Moreover one would, on the basis of these calculations, expect that the anisotropy curves for ^{54}Mn and ^{52}Mn would nearly coincide

since the magnetic moments of the two nuclei are approximately equal, as can be inferred from h.f.s. polarization measurements. This, however, is in contradiction to the experimental results. Two suggestions are discussed in order to explain the peculiar form of the curves $W(0)$ and $W(\pi/2)$ versus $1/T^\otimes$:

a. Not all nuclear spins have the same preferred axis of alignment.

For instance, a considerable alignment of the nuclear spins along the crystalline c-axis may occur for only 1/3 of the Mn-ions, whereas for the remaining 2/3 of the ions the nuclear spins may be oriented to a small extent in a plane perpendicular to that axis.

Phenomenologically this situation may be described by a positive instead of a negative value of D for 2/3 of the ions. For these ions one can then show that the lowest h.f.s. levels would not be well resolved and would have low values of $\langle I_z^2 \rangle$. For 2/3 of the ions the gamma ray anisotropy ε would be negative, which becomes important at the lowest temperatures.

Calculations show, that if all nuclei were in a level with $I_z = \pm 6$, then $f_4 = 0.13$ ($f_2 = 0.61$), whereas, if only the level $I_z = 0$ is populated, $f_4 = 0.11$ ($f_2 = -0.39$). It will be of interest to know, which value of f_4 was obtained in the experiment.

The intensity of the gamma radiation as a function of ϑ in case of a (Q, -2) transition and with $I_0 = I_1 = 6$, is according to the formulae of COX and TOLHOEK (Cox 53, Tol 53):

$$W(\vartheta) = 1 - 90/77 f_2 P_2(\cos \vartheta) - 24/11 f_4 P_4(\cos \vartheta),$$

where P_2 and P_4 are the spherical harmonics. Now $P_2 = 0$ for $\vartheta = 55^\circ$, thus if one measures the intensity in that direction, one can deduce f_4 as a function of $1/T$. From the measurements with one counter in the $\vartheta = 55^\circ$ direction, it was determined that for $150 < 1/T^\otimes < 300$, $f_4 = 0.03 \pm 0.02$, whereas for $1/T^\otimes < 100$, $f_4 = 0.01 \pm 0.01$. This result is corroborated by the comparison between $W(0)$ and $W(\pi/2)$:

$$W(0) = 1 - 90/77 f_2 - 24/11 f_4, \quad W(\pi/2) = 1 + 45/77 f_2 - 9/11 f_4.$$

If f_4 is negligibly small, $1 - W(0)$ should be approximately double the value of $W(\pi/2) - 1$. The results show that this is not the case and one can thus accept the values $f_4 = 0.015 \pm 0.005$ and $f_2 = 0.11 \pm 0.005$. It should be noted that these values are independent of the T^\otimes -measurements, and that the errors are mainly due to a possible misalignment of the counters with respect to the crystalline axis. Two conclusions can be drawn from this result:

1. A high degree of orientation of nuclear spins did not exist simultaneously for both groups of Mn ions, since otherwise a larger value of f_4 would have been measured. This conclusion is valid regardless whether

the c-axis or the plane perpendicular to the c-axis was the preferred direction of alignment.

2. The assumptions of the c-axis as a preferred axis for all spins and a small degree of orientation do not agree with the measurement of f_4 , which is too high: if the h.f.s. levels were equidistant, $f_2 = 0.11$ corresponds to $f_4 = 0.003$, whereas the experimental value is $f_4 = 0.015$. The discrepancy is even larger if the lower h.f.s. levels are more closely spaced than the upper levels, which would be the case if the spin-Hamiltonian were correct, since then f_4 is relatively more reduced than f_2 compared with the case of equidistant levels and the same overall splitting. The large experimental value of f_4 favours therefore a h.f.s. splitting with the upper levels closer together than the lower ones; such a situation might occur as a result of the Ce^{+++} — Mn^{++} interactions. It should be mentioned that the results of section 4, particularly in the temperature region $1/T^\circ > 80$ lead to a value of f_4 which is 30% too high in comparison with the value of f_2 , assuming equidistant levels. Therefore the h.f.s. polarization measurements also suggest a closer spacing of the upper levels; because of the magnetic field, however, the levels lie much more equidistant in case of polarization than for alignment and it can be shown that the discussion of the lower limit of μ is practically unaffected by these suggestions.

b. Relaxation of nuclear spins. One could assume that the nuclear spin system does not attain temperatures below 0.01°K , because of long nuclear relaxation times for instance. Under such circumstances the anisotropy would reach a relatively low maximum value, as is actually observed. As shown above, this assumption is in disagreement with the observed magnitude of f_4 . Moreover a relaxation behaviour is not corroborated by the results of anisotropy measurements with various demagnetizing fields. If one demagnetizes to $T^\circ = 0.003^\circ\text{K}$ and waits 45 minutes until a temperature of 0.010°K has been reached, the same counting rates are found as in case of a demagnetization to 0.010°K and starting one minute after demagnetization.

Concluding one may say that, though the behaviour of Mn nuclei in Ce-Mg-nitrate is not well understood, a number of possible orientation mechanisms have to be rejected. The results of anisotropy measurements in small magnetic fields make it very doubtful that the interactions on the Mn ion in a magnetically concentrated salt can be sufficiently described by the above mentioned spin-Hamiltonian.

SAMENVATTING

Sinds in 1951 de eerste resultaten van onderzoeken met gerichte atoomkernen werden bekend gemaakt, heeft dit gebied van onderzoek een aantal interessante uitbreidingen ondergaan. Terwijl het pionierswerk was gericht op het vaststellen van een anisotropie in de intensiteitsverdeling van gammastraling van gerichte ^{60}Co kernen, zijn sindsdien ook anisotropiemetingen betreffende α - en β -emissie uitgevoerd. Metingen van de intensiteitsverdeling van gammastralingen van verscheidene kernen zijn van nut geweest voor het verzamelen van kernspectroscopische gegevens.

Daarnaast leek het interessant om na te gaan of, in overeenstemming met de theoretische verwachting, gammastraling van gerichte kernen gepolariseerd is. Terwijl lineaire polarisatie van gammastraling enigermate uitvoerig was bestudeerd, was het bestaan van circulaire polarisatie alleen voor ongerichte kernen aangetoond door GUNST en PAGE.

Dit proefschrift heeft in de eerste plaats betrekking op metingen van de circulaire polarisatie van gammastraling, uitgezonden door gepolariseerde ^{60}Co en ^{52}Mn kernen. In de tweede plaats worden metingen besproken van de anisotropie der intensiteitsverdeling van gammastraling van gerichte ^{52}Mn kernen. Daarnaast zijn een aantal aspecten van experimenten met gerichte radioactieve kernen vrij uitvoerig behandeld; in het bijzonder is aandacht besteed aan eigenschappen van paramagnetische kristallen, die bij voornoemde experimenten worden gebruikt.

In hoofdstuk I worden begrippen ingevoerd, die in de volgende hoofdstukken een rol spelen; terwijl in § 1 en § 2 enkele methoden voor het richten van atoomkernen worden geschetst, zijn § 3 en § 4 gewijd aan de kernfysische verschijnselen, die bij gerichte radioactieve kernen optreden.

In hoofdstuk II wordt besproken, dat voor het richten van atoomkernen bij zeer lage temperaturen gebruik kan worden gemaakt van het magnetisch veld ter plaatse van de kern in paramagnetische ionen.

In § 1 en § 2 wordt de magnetische wisselwerking van de kern met de elektronenbeweging in paramagnetische ionen behandeld; in het bijzonder wordt aandacht besteed aan eventuele anisotropie van deze wisselwerking.

In § 3 volgt een discussie van een aantal aspecten van de adiabatische demagnetisatie van paramagnetische kristallen voor het verkrijgen van zeer lage temperaturen. Een uiteenzetting over twee soorten van kernorientatie, namelijk polarisatie en alignering van kernspins, wordt gegeven in § 4 en § 5.

Hoofdstuk III geeft in hoofdzaak de mathematische behandeling van

de richtingsverdeling (§ 1 en § 2) en de circulaire polarisatie (§ 4 en § 5) van gammastraling, uitgezonden door gerichte kernen. In § 3 wordt besproken hoe men in sommige gevallen uit de richtingsverdeling als functie van de temperatuur de grootte van het kernmagnetische moment kan bepalen. De essentiële inhoud van deze paragrafen is grotendeels ontleend aan de publicaties van COX, TOLHOEK en DE GROOT. § 6 bevat een theoretische discussie, afkomstig van LIPPS en TOLHOEK, over de waarneming van de circulaire polarisatie van gammastraling; in § 7 worden, in chronologische volgorde, de experimenten genoemd waarbij circulaire polarisatie van gammastraling een rol speelde.

In hoofdstuk IV wordt behandeld de meting van de draaizin en de grootte van de circulaire polarisatie van gammastralen, afkomstig van gerichte ^{60}Co kernen. De beschrijving van de gebruikte apparatuur wordt gegeven in § 2 en fig. 32.

In hoofdstuk V vindt men een beschrijving van een analoog experiment met gepolariseerde ^{52}Mn kernen. In beide gevallen werd behoorlijke overeenstemming tussen de experimenteel bepaalde en de theoretisch berekende grootte van de circulaire polarisatie gevonden (IV, § 5, en V, § 5); verder kon uit de gemeten draaizin van de circulaire polarisatie worden geconcludeerd dat de magnetische momenten der beide kernen het positieve teken bezitten. In § 3 en § 4 worden metingen vermeld van de richtingsverdeling der gammastraling van gepolariseerde ^{52}Mn kernen; de resultaten van deze metingen waren:

- a) de gammastralingen van ^{52}Mn zijn quadrupoolstralingen, gepaard gaande met een kernspinvermindering van twee eenheden; de aangeslagen niveaus van ^{52}Cr hebben bijgevolg de spinwaarden 2, 4 en 6.
- b) als waarde voor het magnetisch moment μ van ^{52}Mn werd gevonden $\mu = 2.8$ n.m. Een discussie van de mogelijke fout in deze waarde wordt gegeven in § 4.

§ 6 bevat een beschrijving van metingen van lineaire polarisatie van gammastralen van gepolariseerde ^{52}Mn kernen en in § 7 worden experimenten met gealigneerde ^{52}Mn kernen besproken.

CONTENTS

| | Page |
|---|------|
| CHAPTER I. INTRODUCTION AND SUMMARY | 7 |
| § 1. Methods for nuclear orientation | 7 |
| § 2. Low temperature technique | 9 |
| § 3. Anisotropy of radiations from oriented radioactive nuclei . | 9 |
| § 4. Polarization of radiation from oriented nuclei..... | 12 |
| CHAPTER II. ORIENTATION OF NUCLEAR SPINS | |
| § 1. General remarks | 14 |
| § 2. Crystal fields and hyperfine structures | 15 |
| § 3. Low temperature aspects of nuclear orientation | 27 |
| § 4. Magnetic h.f.s. polarization | 35 |
| § 5. Magnetic h.f.s. alignment | 45 |
| CHAPTER III. NUCLEAR PHYSICS | 50 |
| § 1. Anisotropy of gamma ray intensities | 50 |
| § 2. Disorientation by preceding beta-transition | 55 |
| § 3. Determination of the magnitude of the nuclear magnetic moment | 59 |
| § 4. Circular polarization of gamma radiation | 62 |
| § 5. Polarization of gamma radiation from oriented nuclei..... | 65 |
| § 6. Detection of polarization of gamma radiation | 70 |
| § 7. Other experiments related to circular polarization of gamma rays | 77 |
| CHAPTER IV. CIRCULAR POLARIZATION OF GAMMA RADIATION EMITTED FROM POLARIZED ^{60}Co -NUCLEI | 82 |
| § 1. Introduction | 82 |
| § 2. Apparatus for the detection of circular polarization | 83 |
| § 3. Magnitude of the effect | 87 |
| § 4. Experiment | 91 |
| § 5. Discussion of experimental results | 95 |
| CHAPTER V. ANISOTROPY AND POLARIZATION OF GAMMA RAYS EMITTED FROM ORIENTED ^{52}Mn NUCLEI | 100 |
| § 1. Introduction | 100 |
| § 2. Decay scheme | 101 |
| § 3. Experiment I..... | 102 |
| § 4. Experiment II | 105 |
| § 5. Circular polarization | 115 |
| § 6. Linear polarization | 123 |
| § 7. Alignment | 126 |

REFERENCES

- Abr 51a Abragam, A., and Pryce, M. H. L., Proc. roy. Soc., London **A 205** (1951) 135.
- Abr 51b Abragam, A., and Pryce, M. H. L., Proc. roy. Soc., London **A 206** (1951) 164, 173.
- Abr 55 Abragam, A., Horowitz, J., and Pryce, M. H. L., Proc. roy. Soc., London **A 230** (1955) 169.
- Abr 57 Abraham, M., Kedzie, R. W., and Jeffries, C. D., Phys. Rev. **106** (1957) 165.
- Amb 53 Ambler, E. Grace, M. A., Halban, H., Kurti, N., Durand, H., Johnson, C. E., and Lemmer, H. R., Phil. Mag. **44** (1953) 216.
- Amb 55a Ambler, E., and Hudson, R. P., Rep. Progr. Phys. **18** (1955) 251.
- Amb 55b Ambler, E., Hudson, R. P., and Temmer, G. M., Phys. Rev. **97** (1955) 1212.
- Amb 57 Ambler, E., Hayward, R. W., Hoppes, D. D., Hudson, R. P., and Wu, C. S., Phys. Rev. **106** (1957) 1361.
- App 57 Appel, H., and Schopper, H., Z. f. Phys. **149** (1957) 103.
- Arg 53 Argyres, P., and Kittel, C., Acta Metallurgica **1** (1953) 241.
- Bec 39 Becker, R., and Döring, W., Ferromagnetismus J. Springer, Berlin (1939).
- Bet 29 Bethe, H. A., Ann. Physik **3** (1929) 133.
- Bet 36 Beth, R. A., Phys. Rev. **50** (1936) 115.
- Beu 57 Beun, J. A., Thesis, Leiden 1957.
- Bla 52 Blatt, J. M., and Weisskopf, V. F., Theoretical Nuclear Physics, 1952, Wiley, New York.
- Ble 51a Bleaney, B., Phil. Mag. **42** (1951) 441.
- Ble 51b Bleaney, B., Proc. Phys. Soc. **A 64** (1951) 315.
- Ble 51c Bleaney, B., and Ingram, D. J. E., Proc. roy. Soc. **205** (1951) 336.
- Ble 53 Bleaney, B., and Stevens, K. W. H., Rep. Progr. Phys. **16** (1953) 108.
- Ble 54 Bleaney, B., and Trenam, R. S., Proc. roy. Soc. **A 223** (1954) 1.
- Ble 55 Bleaney, B., and Baker, J. M. Proc. Phys. Soc., London, **A 68** (1955) 1090.
- Bli 53 Blin-Stoyle, R. J., Grace, M. A., and Halban, H., Progr. Nucl. Phys. Vol. **3**, Pergamon Press, London 1953 pp. 63—83.

- Bli 55 Blin-Stoyle, R. J., Grace, M. A., and Halban, H., Beta and gamma ray spectroscopy, edited by K. Siegbahn North. Holl. Publ. Comp. 1955 pp. 600—612.
- Bli 57 Blin-Stoyle, R. J., and Grace, M. A., Handbuch der Physik, **42**, Springer Verlag 1957.
- Boe 57a Boehm, F., and Wapstra, A. H., Phys. Rev. **106** (1957) 1364.
- Boe 57b Boehm, Novey, Barnes and Stech, Preprint.
- Bor 33 Born, M., Optik, Springer Verlag, Berlin 1933.
- Bow 55 Bowers, K. D., and Owen, J., Rep. Progr. Phys. **18** (1955) 304.
- Bro 49 de Broglie, Mécanique ondulatoire du photon et théorie quantique des Champs, Paris, Gauthiers-Villars 1949, p. 65.
- Bru 57 Brussaard, P. J., Private communication.
- Car 49 Carrara, N., Nuovo Cimento **6** (1949) 50.
- Car 56 Carver, T. R., and Slichter, C. P., Phys. Rev. **102** (1956) 975.
- Cas 36 Casimir, H. B. G., de Haas, W. J., and de Klerk, D., Physica **6** (1936) 255; Communications Kamerlingh Onnes Lab., Leiden **256b**.
- Coo 49 Cooke, A. H., Proc. phys. Soc. London **A 62** (1949) 269.
- Coo 53 Cooke, A. H., Duffus, H. J., and Wolfe, W. P., Phil. Mag. **44** (1953) 623.
- Coo 55a Cooke, A. H., Progress in Low Temperature Physics I, edited by C. J. Gorter, North Holland Publishing Comp. Amsterdam 1955, pp. 224—244.
- Coo 55b Cooke, A. H., and Duffus, H. J., Proc. roy. Soc. **A 229** (1955) 407.
- Cox 53 Cox, J. A. M., Physica **19** (1953) 673.
- Dan 51 Daniels, J. M., Grace, M. A., and Robinson, F. N. H., Nature **168** (1951) 780.
- Dan 52 Daniels, J. M., Grace, M. A., Halban, H., Kurti, N., and Robinson, F. N. H., Phil. Mag. **43** (1952) 1297.
- Dan 53 Daniels, J. M., and Robinson, F. N. H., Phil. Mag. **44** (1953) 630.
- Dan 57 Daniels, J. M., Can. Journ. of Phys. **35** (1957) 1133.
- Dav 52 Davisson, C. M., and Evans, R. D., Rev. Mod. Phys. **24** (1952) 79.
- Dav 55 Davisson, C. M., Beta and gamma ray spectroscopy, edited by K. Siegbahn, North Holl. Publ. Comp. 1955 p. 24.
- Deb 26 Debye, P. Ann. Phys. **81** (1154) 1926.
- Deb 57 Debrunner, P., and Kündig, W., Helv. Phys. Acta **30** (1957) 261.

- Deu 57 Deutsch, M., Gittelman, B., Bauer, R. W., Grodzins, L., and Sunyar, A. W., *Phys. Rev.* **107** (1957) 1733.
- Did 57a Diddens, A. N., Huiskamp, W. J., Severiens, J. C., Miedema, A. R., and Steenland, M. J., *Nuclear Physics*, **5** (1957) 58.
- Did 57b Diddens, A. N., Thesis, Groningen (1957).
- Dob 56 Dobrowolski, W., Jones, R. V., and Jeffries, C. D., *Phys. Rev.* **101** (1956) 1001 and **104** (1956) 1378.
- Dob 57 Dobrov, W. and Jeffries, C. D. *Phys. Rev.* **108** (1957) 60.
- Ehr 11 Ehrenfest, P., *Journ. der Russ. Phys. Ges.* **48** (1911) 17.
- Ell 53a Elliot, R. J., and Stevens, K. W. H., *Proc. roy. Soc. A* **218** (1953) 553.
- Ell 53b Elliot, R. J., and Stevens, K. W. H., *Proc. roy. Soc. A* **219** (1953) 387.
- Fan 49 Fano, U., *Journ. Opt. Soc. Am.* **39** (1949) 859.
- Fan 57 Fano, U., *Nuovo Cimento* **5** (1957) 1358.
- Fel 57 Feld, B. T., *Phys. Rev.* **107** (1957) 797.
- Fer 30 Fermi, E., *Zeitschr. f. Phys.* **60** (1930) 320.
- Fra 38 Franz, W., *Ann. Physik* **33** (1938) 689.
- Fra 57 Frauenfelder, H., Bobone, R., von Goeler, E., Levine, N., Lewis, H. R., Peacock, R. N., Rossi, A., and De Pasquali, G., *Phys. Rev.* **106** (1957) 386.
- Fre 23 Fresnel, A., *Oeuvres complètes* (1866) 763.
- Gia 27 Giaque, W. F. *J. Amer. Chem. Soc.* **49** (1927) 1864.
- Gol 57 Goldhaber, M., Grodzins, L., Sunyar, A. W., *Phys. Rev.* **106** (1957) 826.
- Goo 46 Good, W. M., Peaslee, D., and Deutsch, M., *Phys. Rev.* **69** (1946) 313.
- Gor 34 Gorter, C. J., *Phys. Z.* **35** (1934) 923.
- Gor 48a Gorter, C. J., *Les phénomènes cryomagnétiques (Cérémonies Langevin et Perrin)* Paris (1948) 77.
- Gor 48b Gorter, C. J., *Communications Kamerlingh Onnes Lab., Leiden, Suppl.* **97d**, *Physica* **14** (1948) 504.
- Gor 51 Gorter, C. J., Poppema, O. J., Steenland, M. J., and Beun, J. A., *Communications Kamerlingh Onnes Lab., Leiden, no.* **287b**, *Physica* **17** (1951) 1050.
- Gra 54 Grace, M. A., Johnson, C. E., Kurti, N., Lemmer, H. R., and Robinson, F. N. H., *Phil. Mag.* **45** (1954) 1192.
- Gra 55 Gray, T. P., and Satchler, G. R., *Proc. phys. Soc. A* **68** (1955) 349.

- Gri 56 Griffing, D. F., and Wheatley, J. C., *Phys. Rev.* **104** (1956) 389.
- Gro 52 Groot, S. R. de, *Physica* **18** (1952) 1201.
- Gro 55 Groot, S. R. de, and Tolhoek, H. A., *Beta and gamma ray spectroscopy*, edited by K. Siegbahn, North Holland Publishing Company, Amsterdam (1955) pp. 613—623.
- Gun 53 Gunst, S. B., and Page, L. A., *Phys. Rev.* **92** (1953) 970.
- Hal 51 Halpern, O. *Nature* **168** (1951) 782.
- Han 56 Handel, J. v. d., *Handbuch der Physik* **15**, Springer Verlag, Berlin, 1956, pp. 1—38.
- Har 55 Hartogh, C. D., Tolhoek, H. A., and Groot, S. R. de, *Physica* **20** (1955) 1310.
- Hei 54 Heitler, W., *Quantum theory of radiation*, Oxford University Press, London (1954).
- Hei 57 Heine, V., *Phys. Rev.* **107** (1957) 1002.
- Hui 56 Huiskamp, W. J., Steenland, M. J., Miedema, A. R., Tolhoek, H. A., and Gorter, C. J., *Physica* **22** (1956) 587; *Communications Kamerlingh Onnes Lab., Leiden*, no. **304**.
- Hui 57 Huiskamp, W. J., Diddens, A. N., Severiens, J. C., Miedema, A. R., and Steenland, M. J., *Physica* **23** (1957) 605, *Communications Kamerlingh Onnes Lab., Leiden*, no. **308b**.
- Hum 43 Humblet, M. J., *Physica* **10** (1943) 585.
- Jah 37 Jahn, H. A., and Teller, E., *Proc. roy. Soc., London* **A 161** (1937) 220.
- Jau 55 Jauch, J. M., and Rohrlich, F., *The theory of photons and electrons*. Addison-Wesley Publ. Comp. Cambridge, Massachusetts, 1955.
- Jef 57 Jeffries, C. D., *Phys. Rev.* **106** (1957) 164.
- Jud 55 Judd, B. R., *Proc. roy. Soc. A* **232** (1955) 458.
- Kei 54 Keister, G. L., *Phys. Rev.* **96** (1954) 855 A.
- Kle 29 Klein, O., and Nishina, Y., *Z. Phys.* **52** (1929) 853.
- Kle 48 Klerk, D. de, *Onderzoekingen over adiabatise demagnetisatie*. Thesis, Leiden, 1948.
- Kle 55 Klerk, D. de, and Steenland, M. J., *Progress in low temperature physics*, North Holland Publishing Company, Amsterdam 1955, pp. 273—335.
- Kle 56 Klerk, D. de, *Handbuch der Physik* **15** (1956) pp. 38—209. Springer Verlag, Berlin.

- Kur 35 Kurti, N., and Simon, F., Proc. roy. Soc. London, **A 149** (1935) 152.
- Kur 55 Kurti, N., Conférence de Physique des basses températures, Paris, 1955.
- Kur 57 Kurti, N. Conf. low temp. physics Madison, 1957.
- Lan 57 Landau, Nuclear Physics **3** (1957) 127.
- Lee 56 Lee, T.D. and Yang, C.N. Phys. Rev. **104** (1956) 254.
- Lee 57a Lee, T. D., and Yang, C. N., Phys. Rev. **105** (1957) 1671.
- Lee 57b Lee, T. D., Oehme, R., and Yang, C. N., Phys. Rev. **106** (1957) 340.
- Lip 54a Lipps, F. W., and Tolhoek, H. A., Physica **20** (1954) 85.
- Lip 54b Lipps, F. W., and Tolhoek, H. A., Physica **20** (1954) 395.
- Lun 57 Lundby, A., Patro, A. P., and Stroot, J. P., Nuovo Cimento, **6** (1957) 745.
- Maz 57 Mazari, M., Buechner, W. W. and Sperduto, A., Phys. Rev. **107** (1957) 1383.
- Men 55 Mendelsohn, K., Conférence de Physique des basses températures, Paris (1955).
- Moz 55 Moszkowski, S. A., Beta and gamma ray spectroscopy, edited by K. Siegbahn, North Holland Publishing Company, Amsterdam 1955.
- Osb 46 Osborne, R. K. and Deutsch, M., Phys. Rev. **71** (1946) 467A.
- Pag 57 Page, L. A., Phys. Rev. **106** (1957) 394.
- Pau 24 Pauli, W., Naturwiss. **12** (1924) 741.
- Pea 46 Peacock, W. C. and Deutsch, M., Phys. Rev. **69** (1946) 306.
- Pip 57 Pipkin, F. M. and Culvahouse, J. W., Phys. Rev. **106** (1957) 1102.
- Pol 42 Polder, D., Physica **9** (1942) 709.
- Pop 52 Poppema, O. J., Beun, J. A., Steenland, M. J., and Gorter, C. J. Physica **18** (1952) 1235; Communications Kamerlingh Onnes Lab., Leiden, **291a**.
- Pop 54 Poppema, O. J., Thesis, Groningen 1954.
- Pop 55 Poppema, O. J., Steenland, M. J., Beun, J. A., and Gorter, C. J., Physica **21** (1955) 233; Communications Kamerlingh Onnes Lab., Leiden, no. **298b**.
- Pos 57a Postma, H., Huiskamp, W. J., Miedema, A. R., Steenland, M. J., Tolhoek, H. A. and Gorter, C. J., Physica **23** (1957) 259.
- Pos 57b Postma, H., Huiskamp, W. J., Miedema, A. R., Steenland, M. J. Tolhoek, H. A. and Gorter, C. J., Physica, to be published.
- Poy 09 Poynting, J. M., Proc. roy. Soc. London, **82** (1909) 565.
- Pry 50 Pryce, M. H. L., Phys. Rev. **80** (1950) 1107.

- Ram 56 Ramsey, N. F., *Molecular Beams*, Oxford University Press, London 1956.
- Ros 48 Rose, M. E., U.S. At. En. Comm. Report AECD 2119 (1948).
- Ros 55 Rose, M. E., *Multipole fields*, J. Wiley and sons, New York, 1955.
- Sal 57 Salam, A., *Nuovo Cimento* **5** (1957) 299.
- Sch 57a Schopper, H., *Phil. Mag.* **2** (1957) 710.
- Sch 57b Schopper, H., Appel, H., Galster, S., and Hartwig, G., *Proc. Coll. on Nuclear structure*, Rehovoth, Israel 1957.
- Seh 54 Sehr, R., *Zeit. Phys.* **137** (1954) 523.
- Ste 52a Steenland, M. J., Thesis, Leiden, 1952.
- Ste 52b Stevens, K. W. H., *Proc. phys. Soc. London A* **65** (1952) 209.
- Ste 53 Steenberg, N. R., *Proc. phys. Soc. A* **66** (1953) 391.
- Ste 57 Steenland, M. J., and Tolhoek, H. A., *Progress in low temperature physics II*, North Holland Publishing Company, Amsterdam (1957) pp. 292—337.
- Tol 52 Tolhoek, H. A., *Physica* **18** (1952) 1257.
- Tol 53 Tolhoek, H. A., and Cox, J. A. M., *Physica* **19** (1953) 101.
- Tol 56 Tolhoek, H. A., *Rev. Mod. Phys.* **28** (1956) 277.
- Tou 57 Touschek, B. F., *Nuovo Cimento* **5** (1957) 754.
- Tre 53 Trenam, R. S., *Proc. phys. Soc. London A* **66** (1953) 118.
- Tru 56 Trumpy, G., *Nuclear Physics* **2** (1956) 664.
- Vle 32 Vleck, J. H. van, *The theory of electric and magnetic susceptibilities*. Oxford University Press (1932).
- Vle 34 Vleck, J. H. van, and Penney, W. G., *Phil. Mag.* **17** (1934) 961.
- Voy 57a Voy, K. W. Mc., *Phys. Rev.* **106** (1957) 828.
- Voy 57b Voy, K. W. Mc., and Dyson, F. J., *Phys. Rev.* **106** (1957) 1360.
- Waa 57 Waard, H. de, and Poppema, O. J., *Physica* **23** (1957) 597.
- Whe 55a Wheatley, J. C., Griffing, D. F., and Hill, R. D., *Phys. Rev.* **99** (1955) 334.
- Whe 55b Wheatley, J. C., Huiskamp, W. J., Diddens, A. N., Steenland, M. J., and Tolhoek, H. A., *Physica* **21** (1955) 841; *Communications Kamerlingh Onnes Lab., Leiden*, no. **301b**.
- Whe 56 Wheatley, J. C., and Estle, T. L., *Phys. Rev.* **104** (1956) 264.
- Wu 57 Wu, C. S., Ambler, E., Hayward, R. W., Hoppes, D. D., and Hudson, R. P., *Phys. Rev.* **105** (1957) 1413.

